Manned MZU-003

Monograph 10

BIOTELEMETRY OF THE TRIAXIAL BALLISTOCARDIOGRAM AND ELECTROCARDIOGRAM IN A WEIGHTLESS ENVIRONMENT

W. Carroll Hixson

Dietrich E. Beischer

SCHAVNMED-P-23

U. S. NAVAL SCHOOL OF AVIATION MEDICINE
U. S. NAVAL AVIATION MEDICAL CENTER
PENSACOLA, FLORIDA

BIOTELEMETRY OF THE TRIAXIAL BALLISTOCARDIOGRAM AND ELECTROCARDIOGRAM IN A WEIGHTLESS ENVIRONMENT

W. Carroll Hixson and Dietrich E. Beischer

Monograph No. 10

APPROVED BY

Captain Ashton Graybiel, MC USN
Director of Research

RELEASED BY

Captain H. C. Hunley, MC USN
Commanding Officer

8 September 1964

This research was conducted under the sponsorship of Office of Biotechnology and Human Research, Order No. R-20, National Aeronautics and Space Administration Headquarters, Washington, D. C.

U. S. NAVAL SCHOOL OF AVIATION MEDICINE
U. S. NAVAL AVIATION MEDICAL CENTER
PENSACOLA, FLORIDA

ABSTRACT AND SUMMARY

BIOTELEMETRY OF THE TRIAXIAL BALLISTOCARDIOGRAM AND ELECTROCARDIOGRAM IN A WEIGHTLESS ENVIRONMENT

W. Carroll Hixson and Dietrich E. Beischer

The effect of the earth's gravitational field on suspension systems used in ballistocardiography has limited the collection of multidimensional motion data adequate to describe in detail the instantaneous spatial distribution of the whole-body cardiovascular force pattern.

Biotelemetry instrumentation (Figures 3.1 and 3.2) was developed to record the cardiac-originated inertial accelerations of a subject freely floating in the weightless environment realized in a jet aircraft flying a Keplerian trajectory (Figures 7.5 and 7.6). The weightless state served as an ideal suspension system and allowed unrestricted motion of the subject with six degrees of freedom.

The report describes in detail the design and development of the Constraint Platform with attached Biotelemetry Module (Figure 4.1) used to transduce, signal condition, and telemeter the physiological measurements. A similar description is given of the airborne receiving station (Figure 7.1) used to receive, display, and store the telemetered data.

Linear and angular acceleration measurements were performed with this equipment and the results represent the first recording of a triaxial inertial acceleration ballistocardiogram (Figures 8.1 through 8.6). Triaxial electrocardiographic data were simultaneously measured and telemetered to permit correlation of the mechanical and electrical events of the cardiac complex.

The linear acceleration patterns were also displayed in loop form (Figure 9.1) and in a three-dimensional arrangement (Figure 9.2) to facilitate interpretation of their spatial relationship. Analog computer operations were performed on the flight data (Figures 9.5 and 9.6) to obtain a continuous trace of the absolute magnitude of the instantaneous BCG and ECG vector (Figure 9.7). Differences between the flight BCG and the laboratory based BCG data are noted and discussed.

A discussion of the instrumental approach outlines performance and limitations of such measurements in the weightless environment and makes suggestions for ballistocardiographic studies in large size manned orbiting space laboratories.

ACKNOWLEDGMENTS

The splendid cooperation of the following persons and organizational units of Wright-Patterson Air Force Base, Dayton, Ohio is most gratefully acknowledged: Margaret Jackson, Psychophysiological Stress Section, 6570th Aerospace Medical Laboratories, whose liaison activities resulted in excellent cooperation between the USAF and USN participants; D. Griggs, Guidance and Flight Control Branch, Flight Test Engineering Division, whose whole-hearted efforts as flight test director resulted in smooth implementation of the airborne experimental program; F. A. Post, Captain, USAF, Bomber Operations Division, Directorate of Flight Test, who served as chief project pilot; and S/Sgts H. F. Espenson, C. W. Sears, and E. P. Bunch who were responsible for the airborne launch and recovery of the subject.

The following persons from the U. S. Naval School of Aviation Medicine, Pensacola, Florida, have contributed greatly to the success of the study: C. L. Browning, Jr., and C. A. Lowery, electronic technicians, who were responsible for construction of the instrumentation equipment and their operation in the zero g environment; M. C. Carver, LCDR, MC, USN, who served as project flight surgeon; C. S. Ezell, laboratory technician, who helped in ground support and data analysis; and R. F. Wiencek, AA, USN, who deserves special credit for his patience and cooperation as the research subject.

The project received support from the National Aeronautics and Space Administration, Office of Biotechnology and Human Research, under NASA Order No. R-20. The encouragement provided by Dr. F. B. Voris, Chief, Human Research, of this Office, contributed significantly to the successful completion of the project.

TABLE OF CONTENTS

1. INTRODUCTION

The contributions of ballistocardiography to an understanding of the dynamics of the cardiovascular system will be greatly enhanced by a definitive description of the instantaneous spatial distribution of the multidimensional force patterns of the circulatory system. The merits and pitfalls of different techniques of suspension in the terrestrial environment (swing pendulum, rod, mercury, and air-bearing, as well as others) have been discussed and reviewed in pertinent literature. Though some of these systems allow motion with more than one degree of freedom, the physical characteristics of each place restrictions on obtaining a true spatial description of mechanical cardiovascular activity.

The "ideal" whole-body ballistocardiograph system requires the body suspension to allow unrestricted, frequency independent motion with six degrees of freedom. The inertial translations and rotations of the body arising from its cardiac-originated mass motions must not be modified by the introduction of external inhibitive or perturbative forces. Such a system can be imagined in form of an unrestrained free-floating body in space. The motion of such a body in a weightless environment, relieved from mechanical coupling to ground, would not be subject to the restoring and damping forces acting to various degrees on all existing terrestrial suspension sytems. With free-flotation of the body, frequency dependent phase and amplitude errors due to the dynamics of the suspension system proper would be eliminated, and recordings with minimal distortion achieved. The reduction of the number and complexity of perturbation effects would bring the BCG records derived from measurements of the triaxial inertial linear and angular accelerations closer to a true rendition of the instantaneous cardiovascular force patterns.

The actual physical realization of the dream of ballistocardiographers —the collection of BCG data in a suspension system with six degrees of unrestricted motion—is the subject of this report. The gravity free state experienced for a short time during the ballistic flight of an aircraft performing Keplerian trajectories provided the environment for the experiments. By allowing the subject to free-float during the weightless period and telemetering the instantaneous linear and angular accelerations of his body to an on-board data collection station, it was possible to display the first triaxial inertial acceleration ballistocardiogram ever recorded.

An introductory summary of the experimental approach developed for the study follows. For experimentation in a weightless environment, arrangements were made for flight time on a KC-135 jet aircraft which was custom modified to fly zero g missions. With this aircraft, zero g profiles could be flown with periods of weightlessness extending to thirty seconds. To provide bodily protection to the subject during free-flotation, a Fiberglas couch was custom molded to his outer contours. To this couch, identified as the Constraint Platform, were attached miniature transducers, signal-conditioning amplifiers, and telemetry equipment which permitted

the triaxial BCG and ECG data to be transmitted to an on-board data display and storage receiving station. The radio frequency telemetry link removed the need for hard wire interconnections between the subject and data station, eliminating restrictions on his free-flotation.

These data, as well as related trouble-shooting measurements, were simultaneously displayed in real time on an optical galvanometer recorder, and stored in both analog and composite telemetry video form on a multichannel magnetic tape instrumentation recorder. Approximately 50 zero g profiles were flown to determine the optimal conditions for operation of the over-all instrumentation system.

The method and related instrumentation developed for this study will have specific application in the collection of information on the functional state of the heart and larger vessels during prolonged exposure to the gravity free state present in manned orbiting laboratories stationed in space for extended intervals. Particular advantages will result in the detection of changes in the force patterns during long-time exposure.

The assessment of cardiovascular forces on the stability of a space vehicle or platform is suggested as another application. Quantitative information on these forces may be of specific importance to the design of attitude stabilization systems for low-mass, manned space vehicles equipped for astronomical observations.

It is also expected that the triaxial BCG-ECG data collected in this study will be an immediate contribution to interpretation of the spatial distribution of mechanical cardiovascular activity, and they should prove helpful in the assessment of the quality of presently used earthbound ballistocardiography practices.

2. WEIGHTLESS ENVIRONMENT AND ITS OPERATIONAL BOUNDARIES

Through the excellent cooperation of the 6570th Aerospace Medical Research Laboratories and the Flight Test Engineering Division Agencies at Wright-Patterson Air Force Base, Ohio, their zero g KC-135 jet aircraft was made available to the U. S. Naval School of Aviation Medicine for the measurement of the triaxial ballistocardiogram in a weightless environment. The minimal goal during each zero g maneuver of the aircraft was to place and maintain the subject in a true free-flotation state for a time sufficiently long to record at least three sequential ballistocardigram complexes. The KC-135 flight procedures involved in the measurement of these data, along with the limitations imposed on the program by the operational nature of the airborne environment, are outlined in the following sections to show the working boundaries within which the project had to be implemented.

FLIGHT PROCEDURES

The Zero g Maneuver

The KC-135 jet aircraft used to fly the Keplerian trajectories was a modified four engine military refueling tanker which served as the prototype for the current 707-720 series of commercial jet airliners. Built-in features developed to facilitate on-board experimentation included an extensive free-flotation cabin area with all wall, ceiling, and deck surfaces clear of protruding obstructions and completely lined with insulation materials capable of absorbing heavy impact loads; accelerometers to measure the time-acceleration profile of each maneuver; a recorder to display the profile and related experimental data; heavy-duty inverters to supply 115 VAC, 60 cps, single phase power to on-board instrumentation, equipment, and systems; flush mounted wall and ceiling light fixtures to provide high intensity illumination for photographic documentation purposes; and ancillary life support equipment. An over-all view of the actual aircraft used for this experiment is shown in Figure 2.1.

A typical zero g profile was initiated from straight and level flight at a speed of 374 knots indicated (510 knots true air speed) and at an altitude which varied between 22,000 and 26,000 feet, the exact height being selected for minimum air turbulence in the maneuver strata (Figure 2.2). The onset of the profile was marked by a constant 2 g pull-up which was maintained until the aircraft reached a pitch angle of approximately 45 degrees climb when it was pushed over into the zero g condition. By holding the aircraft on a Keplerian trajectory course the desired state of weightlessness was maintained. When the nose attitude of the aircraft decreased to a predetermined pitch angle, usually between 30 and 40 degrees, a 2 g recovery pull-up was made and the aircraft returned to its original altitude. Straight and level flight was re-established or a second maneuver initiated immediately.

Figure 2.1 Over-all view of the KC-135 jet aircraft used to fly the zero g maneuver.

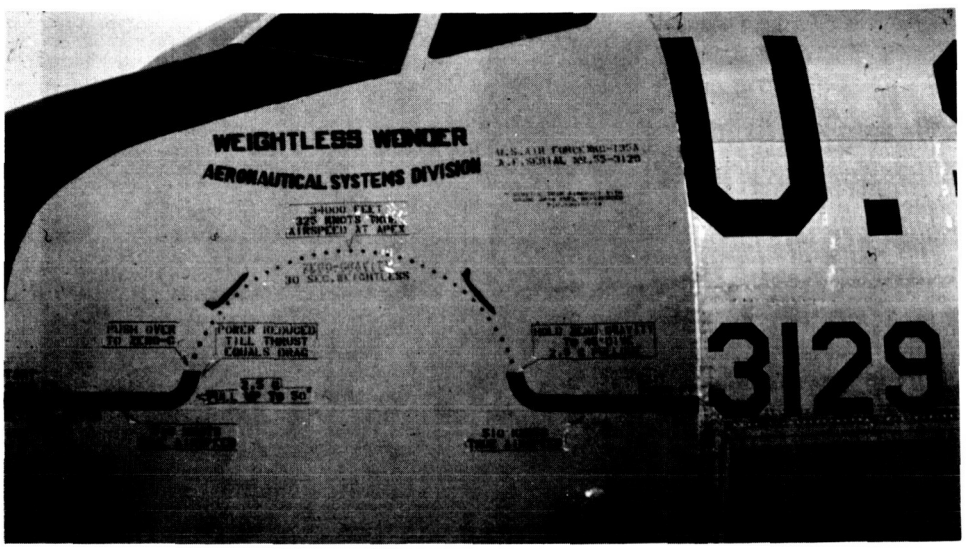

Figure 2.2 Close-up view of the nose section of the KC-135 aircraft which illustrates the flight profile of a typical zero g maneuver.

Weightless periods of twenty to thirty seconds duration were reached during each zero g maneuver; however, the time available for measurements ranged from two to fifteen seconds only. Air turbulence, for example, caused free-floating objects to touch portions of the airframe, thus terminating the measurements in progress.

Free Flotation of the Subject

At the onset of the weightless period in each zero g maneuver, the subject was raised from the deck of the aircraft and allowed to free-float within the confines of the vehicle without any physical attachment or coupling to the airframe. Since the subject was isolated from the airframe, vibrations of the airframe or very slight deviations of the aircraft flight profile from the Keplerian trajectory did not disturb the free-floating state of the subject.

It should be noted that a weightless environment *per se* is not sufficient to satisfy the project objectives of measuring the unperturbed

inertial ballistocardiogram of a human subject. The subject must be decoupled from any larger mass which would modify, alter, or distort the cardiac-originated body accelerations. For this particular project, the BCG measurements could not be made with the subject coupled to the airframe of the KC-135 even if the flight profile conformed exactly to a given Keplerian trajectory and the airframe could be considered in a true zero g condition. It is obvious that the magnitude of the cardiac-originated

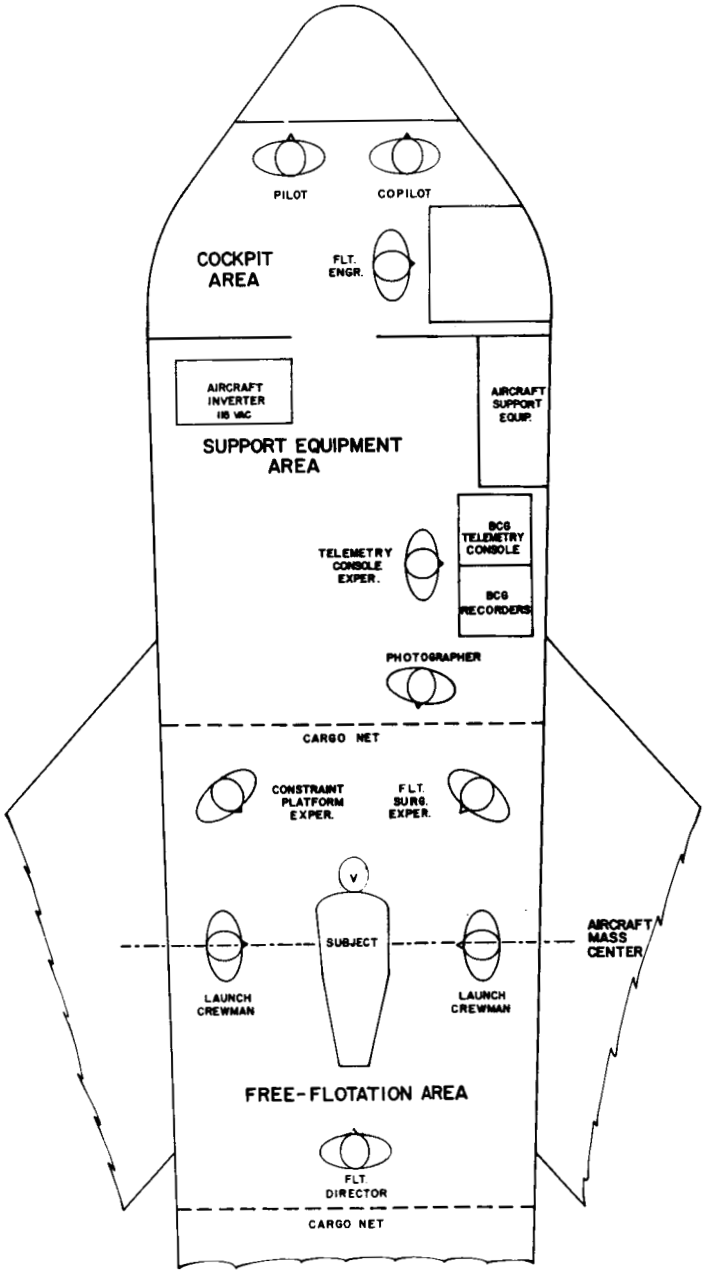

Figure 2.3 Pictorial plan view of the KC-135 aircraft showing the operational positions of the on-board personnel during a typical zero g maneuver.

mechanical forces is not sufficient to impart a measurable acceleration to the mass of the KC-135 aircraft.

The procedures for the placement of the subject in the free-flotation state are best described by listing the on-board personnel and their duties during the zero g maneuvers (Figure 2.3). In-flight personnel included the basic crew consisting of pilot, copilot, and flight engineer; a flight director who supervised the operational aspects of the on-board experimentation and free-flotation procedures; two launch crewmen who manually released and recovered the subject during the zero g maneuvers; an experimenter who was responsible for the operation of the telemetry instrumentation installed on the subject's Constraint Platform; another experimenter who operated all of the telemetry receiving station equipment including the on-board data recorders; a flight surgeon who monitored the performance of the subject during the entire flight; a photographer for still and motion picture documentation of the on-board experimental procedures; and the subject.

A brief summary of the basic operations performed before and during each flight follows: Before each flight, all on-board personnel attended a briefing where the details of the planned experimental program were outlined and integrated with the scheduled flight plan. Following this briefing, the instrumentation system was given a final ground check with the subject in the Constraint Platform and all equipment activated. The aircraft was then flown to a restricted area where the zero g maneuvers were performed under ground-based radar surveillance. Enroute to this area, the BCG instrumentation installed in a Telemetry Console was turned on and allowed to reach operating temperature. After the subject had been placed in a Constraint Platform the entire instrumentation system including the biotelemetry equipment installed on the Constraint Platform was given a final check and calibrated.

When the subject and all other on-board personnel were ready for the first maneuver, the pilot gave the signal for entry pull-up. At this time, the battery operated biotelemetry system installed on the Constraint Platform was turned on and the data display and storage recorders activated. When the weightless state was reached, the pilot signalled the flight director to begin the subject launch operations. The two launch crewmen then lifted the subject from the deck, stabilized his motions, and released the Constraint Platform placing it in the free-flotation state. The ability of these personnel to release the subject without imparting any significant linear or angular motions to the Constraint Platform influenced to a considerable degree the length of the free-flotation period.

After the aircraft had gone over the top of the trajectory and reached a predetermined pitch angle, usually 20 degrees nose-down, the pilot would signal that recovery operations should be initiated. The launch personnel would then return the subject to the deck of the aircraft. After the launch personnel had secured the subject, the pilot initiated the recovery pull-up at which time the instrumentation and recorders were turned off. At the end of the maneuver the flight surgeon checked the well-being of the subject.

OPERATIONAL BOUNDARIES

Instrumentation Considerations

The minimal amount of time available for experimentation served as an important design criterion for the development of the instrumentation system. This time limitation obviously required the system to have a high degree of reliability and to maintain measurement accuracy throughout each flight. Since quantification of the data was a primary objective of the project, in-flight verification of calibration accuracy of both the signal-conditioning and telemetry equipment was a necessity. The time limitation also required that the calibration procedures be performed without difficulty by the airborne instrumentation operators.

The need for sturdy airborne equipment and components rather than general purpose laboratory instruments was another obvious requirement of the experiment. Impact loads encountered during landing of the aircraft, vibration characteristics of the airframe, acceleration loads, air turbulence, a wide range of ambient cabin temperatures, and potential in-flight changes of ambient cabin pressure had to be considered in instrument design and construction. Of particular importance to the basic design of the BCG instrumentation system was the flight profile g load. Because of this acceleration load, which ranged between 2 and 2½ g, the BCG instrumentation channels were subjected to tremendous overloads before and after each measurement interval. Since the linear acceleration BCG channels were set up to measure cardiac-originated accelerations with an expected peak-to-peak level of approximately 0.0025 g, the entry and recovery operations of the aircraft produced an overload signal almost 1000 times greater than channel capacity. Special efforts were necessary to prevent this overload from interfering with the collection of data during the short period of weightlessness.

Another most significant instrumentation design criterion established by the nature of the KC-135 zero g environment was the need to utilize radio frequency telemetry techniques to transmit the desired data from the Constraint Platform to the on-board data display and storage recorders. Although hard-line interconnections would have greatly simplified the design and operation of the system, the need for complete isolation of the subject from the airframe made this approach undesirable. A highly flexible cable could have been developed to connect the output of the signal-conditioning equipment to the input circuitry of the recorders. However, a cable might have restricted the motion of the Constraint Platform during the free-flotation period and thus have resulted in loss of BCG data. Of equal bearing on the decision to use telemetry techniques was the fact that an interconnecting cable might seriously hamper release and recovery operations by the launch personnel during the zero g maneuvers.

The need for telemetry transmission of the data and their on-board reception, display, and storage obviously added to the complexity of the over-all system. Specifically, the signal-to-noise ratio characteristics of a telemetry system are limited and cannot closely approach those attainable with hard-line modes of data transmission. With any telemetry system, this ratio can be maximized only if the data are of such form as to fully utilize

the entire signal handling capabilities of the system. For the FM-PM system used in this project, the maximum signal-to-noise ratio characteristics of each channel could be realized only if the peak-to-peak level of the BCG and ECG signals drove each voltage controlled subcarrier oscillator to its full ± 7.5 per cent deviation limits.

For the ECG channels, the noise characteristics of the telemetry system could be readily optimized since the nominal peak-to-peak values of these data and their expected variations could be determined from laboratory based measurements and the channel sensitivities set up to achieve near maximum frequency deviation. The same procedure could be followed for the linear acceleration ballistocardiograms along the longitudinal and transverse (side-to-side) body axes with data derived from measurements made on an air-bearing BCG bed installed in the laboratory. However, little quantified data were available for either the dorsoventral linear acceleration BCG signal or any of the three angular acceleration BCG signals. Thus the optimal sensitivity levels for the telemetry channels associated with these measurements could not be established on an *a priori* flight basis. For this reason it was necessary to fly an extensive series of preliminary zero g maneuvers to determine these levels empirically before the final data collection phase of the project could be initiated.

Other environmental factors which affected the instrumentation design, but which could not be completely evaluated except under actual conditions of weightlessness, were resonances of the Constraint Platform and the generation of artifacts by the subject release procedures. Since free-flotation of the subject was to be accomplished by manual release of the Constraint Platform, a possibility existed that the launch personnel would impart angular velocity components to the platform at the moment of launch. These angular velocities would remain in effect during free-flotation, and the resultant centripetal accelerations would activiate the triaxially mounted accelerometers used to record the linear BCG accelerations of the subject. If of sufficient magnitude, these centripetal acceleration signals would appear in the recorded data as static offset g levels about which the dynamic BCG signals occurred. Because these angular velocities would occur simultaneously about the three reference axes, and since the exact instantaneous center of mass of the subject and Constraint Platform combination would not be known, conventional circuitry using two accelerometers in a balanced or canceling configuration would not be feasible. As the offset g levels might be of sufficient magnitude to prevent the full utilization of the pertinent telemetry channels, the instrumentation design had to allow for this potential source of artifact.

Other limitations on the over-all instrumentation system involved the minimal ground time available for test and setup of the system between flights. This was due primarily to the nonavailability of aircraft power at all times and the relatively short time available for maintenance between morning and afternoon flights.

Subject Considerations

The lightweight Fiberglas Constraint Platform, tightly molded to the body contours of the subject and equipped with quick-release type torso

and limb restraint straps, was developed for protection of the subject during the zero g maneuvers of the KC-135 aircraft. The molding operations were performed while the subject maintained the conventional clinical BCG reclining posture. The same analytical techniques which have been developed for terrestrial ballistocardiography and which are based on rigid-body mathematics could then be applied to the resultant data. In addition to providing bodily protection for the subject, the Constraint Platform served as a mounting platform for the transducers, signal-conditioning amplifiers, and telemetry equipment associated with the measurements. The basic design criterion for the unit was to develop a rigid support structure of low mass which would not compromise the personal safety or self-egress capabilities of the subject during the flight maneuvers.

It should be noted that the need for a Constraint Platform was dictated more by operational aspects of the aircraft than by the requirement for a rigid body position. If a weightless environment were available without the need for protection of the subject, whole-body acceleration measurements of cardiac activity could be readily achieved by an instrumentation package attached directly to the upper torso of a free-floating subject physically capable of maintaining a rigid and fixed limb-torso relationship. With the KC-135 aircraft, such an experimental approach would be most difficult, although perhaps not precluded. The subject would need sufficient training in the zero g environment to make him fully confident of his physical safety and thus allow full relaxation while maintaining a fixed and rigid body orientation without limb movements or body tremor that would completely mask cardiac-originated accelerations.

The importance of the potential occurrence of subject-originated body motions to the implementation of this project cannot be overemphasized considering the relatively minute magnitude of the BCG accelerations. In the laboratory situation, those artifacts to the BCG produced by the subject, i.e., slight movements of the limbs, uncontrolled respiration patterns, or body tremor, can usually be minimized by giving more explicit instructions to the subject. However, the airborne environment of the KC-135 vehicle and its operational nature limit time-consuming special instructions.

For each zero g profile, the subject was instructed to suspend his respiratory action immediately before he was launched into free-flotation and to maintain this state with a complete relaxation of the body throughout the weightless period of the maneuver. If for some reason he could not maintain this respiratory state, or if he tensed his body, acceleration artifacts would occur which could completely mask the BCG data. Most significant was the possibility of body tremor. These uncontrolled motions could arise from inadequate control of the aircraft cabin temperature relative to the subject's comfort, the onset of motion sickness, or the lack of confidence in the reliability of his environment.

This most important point of subject confidence must be emphasized since the environment afforded by the KC-135 aircraft and the function performed by the subject in this environment were not always conducive to his full and complete relaxation. The subject's attire while restrained

in the Platform consisted of undershirt, swim trunks, and socks. The individual attire of all other on-board personnel consisted of a flight suit, flight boots, crash helmet, and oxygen mask. In addition, these personnel wore parachutes and were always within a few feet of an oxygen bail-out bottle which would be necessary in case of a bail-out emergency or loss of cabin pressure at the maneuver altitude. The subject was given instructions on emergency procedures along with in-flight practice of self-release from the Constraint Platform and donning his flight gear. The need for such instructions would place some demands on the composure of any volunteer subject. As was proven in the actual flight program, the selected subject was able to relax sufficiently to meet the demands necessary for the measurements.

3. INSTRUMENTATION SYSTEM

DESIGN GOALS

The design goals for the bioinstrumentation aspects of this project may be summarized briefly as follows: to provide a low-mass rigid Constraint Platform which would serve as the reference frame for the ballistocardiogram acceleration measurements and as a semi-enclosed housing for protection of the subject during the zero g maneuvers of the KC-135 jet aircraft; to provide transducers and signal-conditioning equipment for the measurement of the inertial linear and angular ballistocardiogram accelerations of the platform along and about three orthogonal body axes; to provide instrumentation for the triaxial electrocardiogram potentials generated along the same body axes, thus allowing correlation of the mechanical and electrical events occurring within each cardiac cycle; to provide a telemetry transmitting link for the transmission of the BCG and ECG data from the subject without any hard wire connections to the Constraint Platform during its flotation in the weightless state; and to provide an on-board Telemetry Receiving Station with facilities for real-time display and magnetic tape storage of both the subject-related signals and the data collected to define the acceleration profile of the KC-135 vehicle during each of its zero g maneuvers.

GENERAL DESCRIPTION

A block diagram of the Biotelemetry Module which housed the majority of the transducers, signal-conditioning amplifiers, and telemetry transmitting equipment located at the Constraint Platform station is shown in Figure 3.1. The Biotelemetry Module circuitry served eleven different

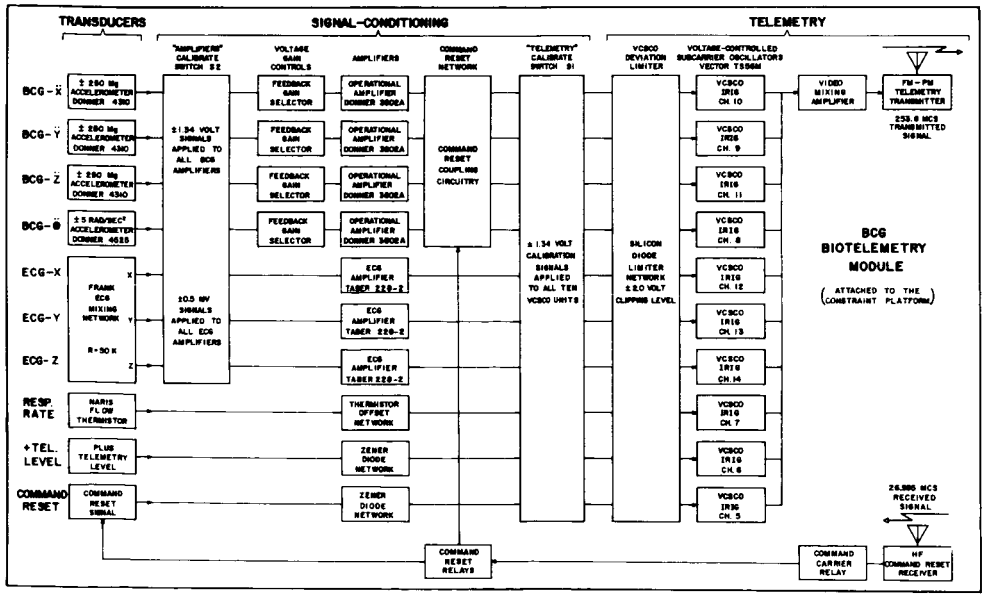

Figure 3.1 Block diagram of the transducers, signal-conditioning, and telemetry elements of the Biotelemetry Module which housed the major components of the instrumentation installed on the Constraint Platform.

measurement functions which are listed as follows: BCG-$\ddot{X}$, the amplitude-time profile of the cardiac-originated linear accelerations of the Constraint Platform along the transverse (side-to-side) body axis of the subject; BCG-$\ddot{Y}$, same as BCG-$\ddot{X}$ except along the longitudinal body axis; BCG-$\ddot{Z}$, same as BCG-$\ddot{X}$ except along the dorsoventral body axis; BCG-$\ddot{\Theta}$, the amplitude-time profile of the cardiac-originated angular accelerations of the Constraint Platform about any single preselected body axis; ECG-X the Frank transverse (side-to-side) electrocardiogram lead; ECG-Y, the Frank longitudinal electrocardiogram lead; ECG-Z, the Frank dorsoventral electrocardiogram lead; Respiration Rate, a measure of the naris air flow patterns of the subject; Plus Telemetry Level, the output voltage of the battery source used to energize the telemetry system; Command Reset, a record of the functioning of the Command Reset Transmitter and Command Reset Receiver equipment; and Plus Amplifier Level, the output voltage of the positive polarity battery source used to energize the signal-conditioning amplifiers. A ten channel FM-PM frequency division multiplexing type telemetry system transmitted these measurements independently (except for the last two which shared the same channel) to the Telemetry Receiving Station installed aboard the aircraft immediately adjacent to the free-flotation area.

The transducers used for the BCG-$\ddot{X}$, BCG-$\ddot{Y}$, and BCG-$\ddot{Z}$ measurements were three force-balance type linear accelerometers mounted orthogonally within the interior of the Biotelemetry Module. An angular accelerometer, which operated also on the force-balance principle, served as the transducer for the BCG-$\ddot{\Theta}$ measurement. A triaxial mounting assembly for this transducer, attached to the bottom of the Constraint Platform at the rear of the Biotelemetry Module, permitted its axis of sensitivity to be readily aligned with any of the three body reference axes. The output lines from the four BCG transducers were routed to four chopper-stabilized DC operational amplifiers via a calibration network. This network consisted of a multipole two-position switch and associated resistors for the on-board calibration of the BCG and ECG signal-conditioning amplifiers. The primary function of the four operational amplifiers was to raise the signals available from the four BCG transducers to the ± 1.5 volt level required to drive the associated voltage-controlled subcarrier oscillators to their full ± 7.5 per cent deviation capabilities. A multiposition sensitivity switch was provided for each amplifier which accurately controlled the closed-loop gain of the combination. This switch allowed the on-board experimenters to change the g sensitivity of each BCG channel between zero g maneuvers according to a prescheduled program.

The output signal from each of the four BCG amplifiers was passed through a network which allowed these signals to be either directly or capacitively coupled to the input of the telemetry system. When direct coupling was selected, the frequency response of the entire transmitting-receiving link extended upward from 0 cps. When capacitive coupling was selected, the frequency response of the entire link was such that the voltage gain was down 0.707 at 0.25 cps. The function of this latter coupling mode was to minimize the effects of potential offset g levels of static form which might be superimposed on the desired dynamic BCG data.

Although capacitive coupling would be of advantage if these static g levels did exist, loss of data would necessarily result due to blocking effects produced by system overloads which would always occur before

the free-flotation state was reached. These overloads, produced by the aircraft pull-in g level and the handling of the Constraint Platform by the launch personnel immediately before its release to the free-flotation state, would be in the form of accelerations with peak-to-peak magnitudes far exceeding the recovery properties of the capacitive coupling system.

To negate this effect, relay circuitry was included which could momentarily short these capacitors to ground and thus minimize their recovery time. Control of this circuitry was provided by a second radio frequency telemetry link which was operated by an experimenter located in the immediate vicinity of the free-flotation area. This experimenter momentarily modulated a portable AM transmitter immediately after the subject was placed in the free-flotation state which then operated the Command Reset Receiver installed inside the Biotelemetry Module. The demodulated carrier signal output of the receiver maintained the reset relays in the energized position as long as the Command Reset Transmitter was modulated. The resultant action minimized the recovery problems associated with the capacitive coupling system.

To time-relate the mechanical and electrical components of the cardiac cycle, the subject's triaxial electrocardiogram was always recorded simultaneously with the BCG data. Electrodes were placed on the subject in a Frank lead configuration (1) which, in conjunction with a resistive mixing network, produced three potentials that theoretically defined the instantaneous electrical activity of the heart along three orthogonal axes. These potentials, identified as ECG-X, ECG-Y, and ECG-Z were raised to telemetry level by three miniature transistorized preamplifiers installed in the Biotelemetry Module.

A bead thermistor transducer was used to record the naris air flow of the subject to obtain a measure of his respirations. This measurement served only a trouble-shooting function in the experiment since it was planned to collect the free-flotation data with the subject in a state of suspended respiration. Thus, if the subject performed as desired, no signal would be transmitted on this channel. However, it was decided to monitor the variable to ensure that, if in-flight noise artifacts did occur, it would be possible to determine if undesired respiratory actions of the subject were the potential source of artifact.

Since the power demands of the Biotelemetry Module were great enough to cause a relatively short battery life, the output voltages from the telemetry battery and the positive polarity signal-conditioning battery were telemetered to the Telemetry Receiving Station to permit the experimenter to visually monitor their status. A resistive mixing network allowed the telemetry channel associated with the signal-conditioning battery level to monitor also the operation of the Command Reset Receiver.

The above-mentioned output signals of the preamplifiers were directed to the input circuitry of the ten voltage-controlled subcarrier oscillators. Each of these signals was first passed through a biased silicon diode circuit which limited the maximum frequency deviation of each oscillator under overload conditions to approximately ± 10 per cent. This limiting action was most necessary to prevent the loss of data due to the potential cross-modulation effects produced by one overloaded channel on other channels operating in the nonoverloaded state. A single multigang switch permitted the inputs of the ten subcarrier oscillators to be removed from the signal-conditioning equipment and connected to a common voltage

calibration source of either plus or minus polarity. The output signals of the ten subcarrier oscillators were resistively added and applied to the input of a mixer amplifier. The composite video output signal of this amplifier drove the phase modulated transmitter to its full 125 kc deviation. The RF output of this transmitter was then coupled to a half-wave dipole antenna molded into the surface of the Constraint Platform.

The resultant FM-PM carrier was transmitted to a telemetry receiver installed in the Telemetry Receiving Station, a block diagram of which is shown in Figure 3.2. The output of this receiver, in composite video form,

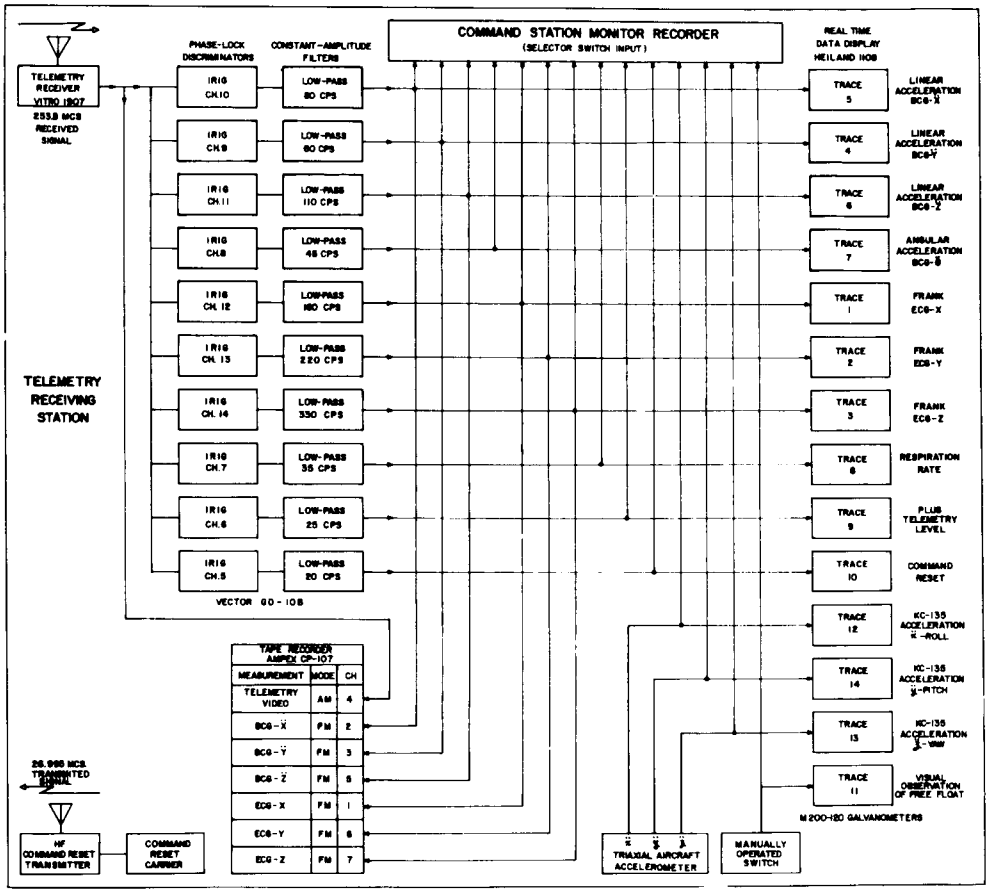

Figure 3.2 Block diagram of the basic elements of the Telemetry Receiving Station installed aboard the KC-135 aircraft for reception, display, and storage of the BCG, ECG, and other data transmitted from the Constraint Platform.

was recorded on a single wideband channel of an on-board, seven-channel magnetic tape instrumentation recorder to permit later laboratory analysis of the raw telemetry data. The receiver output was also routed to ten phase-lock type FM discriminators which translated the composite video signal to its original analog form. These ten analog signals were then displayed in real time on a multichannel light beam galvanometer recorder equipped with a latensification lamp for quick visual readout of the simultaneously displayed data. The linear accelerations of the aircraft along its roll, pitch, and yaw axes, identified as $\ddot{x}$, $\ddot{y}$, and $\ddot{z}$ respectively, were

also displayed on this recorder. In addition, one galvanometer was activated by the flight surgeon to mark the interval when the subject visually appeared to be in the free-flotation state. As with the respiration rate signal, this channel served only a trouble-shooting function in case difficulties were encountered in the collection of the BCG data.

The BCG-$\ddot{X}$, BCG-$\ddot{Y}$, BCG-$\ddot{Z}$, BCG-$\ddot{\theta}$, ECG-X, ECG-Y, and ECG-Z discriminator output signals were independently recorded on the remaining six channels of the tape recorder. These channels, of the FM recording type, allowed the crucial measurements to be reproduced in the laboratory with a greater signal-to-noise ratio than that afforded by the ground-based demodulation of the composite video signal recorded on the wide-band channel of the tape recorder. A single channel, direct-writing recorder with a 20 position input selector switch was made part of the on-board installation to aid in the ground setup of the system and to serve as an in-flight monitor of each individual measurement channel.

4. CONSTRAINT PLATFORM

DESIGN CRITERIA

For this study, the bed type assembly developed to house the subject and the related instrumentation has been identified as the Constraint Platform. The term constraint is used in the sense of supporting firmly the subject to maintain his head, torso, and limbs in a fixed positional configuration with minimal occurrence of relative motion. Constraint was necessary for two main reasons: first, to prevent inadvertent motions of the subject which would produce high-level acceleration artifacts of sufficient magnitude to mask the low-level BCG acceleration data; second, to allow the subject and the Constraint Platform to approximate a single rigid structure whose instantaneous changes of mass center due to the mechanical cardiac activity could be interpreted in the language of rigid-body mathematics developed in past BCG analytical studies. As with all existing whole-body BCG techniques, this approximation can be only approached, not realized. Due primarily to the elasticity and compliance characteristics of the internal organs of the body, the treatment of the over-all transmission system as a rigid body has its limitations.

Specific design criteria for the Constraint Platform included the need for tight coupling between the subject and the accelerometers used to measure cardiac activity; a rigid structure free of internal resonances in the BCG frequency spectrum; a physical configuration allowing the accelerometers to be placed as close to the center of mass (subject plus platform) as possible; and low mass as compared to the subject so that perturbations of the cardiac-originated platform accelerations due to loading effects would be minimized.

Each of the above criteria is inherent in ballistocardiographic techniques. However, the manner in which the constraint was to be provided and its resultant mass were dictated almost wholly by the operational requirements imposed by the airborne environment. Of primary importance was the necessity of maintaining a minimum of personal hazard to the subject with the Constraint Platform to provide maximal protection to the subject during his free-flotation period. Since any change in aircraft velocity during the free-flotation period would result in a displacement of the subject in the opposite direction relative to the cabin, additional protection of the subject against potential impacts was important. This protection was provided to a great degree by the shock-absorbing materials used to line the walls of the KC-135 testing area and the use of flush-mounting techniques for such auxiliary equipment as camera lights, communications panels, and electrical connectors.

The design of the constraint method had to provide for ready self-egress of the subject within a short time since preparations for bail-out had to be completed in less than one minute. As the Constraint Platform was to be manipulated by two men during the free-flotation period, its design had to allow for ease of handling by launch personnel. This was of particular importance during the recovery of the subject and his return to the deck of the aircraft. The platform was to be constructed of sufficient mechanical strength to accommodate the increased weight of subject and instrumentation package during the zero g maneuvers.

CONSTRUCTION

A side view of the Constraint Platform is shown in Figure 4.1. The main parts of the unit were a rigid Fiberglas couch, custom molded to the body contours of the subject; a tubular aluminum skid-like supporting structure; a quick-release strap assembly; a visor for facial protection of the subject; the Biotelemetry Module which housed the majority of the instrumentation components; and a triaxial mount for the angular accelerometer transducer.

To fabricate the couch, a negative mold of the subject was made from plaster of Paris impregnated bandage material which was formed to his outer body contours. This mold was then used to cast a positive hydrastone mold of the subject. This latter mold was then covered with tailored sections of Fiberglas cloth which were held in place by a poly-based resin worked into the cloth. When this layer hardened, the joints requiring additional strength were reinforced and the entire mold covered with a second layer of the same Fiberglas material. The master mold, cut in sections before the Fiberglas process was initiated, was then removed from the couch.

The fit of the subject to the couch was checked and necessary alterations made. Special effort was devoted to relieving pressure points since

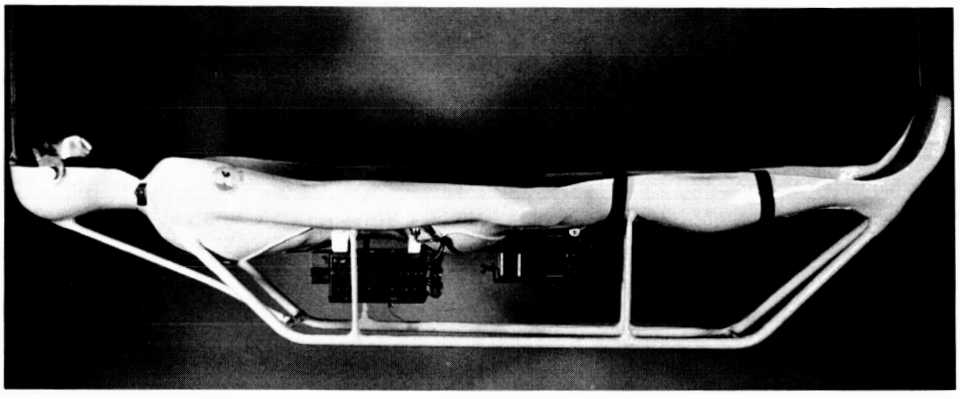

Figure 4.1 Side view of the Constraint Platform showing the basic custom molded Fiberglas couch assembly, its supporting skid structure, the protective visor, the Biotelemetry Module, and the triaxial mount angular accelerometer assembly.

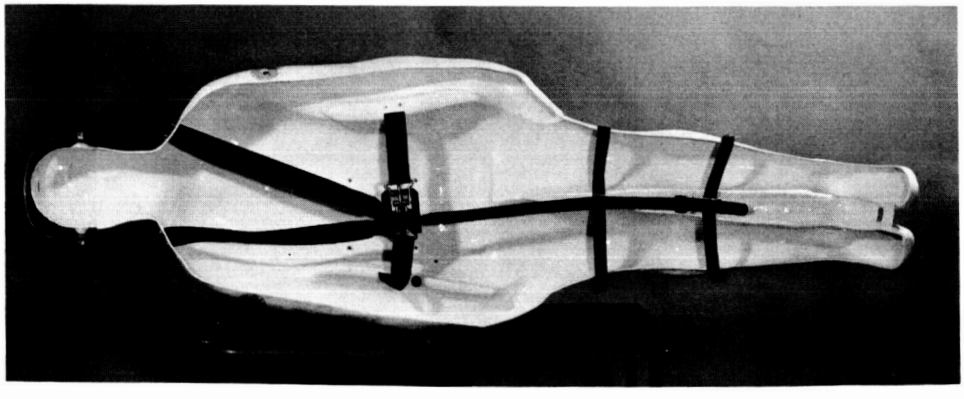

Figure 4.2 Constraint Platform as viewed from the top showing the concave overlap contours of the couch assembly and the quick release torso and limb straps.

the subject would sometimes be required to remain in the platform for several hours. The edges of the Fiberglas couch were extended to provide a concave overlap at the shoulder, arm, and leg levels and thus allow tight coupling of the subject to the couch.

To ensure further that the subject and couch would closely approximate a single rigid structure, prestretched nylon straps were installed (Figure 4.2). The loose ends of two shoulder straps, a belt across the abdomen, and a single longitudinal strap were all held by a quick-release buckle attached to the abdominal belt. Straps at mid-thigh and mid-calf level were held in place by snaps. Even without these straps, the contours of the custom molded assembly provided a high degree of unity of platform and subject.

A protective visor for the subject's face was installed on the Constraint Platform. This assembly was custom shaped from ¼ inch sheet polystyrene and swivel mounted to the couch. A nylon strap prevented undesirable movement of the visor. The interior of the visor was lined with a one inch thick resilient padding material to protect the eyes in case of impact.

The skid-like support served two main operational functions: to protect the instrumentation installed beneath the subject and to provide a stabilized resting position for the platform with a low overturning moment. The latter function was important during the zero g maneuvers of the aircraft when the skid structure had to support additional weight imposed by g loads. A third function of the skid structure was to provide hand holds for the airborne personnel responsible for launch and recovery during zero g maneuvers and for assistance of the subject during air turbulence or significant changes in aircraft velocity.

The Biotelemetry Module containing the three orthogonally mounted linear accelerometers used for the BCG measurements was mounted by means of resin impregnated Fiberglas cloth blocks to the bottom of the couch. This package was centered and leveled so that these accelerometers were as close to the center of mass of the platform and subject as physically possible (about 3 inches displacement in dorsal direction) and in alignment with the three body axes. The angular accelerometer was mounted away from the center of mass (12 inches in footward and 3 inches in dorsal direction) in a triaxial support structure which allowed the axis of sensitivity to be aligned with any of the three orthogonal body reference axes.

A miniature coaxial receptacle for the respiration rate transducer was molded into the side of the head section of the couch. A second receptacle assembly for the ECG electrode cable was molded into the couch at the mid-arm level of the subject. This unit contained also the mixing resistors needed for the ECG lead configuration developed by Frank (1) to measure the spatial triaxial electrocardiogram. To minimize the potential of artifacts due to wire motions, all interconnecting cables as well as the telemetry transmitting antenna and the command reset receiving antenna were cemented to the couch with a neoprene based potting compound.

A close-up photograph of the subject in the Constraint Platform during the calibration phase of an actual flight is shown in Figure 4.3. With the design emphasis placed on the use of lightweight Fiberglas construction, the entire couch assembly including the visor, restraint straps,

interconnecting cables, transmitting antenna, receiving antenna, and supporting skid structure weighed only 12.5 pounds. This amount added to the 11.0 pounds of the miniaturized biotelemetry instrumentation system resulted in a total weight for the finished Constraint Platform of 23.5 pounds, a relatively low weight compared to the weight of the subject (183 pounds).

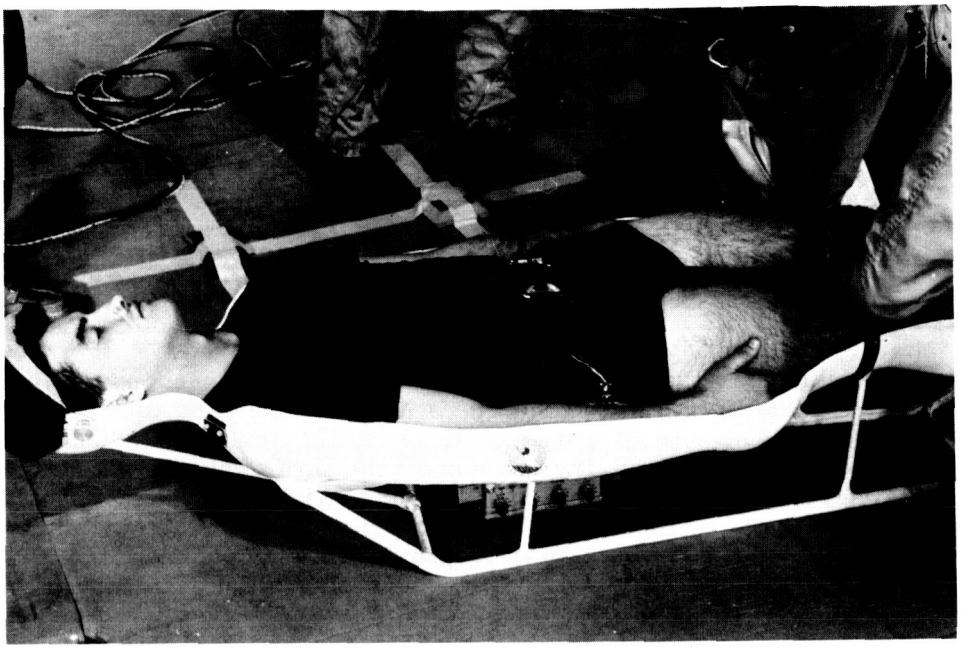

Figure 4.3 Subject positioned in the Constraint Platform aboard the KC-135 zero g aircraft.

5. BIOTELEMETRY MODULE

All of the transducers, signal-conditioning amplifiers, telemetry components, control switches, batteries, and related circuitry located on the Constraint Platform were either installed within, mounted on, or terminated at the Biotelemetry Module. The housing for this unit was a 7" x 6½" x 3½" chassis formed from 0.082 inch thick aluminum with all side junctions welded together to form a rigid structure. Type 5052-0 half-hard aluminum was selected for construction of the chassis because of its good welding properties and its ability to provide better damping characteristics than those available with a harder metal. A removable cover plate of the same material with a 3/8 inch overlap at its edges imparted additional rigidity to the structure.

A photograph of the front panel of the Biotelemetry Module is shown in the Figure 5.1. The four controls at the top of the panel, identified as BCG-$\ddot{X}$, BCG-$\ddot{Y}$, BCG-$\ddot{Z}$, and BCG-$\ddot{\Theta}$, served to control the voltage gain of the four DC operational amplifiers used to raise the low-level output signals derived from the four BCG accelerometers to telemetry level. The two centrally located switches, identified as AMPLIFIERS and TELEMETRY, were used in conjunction with the + CAL and – CAL momentary action pushbuttons to calibrate the system. When the TELEMETRY switch was placed in its CAL position, the input line from each of the ten subcarrier oscillators was returned to ground, which then defined the center frequency of each telemetry channel for zero input signal. By pressing either the + CAL or – CAL pushbuttons, a positive or negative calibration voltage could be applied simultaneously to the input stages of all ten oscillators, resulting in the measurement of their deviation sensitivities. The AMPLIFIERS switch served a similar function for calibration of the voltage gain of the signal-conditioning amplifiers. In this case, it was necessary that the TELEMETRY switch be in its OPR (operate) position so that the input line of each telemetry channel could be connected to the output line of its related signal-conditioning circuit.

To minimize the loss of battery operating time during the setup phases of the airborne program, separate toggle switches were installed for independent control of battery power supplied to the telemetry, reset receiver, bioamplifiers, and BCG accelerometers. The connector at the lower left of the front panel was used to terminate all circuitry external to the Biotelemetry Module which included the Frank ECG mixing network, the respiration rate transducer, and the angular accelerometer. The connector at the right independently terminated the ten output lines of the signal-conditioning elements and the ten lines of the telemetry oscillator units. In addition to serving a test point function, this connector, in conjunction with a mating jumper plug, allowed any signal-conditioning channel to be routed to any telemetry channel.

A photograph of the Biotelemetry Module as viewed from above is shown in Figure 5.2. The components mounted external to the unit include the three nickel cadmium batteries at the left; the cylindrically shaped telemetry transmitter and the three ECG preamplifiers at the top; and the telemetry oscillators at the right. Also seen are the test point jack, antenna connector, and tuning adjustment components of the Command Reset Receiver which was attached directly to the interior of the cover plate. The same top view of the Biotelemetry Module is shown in Figure

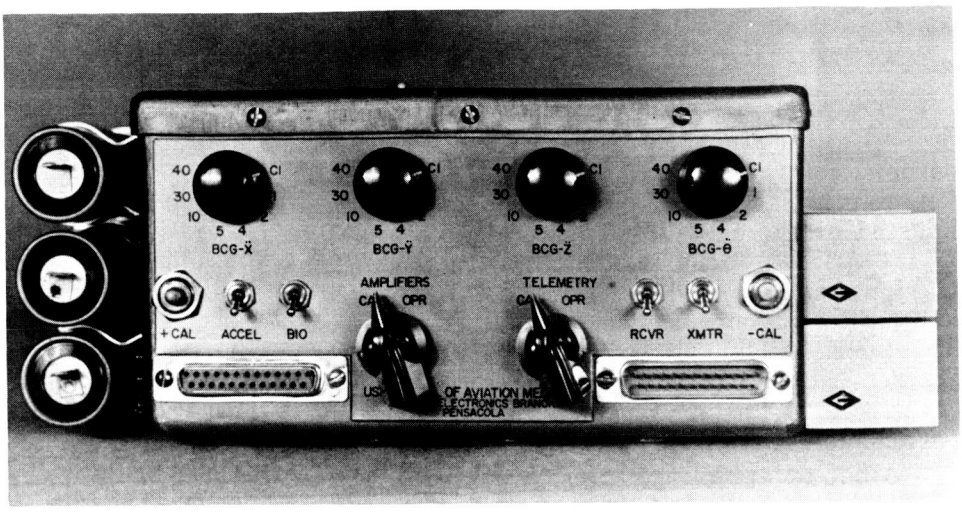

Figure 5.1 Front panel of the Biotelemetry Module showing the basic operator controls.

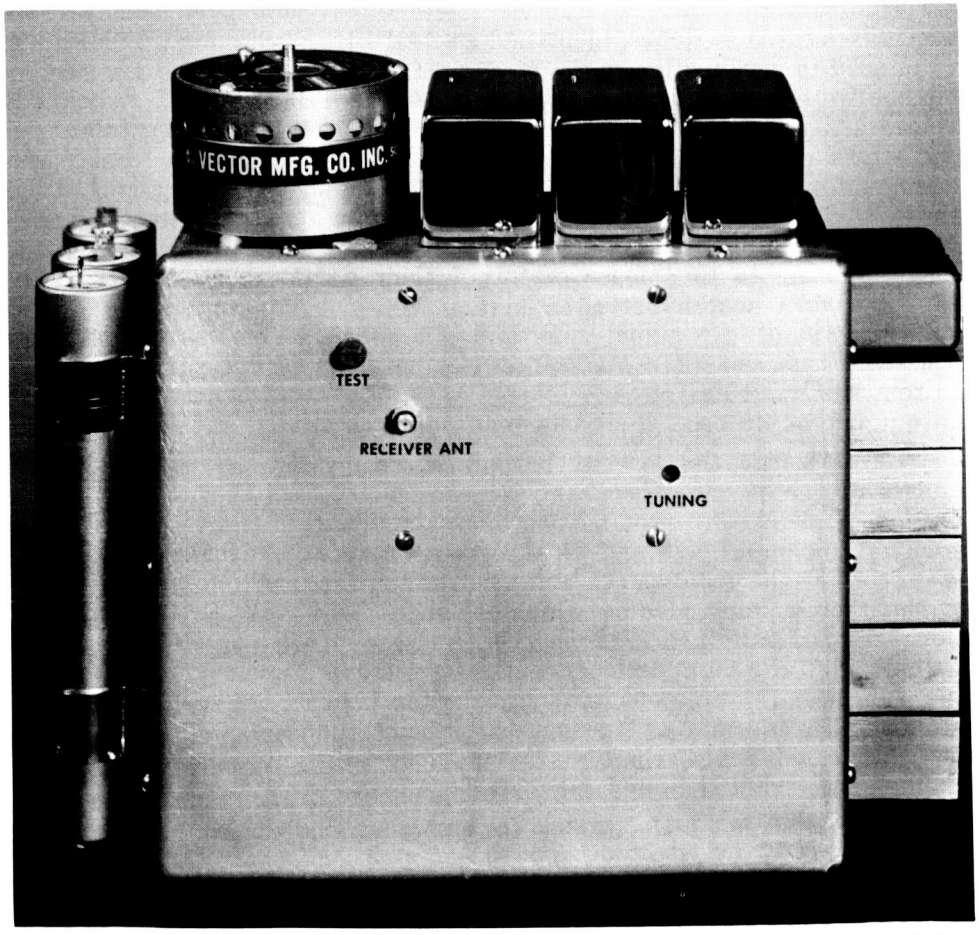

Figure 5.2 Top view of the Biotelemetry Module showing the three nickel-cadmium power sources at the left, the PM telemetry transmitter at the top left, the three ECG preamplifiers at the top right, and the voltage-controlled subcarrier telemetry oscillators at the right.

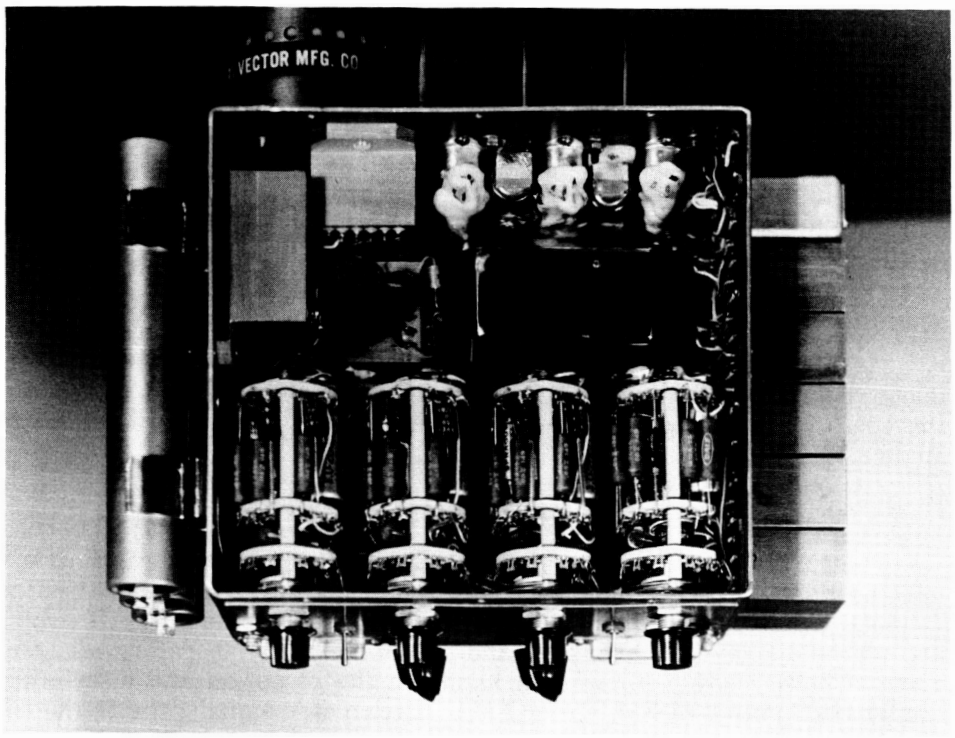

Figure 5.3 Top view of the Biotelemetry Module with its cover removed to show the location and configuration of the internal components.

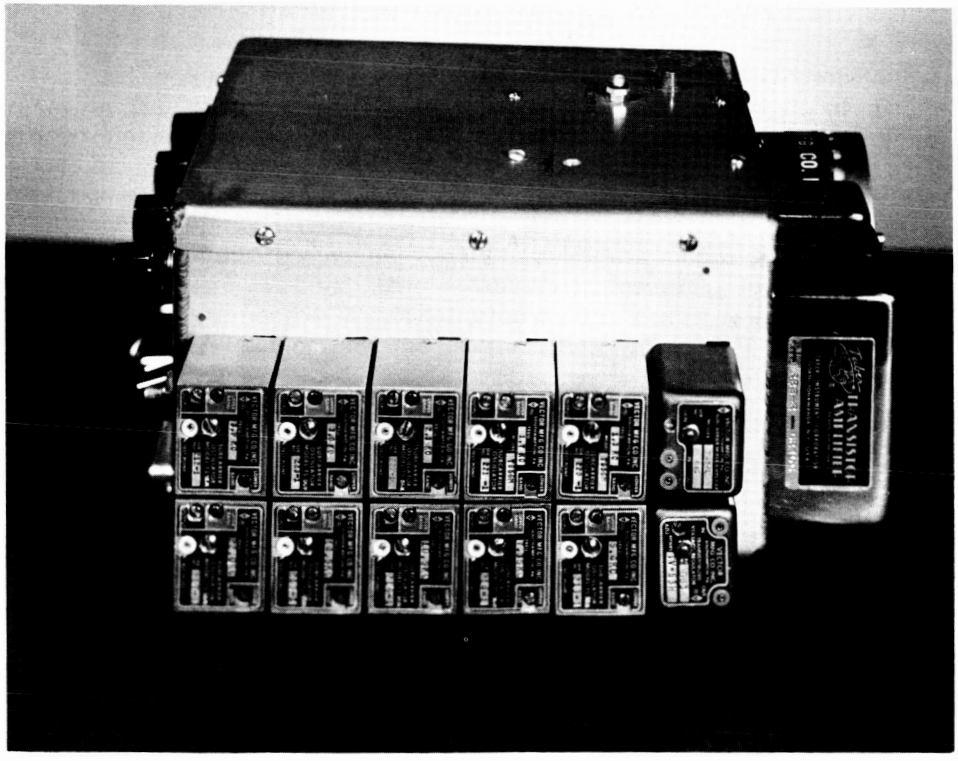

Figure 5.4 Side view of the Biotelemetry Module showing the layout of the voltage-controlled subcarrier telemetry oscillator components.

5.3 with the cover plate removed to show the location and configuration of the major components installed within the chassis. These components included the three orthogonally mounted accelerometers used to measure the linear acceleration BCG data which are at the upper left, the four switches and related feedback network components used to control the sensitivity of the BCG channels which are at the front, and the two mercury cells which served both calibration and voltage limiting functions at the rear. Along the right side may be seen the printed circuit board which terminated the wiring associated with the ten subcarrier oscillators. These units and their related voltage regulator and mixing amplifier may be seen in better detail in the photograph shown in Figure 5.4.

Description of the data telemetry transmitter and the individual telemetry measurements are presented in the following sections to describe the operational function and pertinent circuit details of the Biotelemetry Module.

DATA TELEMETRY TRANSMITTER

The function of this element of the Biotelemetry Module was to transmit the data derived from the Constraint Platform measurements to a Telemetry Receiving Station located aboard the KC-135 aircraft where it could be displayed in real time and stored for later laboratory analysis. Since airborne equipment was on hand for the reception and discrimination of IRIG standard FM/FM or FM/PM telemetry signals, the frequency division multiplex type approach was selected for the transmitting element of the radio frequency link. The primary advantage of this approach, aside from the resultant cost savings to the project, was the availability of multiple data channels with frequency characteristics adequate for the application.

A simplified schematic drawing of the telemetry transmitting link is shown in Figure 5.5. The output signals from the signal-conditioning amplifiers were separately routed to the input stages of the ten voltage-controlled subcarrier oscillators (VCSCO) via the telemetry calibration switch S1 and a silicon diode limit network. The frequency modulated output signals from these oscillators were resistively added together at the input of a mixer amplifier which then raised the composite video signal to a level sufficient to drive the phase modulation circuitry of the transmitter. Radiation of the resultant FM/PM transmitter output signal was established by a half-wave dipole antenna molded into the base of the Constraint Platform.

Each of the ten subcarrier frequencies was generated by a commercially available IRIG voltage-controlled subcarrier oscillator (Vector Manufacturing Company, Model TS-56M) which was factory modified for this project to provide improved modulation sensitivity and environmental temperature characteristics. Pertinent specifications for these units include a modulation sensitivity of ± 1.5 volts for ± 7.5 per cent deviation; a 1 megohm, ± 20 per cent input impedance; a maximum deviation from best straight-line linearity of 0.75 per cent; and special temperature compensation to maintain the output frequency constant to within ± 1 per cent of design bandwidth for any input signal level within its rating over the 0°C to 80°C temperature range. Each oscillator measured approximately 7/8" x 1 1/16" x 1 3/8", weighed 1.75 ounces, and housed top-mounted potentiometers for adjustment of its modulation sensitivity, maximum frequency deviation, and output level. Power to energize the units was obtained from

a single voltage regulator, packaged identically to the oscillators, which delivered a highly stabilized 14 VDC output.

The radio-frequency carrier was generated by an all transistorized, crystal-controlled, phase modulated transmitter (Vector Manufacturing Company Model TRPT-250) which operated at 253.8 mcs with a maximum power output of 250 milliwatts and a nominal peak deviation of 150 KCS. The unit weighed only 8 ounces and was powered from a single 24VDC supply with a maximum current drain of 80 milliamperes. Since precision of data quantification was one of the primary objectives of the project, the ability of this transmitter to operate with a frequency tolerance of ± 0.005 per cent and a total distortion of less than 1.5 per cent over the wide range of temperature, pressure, vibration, and shock extremes which could be encountered in the airborne environment was the most prominent criterion determining its selection.

Limiting circuitry at the input of each subcarrier oscillator was provided to prevent the loss of data due to cross-talk or adjacent channel interference effects which would result from excessive deviations produced by system overloads. The silicon diodes and mercury cells shown in Figure 5.5 prevented the input signal level presented to each oscillator from exceeding a fixed voltage whenever the related signal-conditioning amplifier

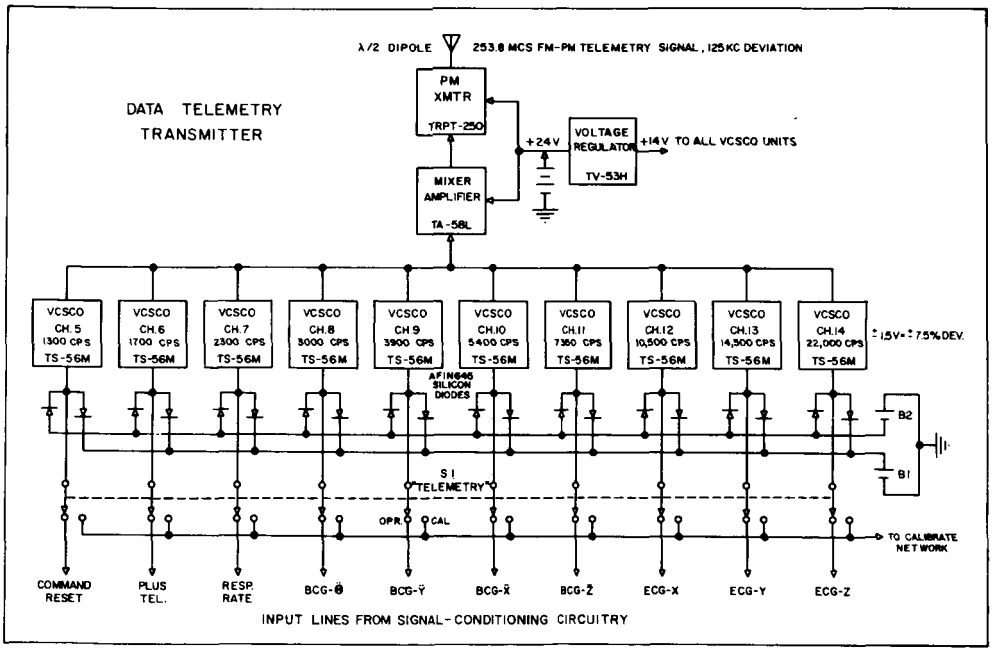

Figure 5.5 Block diagram of the FM-PM data telemetry transmitter component of the Biotelemetry Module.

was in an overloaded state. The series combination of the forward conduction voltage drop of the silicon diodes and the battery voltage limited the input signal of each oscillator to approximately ± 2.0 volts. This clipping level was such that the maximum frequency deviation of each oscillator could not rise above ± 10 per cent. The same batteries used to establish this clipping level also served as reference sources for calibration of the modulation sensitivities of the subcarrier oscillators.

AIRBORNE MEASUREMENTS

The pertinent circuit details of the eleven airborne measurement functions of the Biotelemetry Module are described in the following sections. The design criterion most common to all of these measurements was the need to optimize the signal-to-noise ratio capabilities of the system by providing signal-conditioning circuitry which could deliver a data signal of proper voltage and impedance level to drive the related subcarrier telemetry oscillator to its full deviation. For this particular telemetry system, full ± 7.5 per cent frequency deviation required the signal-conditioning circuitry to produce a data signal with a peak magnitude of ± 1.5 volts.

BCG-$\ddot{X}$, BCG-$\ddot{Y}$, and BCG-$\ddot{Z}$ Measurements

These three measurements served to record simultaneously the linear accelerations of the Constraint Platform along three orthogonal reference axes of the subject. The axis of sensitivity and the polarity convention (2) adopted for these measurements are as follows: BCG-$\ddot{X}$, transverse (side-to-side) body axis with accelerations toward the right considered to be of positive polarity so as to cause an upward deflection of a recording galvanometer; BCG-$\ddot{Y}$, longitudinal body axis with accelerations toward the head considered of positive polarity; and BCG-$\ddot{Z}$, dorsoventral body axis with accelerations toward the back considered of positive polarity.

The function of these measurements was to transduce the low-level BCG acceleration signals to an electrical form capable of satisfying the modulation sensitivity and frequency response characteristics of the telemetry subcarrier oscillators. Under idealized conditions, it would be desirable to have the over-all bandwidth of each BCG channel far exceed the expected frequency spectra of the data. The received data could then be analyzed in the laboratory and frequency weighing functions developed for optimal filtering and display. Since this approach was obviously not feasible, a compromise was necessary in the selection of the frequency response characteristics of the over-all system.

For the low end of the BCG spectrum, a 0.25 cps corner frequency with a 6 db/octave roll-off was selected as a design boundary for faithful reproduction of the low-frequency components of the BCG data. However, because of the lack of *a priori* data describing the potential acceleration artifacts in the BCG data which might be produced in the zero g environment, it was necessary that the system be designed to provide an operating mode whereby all components, including the transducer, would have a frequency response extending upwards from 0 cps. With this response, it would be possible to measure low-frequency, or static offset acceleration levels which might be superimposed on the dynamic BCG data. If these accelerations, which could be produced by such factors as a nonidealized state of weightlessness or the application of centripetal accelerations to the accelerometer as a result of the launch personnel imparting angular velocity components to the Constraint Platform at the time of its release into the free-flotation state, were of sufficient magnitude to preclude the collection of the BCG data, it was desired at least to quantify their magnitude and identify their source. If problems were encountered with system overloads produced by the g loads, the DC response would allow the recovery time advantages of direct coupling to be realized. In essence, the BCG measurement equipment was required to serve both trouble-shooting and data collection functions.

With the design philosophy that a transducer for any measurement should have a frequency response extending beyond the desired frequency

spectra of the data signal, with all frequency shaping determined by the signal-conditioning circuitry, an undamped natural frequency of at least 100 cps was established as a selection criterion for the accelerometer. It was desired also that the transducer have linearity, resolution, hysteresis, and noise properties adequate for accurate quantification of the BCG data. Since the telemetry components dictated the maximum signal-to-noise ratio attainable with the system, the noise requirements of the transducer were not stringent. Of more importance was the need for a transducer which would produce relatively large output voltages for low-level BCG acceleration inputs so that minimal amplification would be required to drive the telemetry channels to their full deviation capabilities. Since little time was available for either ground or airborne setup of the system, it was necessary that the transducer and its associated signal-conditioning amplifier not require any time-consuming balancing or calibration procedures to mantain its absolute acceleration accuracy, and that its calibration be independent of the actual voltage level of the battery power sources to be used to energize the system.

The 2.0 to 2.5 g acceleration level of the KC-135 aircraft which was encountered before each zero g profile required that the transducer withstand such an overload without alteration of its calibration accuracy. It was also necessary that the transducer and its associated signal-conditioning circuitry recover from this overload in a time much less than the experimental period so as to minimize the loss of data and that they be unaffected by vibration and pressure-temperature variations existing in the KC-135 aircraft during flight. Other essential characteristics included the ability to operate from the same plus and minus 24 volt DC power sources used to energize the other elements of the instrumentation and that the output be single-ended and operate about zero volts DC with no signal input.

The transducer selected to meet most of these requirements was a modified version of a standard, commercially available linear force-balance accelerometer (Donner Scientific Company Model 4310). The main elements of the transducer are a seismic mass, a position detector that senses displacements of the mass, a restoring coil located in a permanent magnetic field and physically attached to the seismic mass, and a high gain servoamplifier whose input is derived from the position detector and whose output drives the restoring coil. When an input acceleration is applied to the transducer, the resultant force tends to move the seismic mass. The position detector senses this movement and transmits a corresponding error signal to the servoamplifier. The servoamplifier then sends a feedback current through the restoring coil which produces a restoring torque that returns the seismic mass to its original null position. The voltage across, or the current through, a precision load resistor placed in series with the restoring coil then becomes an analog measure of the input acceleration. The unique feature of these accelerometers that results in many operational advantages is the near infinitesimal displacement of the seismic mass from its quiescent null position for all in-range levels of applied accelerations. With this closed loop mode of operation, the nonlinearities, hysteresis problems, temperature drifts, and changes in zero baseline of conventional open-loop accelerometers as a result of the mechanical characteristics of its displaced seismic mass system are greatly minimized.

Manufacturer's specifications for each of the accelerometers included a full-scale sensitivity of ± 0.25 g to produce a ± 15 volt output signal; a natural frequency of 100 cps with electrical damping set at 70 per cent

of critical; a resolution of better than 0.0001 per cent of full range; a non-linearity of less than 0.05 per cent of full range as measured with the best fitted straight line; a hysteresis of 0.02 per cent of full range; and a zero output of less than 0.05 per cent of full range. Factory modifications of the three BCG accelerometers included a ± 0.001 per cent per degree F temperature compensation; case alignment to within 1/4 degree of the true sensitive axis; standardization of the outputs of all three transducers to within ± 0.01 per cent; and operation from a ± 24 VDC supply.

The excellent noise characteristics of these accelerometers are demonstrated by the data presented in Figure 5.6. These data show the output signals produced by the three accelerometers used for the measurement of the airborne BCG data when placed in a relatively acceleration free terrestrial environment. The top row represents the noise output of each accelerometer under near normal display conditions. No visually perceptible deflection of the baseline occurs even though the gain is slightly greater than that used to display the flight data. In the bottom row of the figure, these signals are shown in greatly magnified form to demonstrate further the low-level noise characteristics of the transducers.

It should be noted that care has been taken not to attribute these noise signals solely to the transducer since the absolute noise level of an accelerometer can be measured only when it is placed in a motionless, i.e. acceleration free, environment so that the analog input signal is at truly zero level. During preliminary laboratory evaluation of these units it was determined that vibrations present in various building structures, due to their natural resonances or the operation of mechanical equipments such as air-conditioners, elevators, or small vehicles, generated acceleration signals far above the noise threshold of the transducers. The location finally selected for the measurement of the data shown in Figure 5.6 was on a concrete slab in an isolated farming community approximately 50 miles from the nearest major city. Even in this environment, it is most likely that the true noise level of the accelerometers is below that shown in Figure 5.6.

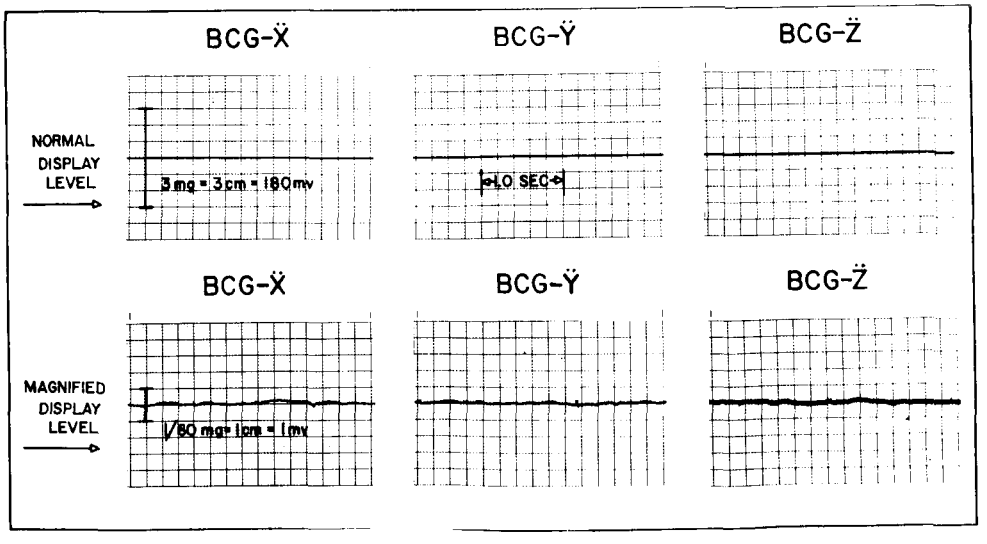

Figure 5.6 Laboratory data showing the low-level noise characteristics of the three linear accelerometers used for the collection of BCG flight data.

The output signal of each accelerometer was raised to telemetry level by a miniature chopper-stabilized DC operational amplifier. This commercially available unit (Donner Scientific Company, Model 3802A) utilized silicon solid-state circuitry with an internal 400 cps chopper drive in a package configuration similar to that used for the accelerometer. The essential characteristics of the amplifier include a typical open-loop gain of 500,000, a 3 db frequency response to 150 kcs, a maximum input current of $5x10^{-10}$ amperes, and a maximum drift of 150 microvolts per 10°C change over the 0°C to 65°C temperature range. The amplifier requires a ±24 VDC power source, can deliver 3 ma at ±15 volts, and weighs only 8 ounces. By utilizing the current output of the accelerometer to supply the input current to the amplifier, a system with excellent drift and gain stability characteristics resulted. A photograph of a single accelerometer and the matching operational amplifier is shown in Figure 5.7.

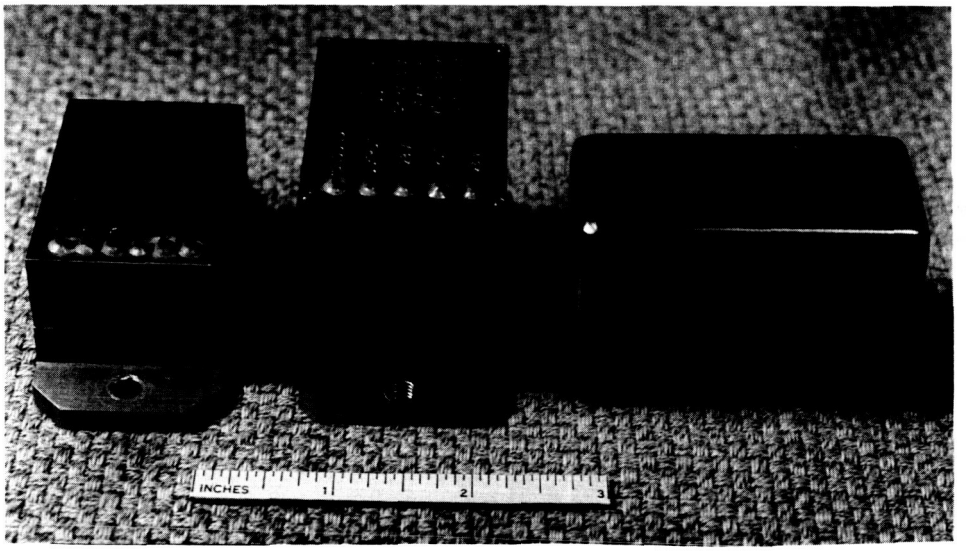

Figure 5.7 BCG Accelerometer (left) BCG Operational Amplifier (center) and ECG Preamplifier (right).

A simplified schematic drawing of a typical BCG channel is shown in Figure 5.8. The acceleration analog current signal developed by the accelerometer through its internal 20,000 ohm load resistor, RL, was directed to the current input terminal of the DC chopper-stabilized operational amplifier which was held at a virtual ground potential by the combined action of the feedback resistor R1 and the high open-loop gain of the amplifier. Precise control of voltage gain, proportional to the ratio of R1 to RL, with excellent stability characteristics resulted. The capacitor C1 connected across the feedback resistor R1 provided a 6 db/octave high frequency roll-off with a 40 cps corner frequency. In the actual circuit, a multiposition switch selected various combinations of R1 and C1 which allowed the system to be setup with polarity inverted voltage gains of 1, 2, 4, 5, 10, 15, and 20. With the 60 millivolt output per milli-g input sensitivity of the accelerometers and the ±1.5 volt input requirements of the telemetry oscillators, these voltage gains resulted in full scale acceleration sensitivities of approximately ±2.5, ±5.0, ±10.0, ±12.5, ±25, ±37.5, and ±50 milli-g.

The series combination of Zener diodes D1 and D2 and resistor R2 connected between the input and output terminals of the amplier limited

the maximum plus and minus excursions of the amplifier output signal when accelerometer overloads occurred. This action, initiated by the forward conduction of one diode and the backward conduction of the other diode prevented these amplifiers from being damaged by the gross overloads which would always occur during each zero g maneuver. The combination also served to minimize further the already low recovery time properties of the DC coupled operational amplifier. Resistor R2 served to protect the amplifier by limiting the current it delivered whenever the diodes were in their conducting states. The Zener potentials of D1 and D2 were such that the dynamic range of the amplifier was approximately ± 16.5 volts. Because of the extremely high back-to-back series resistance of these silicon units when in the nonconducting state, negligible shunting of the feedback resistor occurred when the amplifier was operated within its ± 15 volt dynamic range.

Three different coupling modes were made available to interconnect the output of the amplifier to the input of the telemetry subcarrier oscillator. For each of these modes, optimal system performance resulted when the amplifier gain was set to a value which produced a BCG signal with a peak-to-peak magnitude of approximately ± 1.5 volts at the input of the subcarrier oscillator. If the BCG signal was much less than this value, the data channel would have poor signal-to-noise ratio characteristics. If the BCG was greater than this value, distortion of data would occur as a result of exceeding the deviation sensitivity of the telemetry oscillator. For this overloaded case, the clipping action of diodes D3 and D4 in conjunction with the two 1.34 volt mercury cells limited the maximum excursion of the input signal to ± 2.0 volts. The resistor R4 served to protect the operational amplifier during this clipping action by limiting the current it could supply to the diodes. Since the resistance of R4 was much less than the input impedance of the telemetry oscillator, negligible attenuation of signals below ± 2.0 volts occurred.

In the first mode, established by jumpering terminals A and B, the amplifier was direct coupled to the telemetry oscillator. Then, if the dynamic BCG signals occurred about a true zero g level, the amplifier could be operated with high gain to permit the telemetry system to be driven to its full scale deviation, resulting in optimal signal-to-noise ratio characteristics. However, if the BCG signals were superimposed on an offset acceleration level, nonsymmetrical deviation of the oscillator would occur, resulting in clipping or even loss of the telemetered BCG data. By setting the gain of the amplifier to a lower value it would be possible to record the magnitude of the combined offset acceleration level and the BCG signal. Obviously the BCG data under these recording conditions would have poor signal-to-noise ratio characteristics. Yet, it would be possible to quantify the magnitude of these perturbation accelerations if they did occur and thus determine the possibility of using corrective circuitry or techniques to eliminate the artifacts. With the lowest gain setting available, this coupling mode permitted the measurement of peak-to-peak accelerations up to ± 50 milli-g.

In case these offset accelerations or similar artifacts exceeded ± 50 milli-g, a second mode of direct coupling was provided in the system. By jumpering terminals D and E as well as A and B (Figure 5.8) the input signal to the telemetry oscillator was derived from the junction of the R4-R5 voltage divider combination. This network provided a 10:1 attenuation of the amplfier signal so that offset accelerations up to 250 milli-g, the

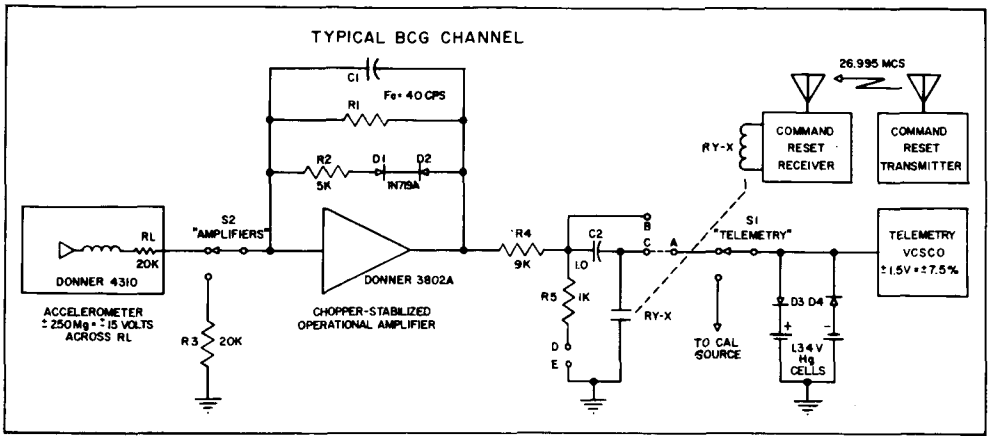

Figure 5.8 Simplified schematic drawing of a typical BCG measurement channel.

full scale sensitivity of the accelerometer, could be measured. In essence, these two coupling modes were required only if artifacts were encountered in the flight program which could make collection of the BCG data difficult or impossible.

The third mode of operation, established by jumpering terminals A and C, involved the capacitive coupling of the amplifier output to the input of the telemetry oscillator. The input resistance of the oscillator in combination with C2 provided a 6 db/octave low frequency roll-off at a corner frequency of 0.25 cps. Thus, if offset accelerations did occur, the resultant offset potential present at the output of the amplifier would not be presented to the input of the subcarrier oscillator as a result of the blocking action of C2. The gain of the amplifier could then be set to a much higher value than possible with direct coupling. This resulted in a better utilization of the deviation capabilities of the subcarrier oscillator and an attendant improvement of the signal-to-noise ratio characteristics of the telemetry channel.

With this approach, the extent of the offset accelerations which could be handled by the system was controlled only by the dynamic range of the amplifier proper. Since the Zener diodes D1 and D2 allowed the amplifier to operate in a linear fashion as long as its output signal did not exceed ± 16.5 volts, the dynamic range of the amplifier was approximately ten times that of the telemetry oscillator. Thus, assuming that the amplifier gain was adjusted to the peak-to-peak magnitude of the dynamic BCG signal (± 1.5 volts), the system could function properly in the presence of static offset acceleration levels up to ten times greater than the BCG signal. If this capability were not required, it would be possible to limit the amplifier output voltage proper to the ± 1.5 volt subcarrier oscillator level which would then eliminate the need for the telemetry limiting diodes D3 and D4.

Such a system might perform ideally in the laboratory, but the gross system overloads, which would always occur during each zero g maneuver before release of the Constraint Platform, would result in the loss of data due to the recovery time problems associated with capacitive coupling. Although the oscillator side of C2 was always held to within ± 2.0 volts of ground by diodes D3 and D4, the time constant of the system was considered to be too long compared to the relatively short free-flotation measurement interval expected for the flights. To allow the advantages of ca-

pacitive coupling to be realized without losing data as a result of recovery time problems, provisions were made to bring the oscillator side of the capacitor to ground potential momentarily by means of relay contacts RY-X. This relay, along with similar relays for each of the other BCG channels, was operated by a Command Reset Receiver installed inside the Biotelemetry Module. This receiver was actuated by a Command Reset Transmitter which was manually operated by an experimenter located in the flotation area of the aircraft. The function of this experimenter was to monitor visually the launch of the Constraint Platform during the zero g runs. When the zero g state was reached and at the instant the subject was released into the free-flotation state, this experimenter would momentarily key the Command Reset Transmitter which would then activate relay RY-X and return the oscillator side of C2 to ground. Since C2 was brought to its proper charge level by the amplifier current passed through the 9000 ohm resistor R4, a much lower time constant resulted than would have existed if the high input impedance of the telemetry oscillator were in the charging path. Thus, any static offset acceleration signals within the dynamic range of the amplifier could be removed immediately from the telemetry oscillator.

If these offset accelerations did not occur, either the direct or capacitive coupling modes of operation would be adequate for the collection of data. However, the need for the lower gain sensitivities of the amplifier was dictated by the requirement that the system serve a trouble-shooting function in case data collection problems were encountered in the flight portion of the program. The experimental approach planned for the flights was to utilize first the DC coupling mode without attenuation to determine if these offset accelerations did exist. If these measurements indicated that these offsets did not exist, BCG data collection would precede in this mode. If the data indicated that the offset accelerations were of appreciable level, the same mode would be used to identify their magnitude. If their level exceeded 50 milli-g, the direct coupling mode with 10:1 attenuation would be used for their quantification. For these cases, collection of BCG data would not be possible if the offset acceleration exceeded the BCG signal by a factor greater than ten. However, if it was found that offset accelerations were present, but less than ten times the BCG signal, the data would be collected in the capacitive coupling mode.

The complete schematic drawing of the actual circuitry for the BCG-$\ddot{X}$ channel is shown in Figure 5.9. The current output of the accelerometer was routed via switches S2 and S3 to the input of the operational amplifier. The function of S2, identified as the AMPLIFIERS switch, was to set the BCG and ECG signal-conditioning amplifiers for the in-flight checkout of gain sensitivity and DC offset level. Switch S3, identified as BCG GAIN, provided manual control of the voltage gain of the operational amplifier which in turn controlled the g sensitivity of the entire system.

When switch S3 was placed in its first position, the input of the amplifier was connected directly to the mercury cell calibration network via R12. With the 20,000 ohm resistance of R12 and the feedback resistor R1, the amplifier voltage gain was unity with polarity conversion. A calibration signal of ± 1.34 volts could then be applied to the amplifier by momentary activation of switches S4 and S5. Capacitor C1 shunted across R1 produced a 6 db/octave roll-off at the higher frequencies which cornered at 40 cps.

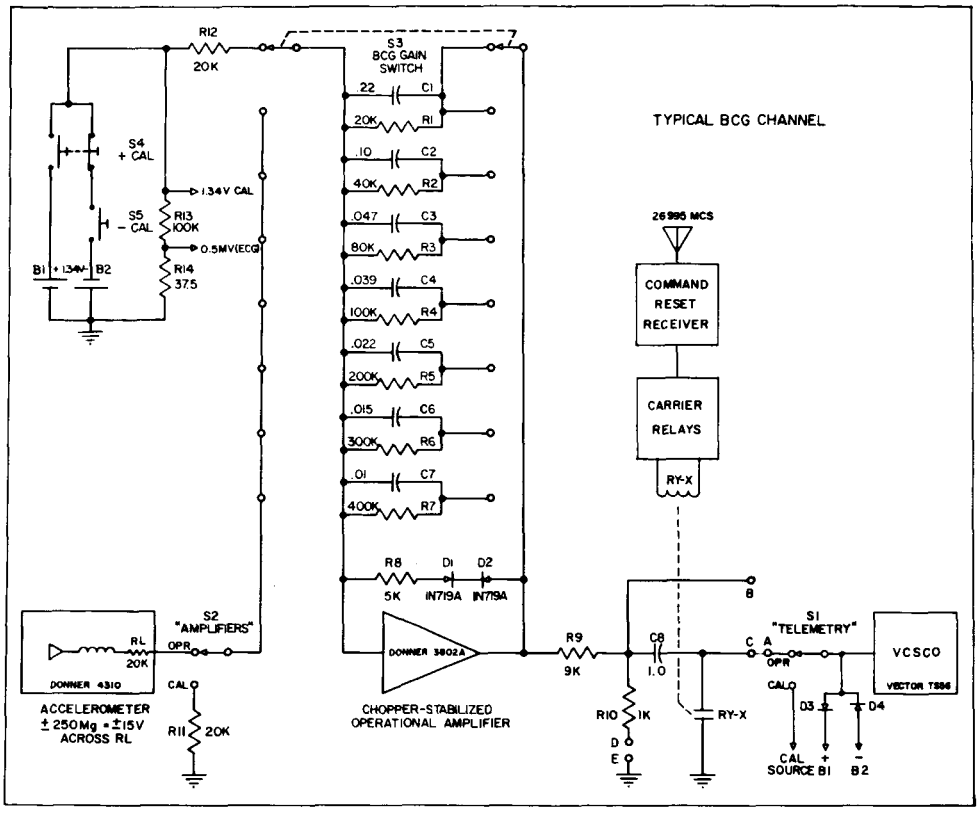

Figure 5.9 Detailed schematic drawing of the BCG-$\ddot{X}$ measurement channel.

When switch S3 was placed in any of its other positions, the input of the amplifier was connected directly to the arm of the switch S2. When S2 was placed in the "Calibrate" position, the amplifier input was returned to ground by another 20,000 ohm resistor R11. This feature allowed the DC offset level of the operational amplifer to be established for each position of S3. As determined during both the preflight checkout period and the actual flight operations, the excellent stability of the amplifiers resulted in negligible shifts in DC output level for variations either in supply voltage or ambient temperature.

When S2 was placed in its "Operate" position, the current input terminal of the amplifier was connected directly to the low end of the accelerometer load resistor RL, thus allowing the collection of the desired data. The acceleration sensitivity was determined by the feedback resistor selected by switch S3. All feedback resistors used in the system were precision wire-wound units with a ± 0.05 per cent tolerance.

BCG-$\ddot{\Theta}$ Measurements

The function of these measurements was to record sequentially the instantaneous angular acceleration of the Constraint Platform about the same three body reference axes as used for the linear acceleration BCG data. A single angular accelerometer, mounted on a support assembly which allowed its axis of sensitivity to be aligned with any of the three orthogonal body axes, served as the measurement transducer. The accelerometer was attached to the support assembly by quick-disconnect fasteners which permitted the axis of sensitivity to be manually changed within ninety seconds so that the triaxial angular acceleration BCG data

could be recorded sequentially during three successive zero g maneuvers of the aircraft.

As noted previously, the necessity for the sequential rather than simultaneous approach to the collection of these data was dictated by both the unknown nature of the variable to be measured and the lack of a commercially available transducer with optimal characteristics. Since angular acceleration BCG data had never been collected with a subject placed in a suspension system that allowed frequency independent motion with six degrees of freedom, the peak-to-peak magnitude of the BCG signals to be expected during the free-flotation state was not known. Thus the *a priori* selection of a transducer with optimal full scale sensitivity and natural frequency characteristics would be difficult. However, in order to obtain some preflight data on the potential magnitude of these signals, measurements were made in the laboratory of the cardiac-originated angular accelerations of the subject about his dorsoventral (Z) reference axis. The subject was placed in the Constraint Platform and the combination supported on a commercial air-bearing BCG bed (Astro Space Laboratories, Model ME 611R). The data collected in this manner obviously did not represent a true angular acceleration BCG signal because of the limited number of degrees of freedom permitted by the BCG bed. Yet extrapolation of the resultant data did indicate that a transducer with a full-scale sensitivity in the range of 1 to 5 radians/sec^2 might prove adequate for the flight program.

With the same design philosophy as used for the selection of the linear acceleration BCG transducer, it was desired to obtain an accelerometer with a frequency response extending far beyond the spectrum of the BCG data, preferably 100 cps or greater, that would have adequate sensitivity, accuracy, temperature stability, and low mass characteristics. Of particular importance was the need for a transducer of low mass so that the mass of the Constraint Platform and associated instrumentation would be only a small percentage of the mass of the subject.

As with the selection of most transducers, conflicts always exist between high sensitivity and low-mass requirements as well as high sensitivity and high natural frequency characteristics. For this application unbonded strain gauge and inductive type liquid rotor angular accelerometers of high sensitivity were not considered because of their excessive weight, varying typically from 5 to 8 pounds, and their low natural frequencies. The weight of rate gyro type devices and the low natural frequency characteristics of the chemical type transducers excluded these instruments.

A compromise solution was effected by selecting an angular accelerometer that operated on the same force-balance principle as the linear accelerometer. This accelerometer (Donner Scientific Company, Model 4525) had a 5 radians/sec^2 full-scale sensitivity, a natural frequency of 39 cps, was electrically damped to 0.7 of critical, and weighed 2 pounds. Because of the 6 pound weight penalty which would have resulted if three units were installed on the Constraint Platform and the fact that the flight tests might prove that instruments with different full-scale sensitivities would be required, it was decided to use only one transducer and to perform the triaxial angular acceleration BCG measurements sequentially. The principal disadvantage of this transducer was its relatively low natural frequency.

Signal-conditioning circuitry identical to that developed for the linear BCG measurements was used for collection of the angular accelerometer

data. The transducer was operated in its current output mode, and since its internal load resistance was 10,000 ohms as compared to the 20,000 ohm load of the linear accelerometers, the voltage gain of its associated operational amplifier was twice that available with the other BCG channels.

A photograph of the angular accelerometer in the lightweight triaxial mount which was attached to the Constraint Platform is shown in Figure 5.10. The mount, constructed of aluminum, was attached to the Constraint Platform behind the Biotelemetry Module. Three sets of orthogonally located tapped holes in conjunction with four extension screws permitted orientation of the accelerometer with its axis of sensitivity parallel to any of the three body axes. To reduce weight further, a light gauge aluminum cover was constructed for the accelerometer to replace the steel cover provided on the original unit. Identification of the actual BCG flight data was provided by BCG-$\ddot{\Theta}_X$, BCG-$\ddot{\Theta}_Y$, and BCG-$\ddot{\Theta}_Z$, nomenclature for the instantaneous angular accelerations of the Constraint Platform about the X, Y, and Z body reference axes, respectively.

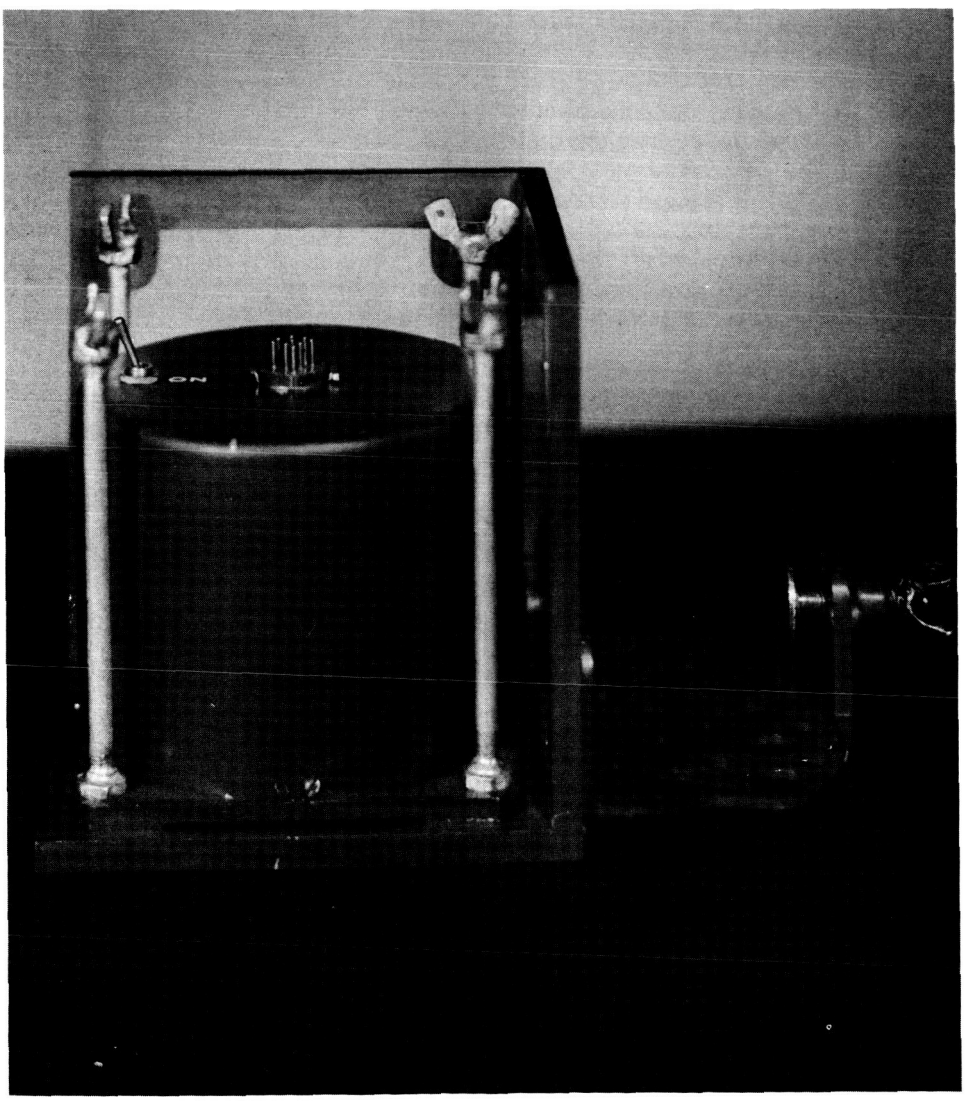

Figure 5.10 Angular accelerometer attached to triaxial mount assembly.

ECG-X, ECG-Y, and ECG-Z Measurements

A simplified schematic drawing of the circuitry used to measure the triaxial electrocardiogram is shown in Figue 5.11. A Frank lead system (1) involving eight torso electrodes and a resistive mixing network was used to derive the electrocardiogram potentials ECG-X, ECG-Y, and ECG-Z, where X, Y, and Z denoted the same body reference axes as used for the BCG measurements. To eliminate muscle potential artifacts attendant with limb placement of electrodes, the positions of the inactive right leg electrode G and the left leg electrode F used in the original Frank system were moved to the sternum and to the lower left quadrant of the abdomen above the inguinal ligament, respectively. A stainless steel mesh, held in place by adhesive backed moleskin tape and physically isolated from the skin surface by Bentonite clay and conventional electrode paste mixed to a putty-like consistency, served to establish low resistance electrical contact with the subject.

The differential output signals from the resistive network were routed through the AMPLIFIERS calibration switch S2 to the three solid-state differential input ECG amplifiers. These amplifiers (Taber Instrument Company, Model 228-2) were developed to the specifications of this activity for general purpose electrocardiographic applications. The voltage gain and output impedance characteristics of these amplifiers were selected to permit the related signal data to drive subcarrier oscillator telemetry systems with full-scale deviation sensitivities ranging from ± 1.5 to ± 5.0. volts. The output impedance characteristics were also sufficiently low to drive a 10,000 ohm load so that a medium frequency galvanometer recorder and an instrumentation tape recorder could be driven simultaneously without the need for additional signal-conditioning amplifiers.

Other features of these amplifiers included a high-frequency response to 75 cps and provisions for control of their voltage gain and low-frequency

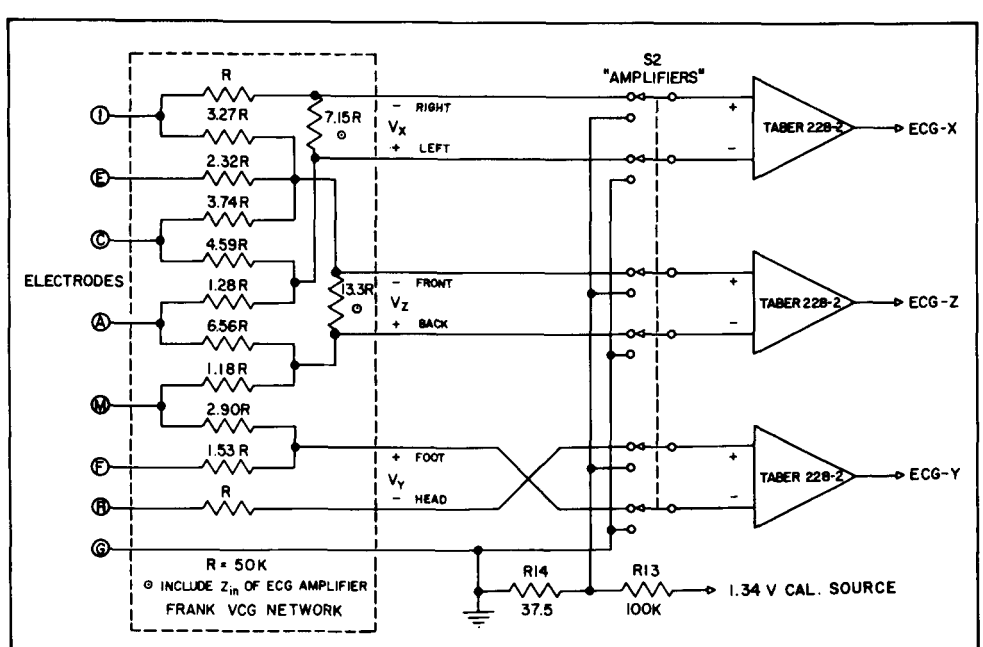

Figure 5.11 Simplified schematic drawing of the triaxial ECG circuitry.

response characteristics. By selecting an appropriate jumper at the amplifier connector, fixed voltage gains of 500, 1000, and 2000 could be made available. By eliminating these jumpers and using an external potentiometer, continuous gain adjustment between 500 and 2000 could be accomplished. Access to the internal coupling capacitor networks allowed the jumper selection of 0.75, 1.5, or 3.0 seconds time constants. A 1.5 seconds time constant was selected for adequate rendition of T wave changes.

As with the BCG amplifiers, the output of each ECG preamplifier drove a related subcarrier oscillator with coupling established through the TELEMETRY calibration switch S1. The + CAL and – CAL pushbutton switches, in conjunction with a resistive dividing network, applied either a 0.5 or 1.0 millivolt DC signal via switch S2 to the input of each amplifier for calibration of system gain.

Respiration Rate

The respiration rate of the subject served only as a trouble-shooting measure and was recorded by means of a transducer assembly clipped to the nostril. This assembly utilized a bead thermistor heated to approximately 200°C which measured the naris air flow. The bead was physically located in the naris air path so that inspiration flow gave a much greater output than the expiration flow. Thus time-amplitude recordings were obtained in which variations were a single function of rate rather than the double rate bipolar display received when the bead thermistor measured both inspiration and expiration flow. A photograph of the transducer assembly is shown in Figure 5.12. The unit was terminated in a miniature coaxial receptable mounted in the head area of the Constraint Platform.

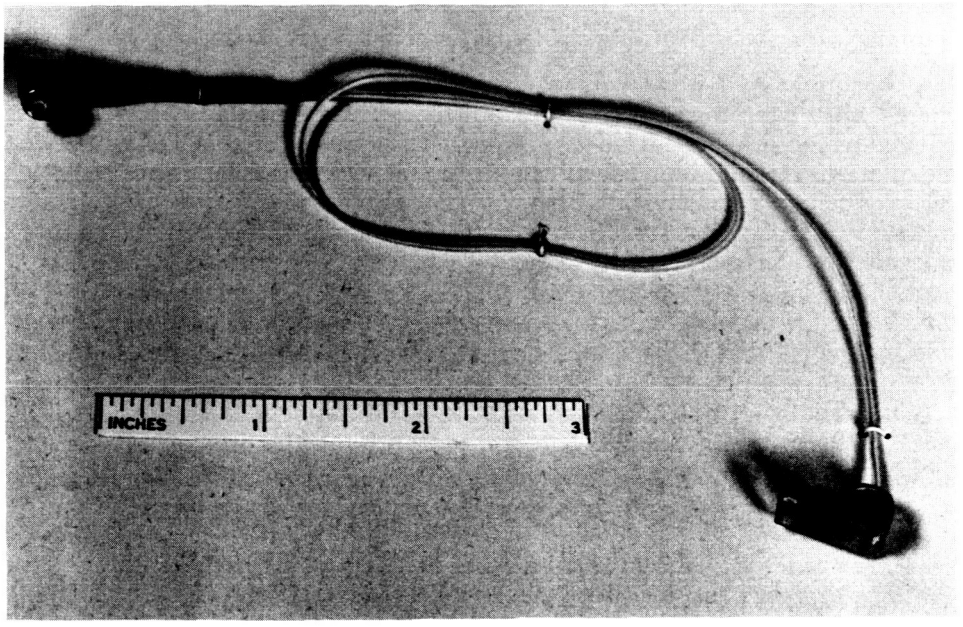

Figure 5.12 Respiration Rate Transducer.

A schematic drawing of the Respiration Rate Circuitry is shown in Figure 5.13 (right). The resistive network connected to the negative power supply was used to bias the output of the transducer to a level which allowed the full deviation of the assigned telemetry channel to be utilized.

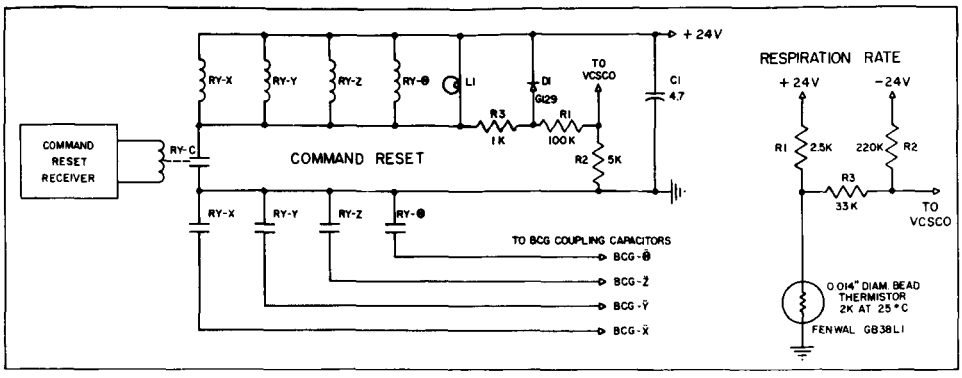

Figure 5.13 Simplified schematic drawings of the Command Reset Circuitry (left) and the Respiration Rate Circuitry (right).

This circuit set the telemetry channel to approximately −4 per cent deviation when respiration was suspended. When the respiration process was started, the rise in output voltage across the thermistor, due to its cooling by the naris air flow, swung the subcarrier oscillator deviation in the positive direction through 0 to approximately +4 per cent.

Command Reset System

A simplified diagram of the Command Reset Receiver System is shown in Figure 5.13 (left). The output of the superregenerative receiver activated relay RY-C which in turn energized the four subminiature SPDT relays RY-X through RY-⊖. As described in the BCG section of this report, the contacts of these slave relays were used to return the low side of BCG coupling capacitors to ground potential whenever overloads were expected.

A simple half-wave coaxial cable dipole antenna served to pick up the 27 MCS carrier frequency transmitted by the Command Reset Transmitter which was operated by an on-board experimenter. The 500 cps modulation signal from the transmitter activated the superregenerative receiver whose rectified pulse-modulated current output drove RY-C. The contacts of this relay then operated the four slave relays which were energized from the same 24 VDC supply used to power the telemetry transmitter. To allow the operation of this system to be continuously monitored, the voltage applied to the slave relays was telemetered to the console by means of another telemetry channel. This channel also served to determine the status of the telemetry battery. The Zener diode D1 allowed a scale expansion of this nominal 24 VDC voltage to permit the actual voltage level to be determined more accurately at the Telemetry Console.

Signal-Conditioning Battery Level

This channel monitored the output voltage of the 24 VDC battery used to supply positive operating voltage to the signal-conditioning amplifiers. Since the current drain on the positive battery was slightly greater than that used for the negative supply, this measurement indicated the battery condition.

Power Sources

The main power sources for the Biotelemetry Module were three nickel-cadmium cells rated at 24 VDC with a 180 mah life span. One cell was used to energize the 10 telemetry subcarrier oscillators, the volt-

age regulator, the mixing amplifier, and the telemetry transmitter. The other two cells were used to supply ±24 VDC to the four BCG transducers, the four BCG amplifiers, and the three ECG amplifiers. The characteristics of the BCG transducers and operational amplifiers were such that the output voltage level and calibration accuracies were relatively independent of actual supply voltage level over the 20 to 24 volt range. However, the DC output of the ECG preamplifiers was sensitive to the actual battery voltage level. This effect was minimized by using shunt Zener diode regulation to maintain the potential at the ECG preamplifier equal to approximately ±22 volts. Other power sources of the Biotelemetry Module included two 45 volt batteries to operate the angular accelerometer, two 1.34 volt mercury cells for the calibration circuits, and three identical 1.34 volt mercury cells for the Command Reset Receiver.

6. TELEMETRY RECEIVING STATION

The main elements of the on-board Telemetry Receiving Station comprised a Telemetry Console which housed the equipment necessary for the reception and discrimination of the FM/PM signal transmitted from the Constraint Platform; a multichannel light-beam galvanometer recorder for the real-time display of both the telemetry and hard wire data signals; a seven-channel magnetic tape instrumentation recorder for electrical storage of preselected measurement data; a Triaxial Aircraft Accelerometer for the measurement of the linear accelerations of the KC-135 aircraft along its roll, pitch and yaw axes; and a single channel heat-stylus type galvanometer recorder with a multipoint selector switch for rapid setup and checkout of the system during both ground and flight operations.

A photograph of the principal components of the Telemetry Receiving Station, as well as related ground checkout equipment, is shown in Figure 6.1. At the left is the Telemetry Console with the shock-mounted light-beam galvanometer recorder installed on top. In the center is the ground checkout rack which, as viewed from top to bottom, housed an audio-frequency oscillator, a monitor oscilloscope, a custom constructed battery charger for the nickel-cadmium batteries used to energize the Biotelemetry Module and Triaxial Aircraft Accelerometer equipment, a frequency counter, an AC vacuum tube voltmeter, and a blower for forced air ventilation of the rack equipment. On the right is the magnetic tape instrumentation recorder with the Triaxial Aircraft Accelerometer atop.

TELEMETRY CONSOLE

Photographs of the Telemetry Console as viewed from the front and rear are shown in Figures 6.2 and 6.3, respectively. For the rear view, a hinged access door has been removed to show details of the interior equipment and wiring. The basic housing for the unit was a standard 19 inch vertical rack enclosure with a reinforced base plate supported by nine individual shock absorbers that served to minimize the effects of aircraft vibration on the performance of the console equipment and to protect it from the shock loads encountered when landing the aircraft.

The switches mounted on either side of the name plate located at the very top of the console were used to control the tape recorder and to synchronize its operation with the 24 channel data display recorder. The equipment installed in the console as viewed from the top to bottom in Figure 6.2 includes the two discriminator panels which housed the ten individually metered phase-lock discriminators; the Data Patch Panel and associated controls for calibration of the system and individual adjustment of the sensitivities of the galvanometers installed in the 24 channel data display recorder; a multipoint switching panel used in conjunction with the single channel recorder; the FM telemetry receiver; the power supply that energized the discriminators; and a blower fan for forced air cooling of the interior equipment. Perforated blank panels are installed above and below the discriminator power supply to facilitate its forced air ventilation. It was important to mount the discriminators as far apart as possible from their power supply because of 60 cps noise interference generated by the relatively high-level magnetic field produced by the latter unit.

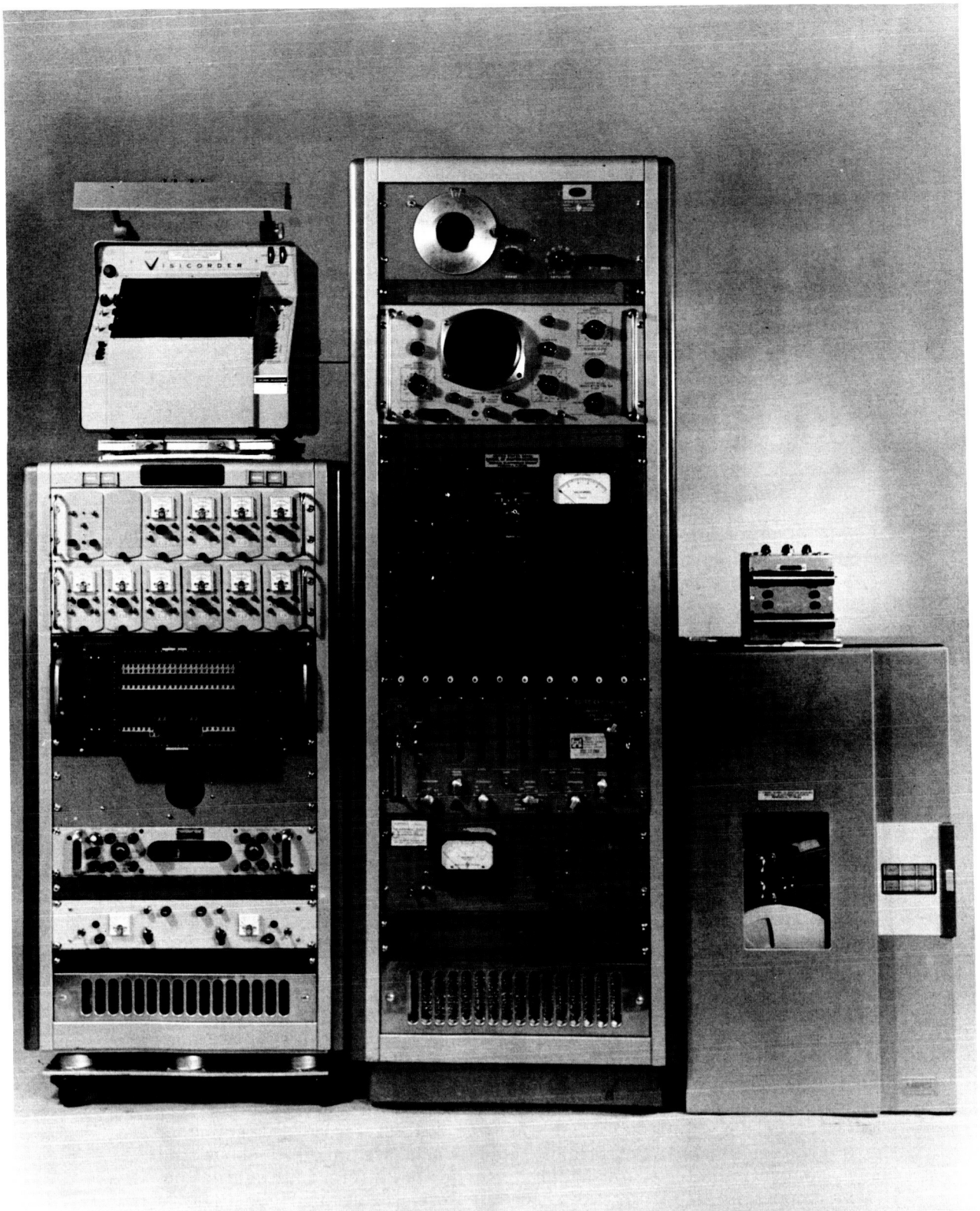

Figure 6.1 Principal components of the Telemetry Receiving Station and related ground checkout equipment.

Photographs of the front and rear views of the Data Patch Panel are shown in Figures 6.4 and 6.5, respectively. In the front view is shown the Data Patch Panel proper, a column of twenty miniature 10 turn potentiometers for setup of the data display recorder galvanometers, and a three unit switch panel allowing selection of a momentary or continuous type calibration signal of either plus or minus polarity to be entered into the Data Patch Panel. The photograph of the rear of this unit shows the various connectors used for termination of the telemetry receiver, discriminators, display recorder galvanometers, tape record and reproduce amplifers, calibration power supplies, and auxiliary control circuits and monitor equipment.

The over-all Telemetry Receiving Station served not only as an airborne center for collection of data but also as a laboratory tool for the preflight setup of the system and the postflight analysis of the data collected in the airborne environment. To permit the rapid interchange between these various modes of operation, the design of the entire station was centered about the Data Patch Panel which terminated all pertinent circuitry of the system. To outline the capabilities of the system, a pictorial view of the circuits available at the Data Patch Panel proper is shown in Figure 6.6. The panel is composed of 391 individually shielded and color-coded nylon circuit cells arranged in a 17x23 matrix with front panel interconnection established by shielded patchcords. Rear access is provided by 0.053 inch taper pins with soldered jumpers used to common or parallel desired cell combinations.

The top two rows of the Data Patch Panel cells terminated the output circuits of the discriminators which were calibrated so that a ± 7.5 per cent deviation of the input signal produced a ± 7.5 volt output signal. For discriminator #1, this signal was available on either A1 or B1 which were paralleled from the rear, the output of discriminator #2 was available at A2 or B2, *et cetera*. The output of each discriminator was reduced by a low-impedance voltage divider to make available a ± 1.5 volt output signal (C and D rows) for a ± 7.5 per cent input deviation in order that the tape recorder and galvanometers could be driven at the same level.

The plus and minus polarity terminals of 20 galvanometers were brought directly to the Data Patch Panel and made available at the E and F cell rows. By jumpering either side of a galvanometer to the ground cells located in row G, a change of display polarity could be readily accomplished. The other end of the galvanometer was patched to the output of a signal-conditioning resistive divider network (available in row H) which provided both proper galvanometer damping and the selection of three fixed sensitivities. By patching the related discriminators into row I, J, or K, galvanometer display sensitivities of either 1, 2, or 4 volts per inch deflection could be selected.

Access to the inputs of the seven record amplifiers of the instrumentation tape recorder was made available at cells N1 through N7 and cells O1 through O7. The outputs of the seven reproduce amplifiers were made available at cells N17 through N23 and O17 through O23. The high sides of the amplifiers were in the N row and the low or ground sides in the O row. Input and output video circuitry associated with the telemetry receiver and discriminators was terminated in the bottom two rows, P and Q, with the high sides on P and low sides on Q. Circuits for the connection of oscilloscope, counter, and oscillator equipment used in the setup and calibration of the system were also terminated in these rows. Rear panel

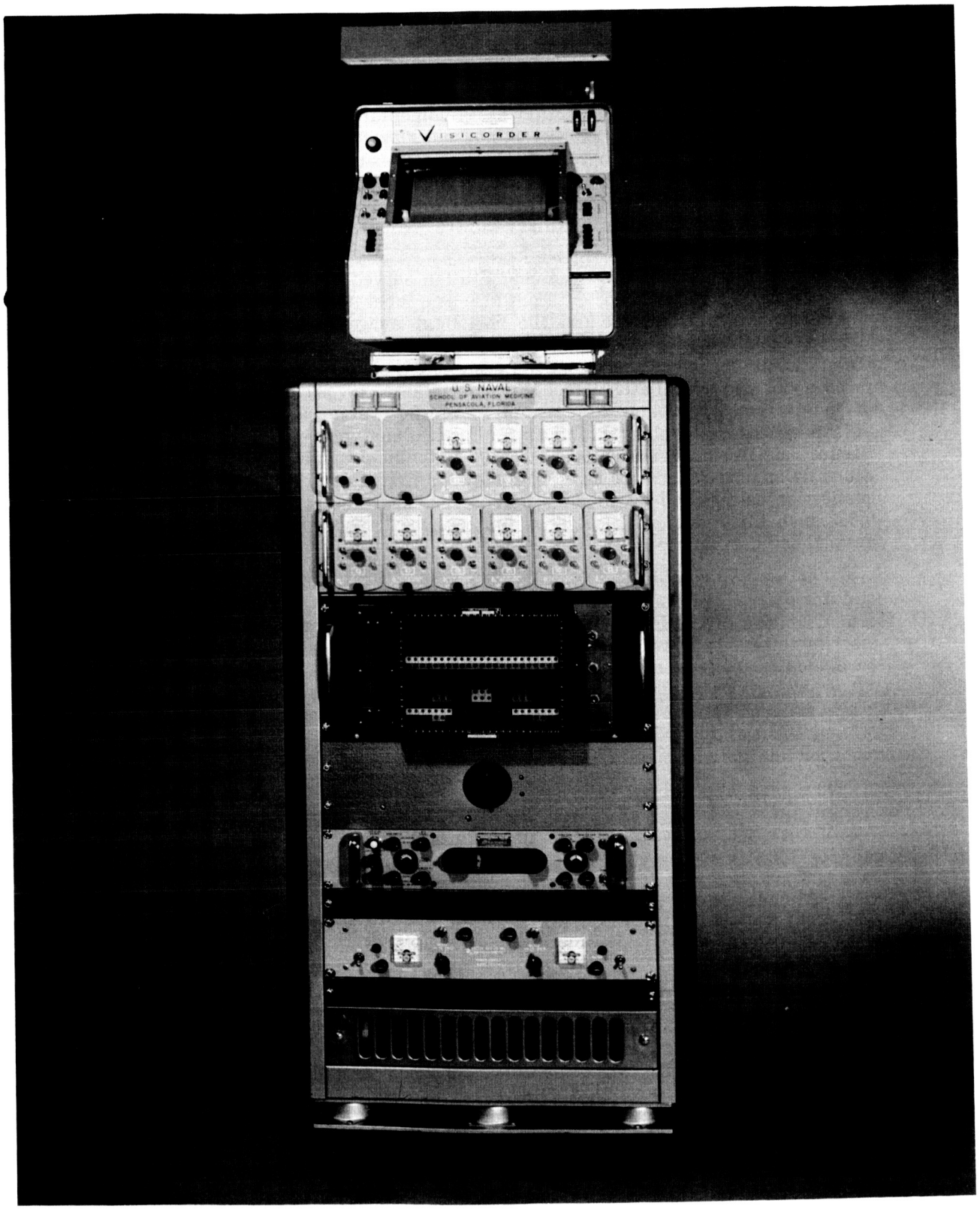

Figure 6.2 Front view of the Telemetry Console.

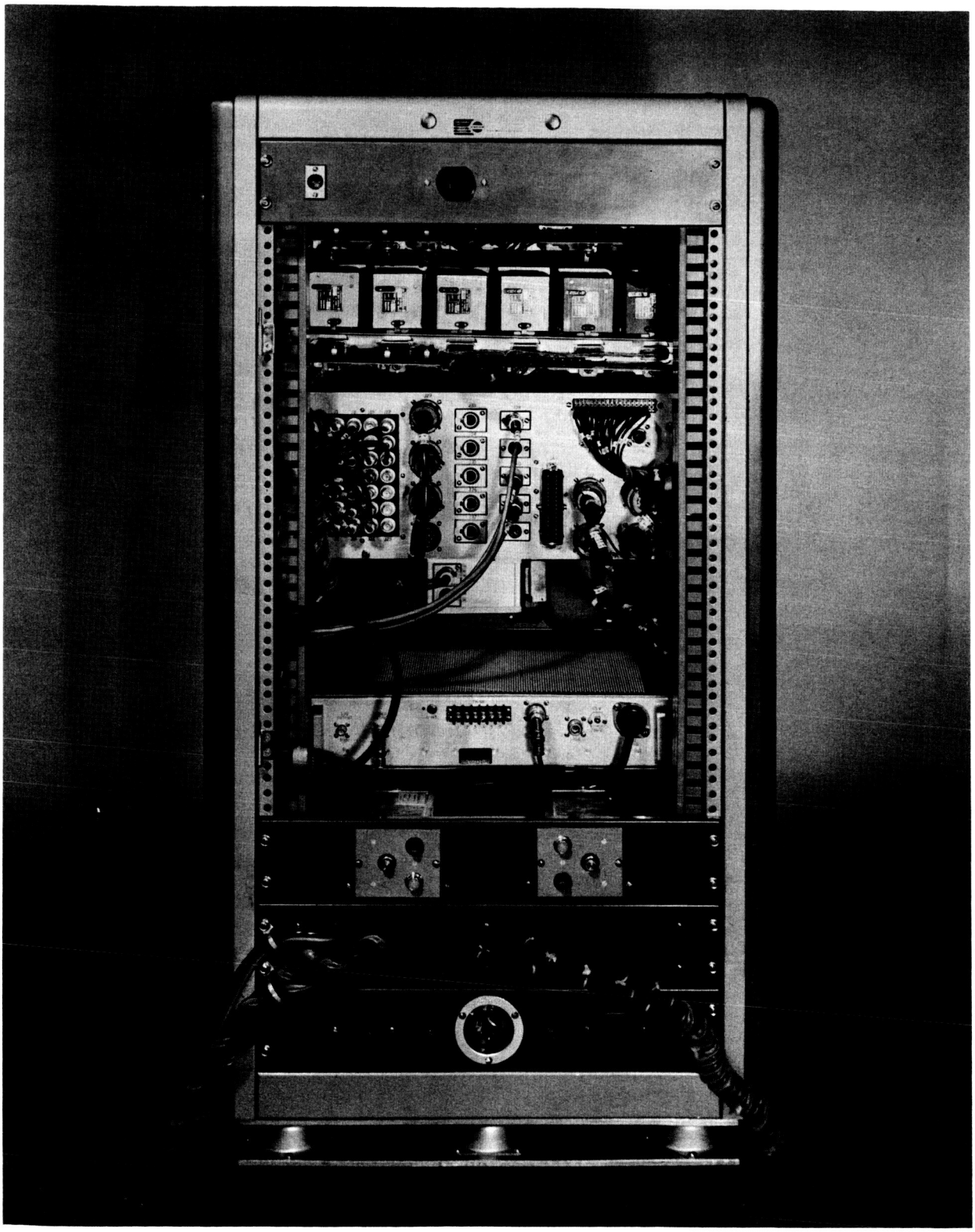

Figure 6.3 Rear view of the Telemetry Console.

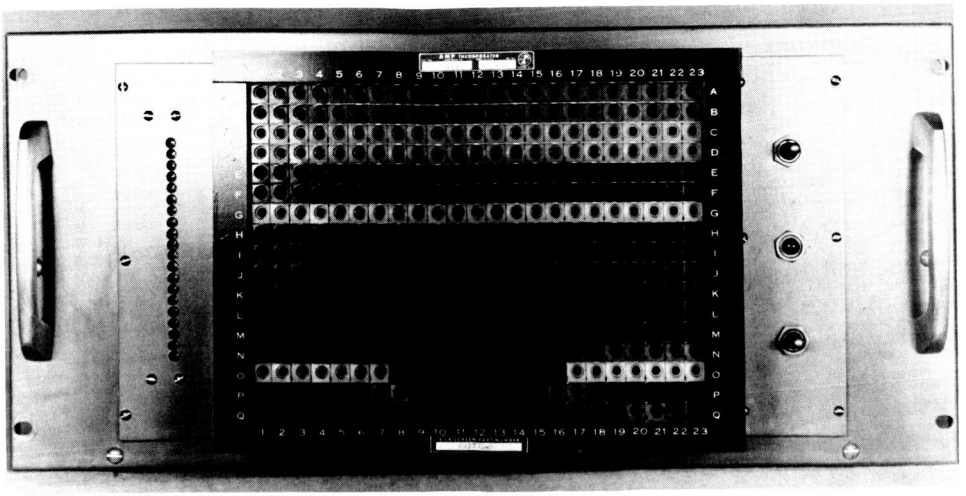

Figure 6.4 Front view of the Data Patch Panel.

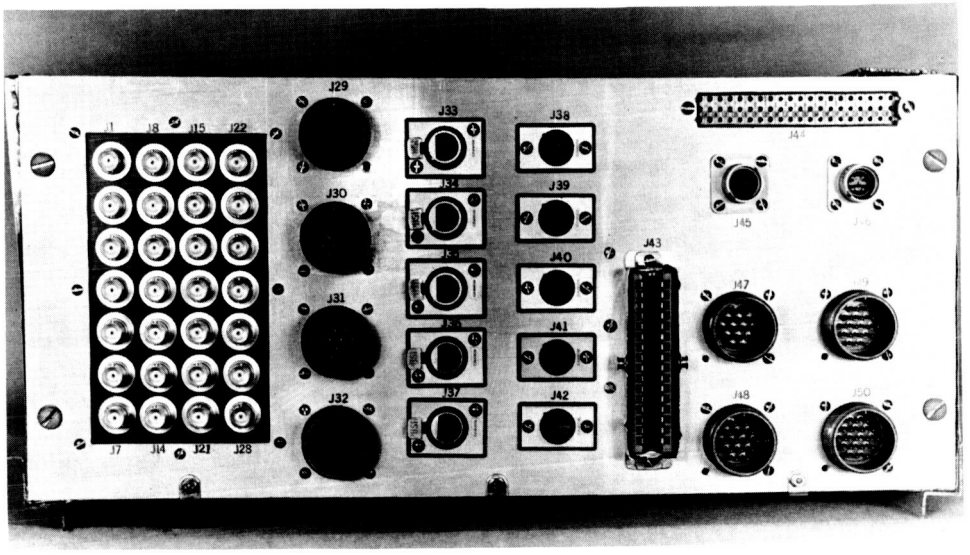

Figure 6.5 Rear view of the Data Patch Panel.

access to these cells was accomplished by means of BNC receptacles. The discriminator circuits available for compensation of tape speed error were made available in the cell group bounded by the L11, L13, M11, and M13 cells.

The cells at the top right of the Data Patch Panel terminated the power supplies installed at the rear of the console. These supplies were used to furnish precise reference voltages for calibration of the system. Cells N8 through N16 and O8 through O16 served to terminate the input circuitry to the multiposition switch associated with the single channel monitor recorder. The remaining cells terminated other basic equipment and served as commoning blocks for multicell interconnections.

TELEMETRY RECEIVER AND DISCRIMINATORS

A Nems-Clarke Model 1907 compact surveillance receiver was used for reception of the 253.8 mcs telemetry data. The receiver was fed from a half-

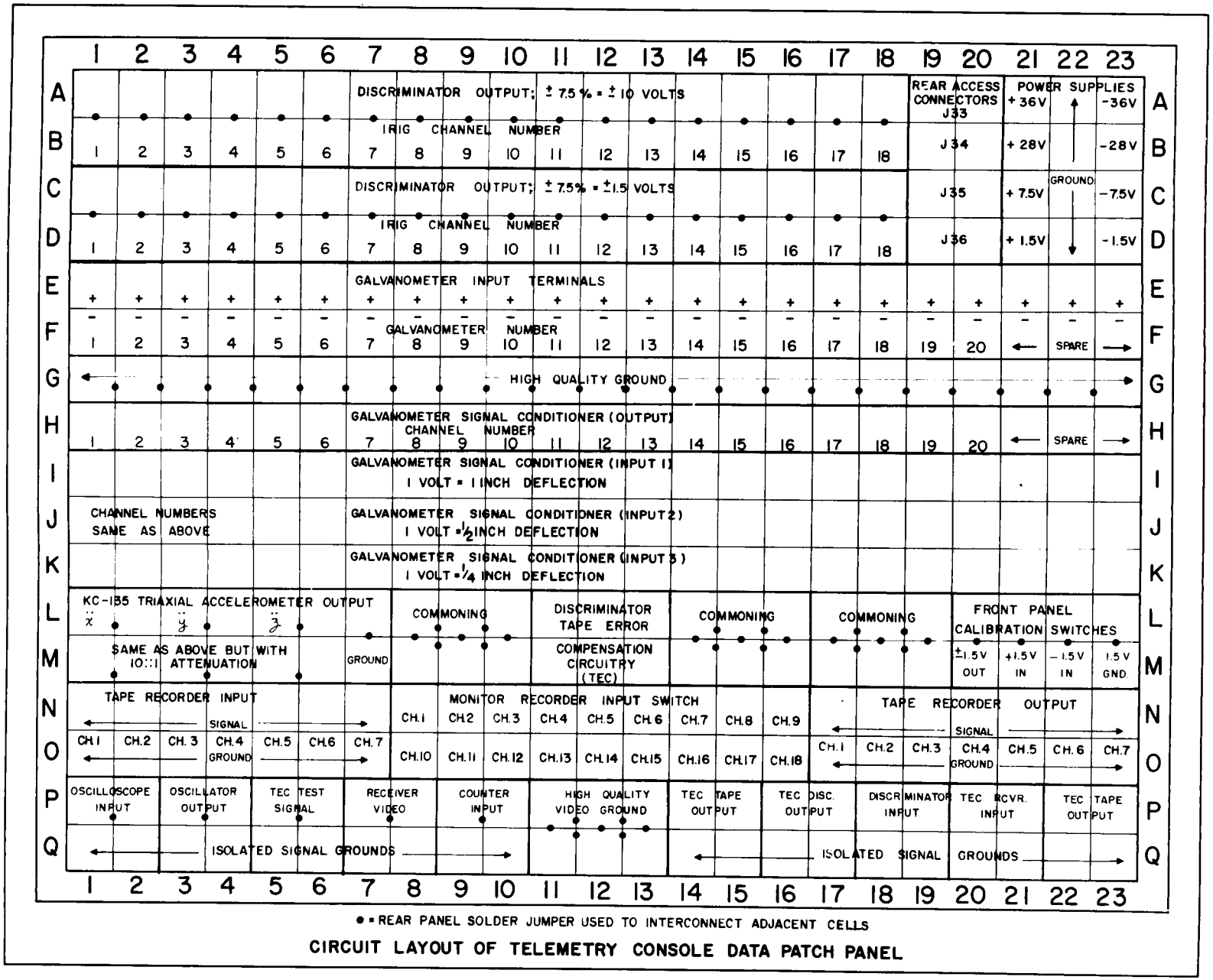

Figure 6.6
Pictorial view of the Data Patch Panel showing the various circuits and equipment terminated at this unit.

wave dipole antenna mounted in the overhead of the aircraft at the center of the free-flotation area. The pertinent specifications of the receiver include a selector switch controlled IF bandwidth that was set to 300kc; video response from 50 cps to 100 kc at the 3 db points; and an unbalanced 600 ohm video output capable of producing 0.774 volts rms with a 4 microvolt input, 100 kcs deviation, and a 1 kcs modulation frequency.

The multiplexed composite telemetry signal output of the receiver was routed through the Data Patch Panel to the paralleled high impedance input circuitry of the 10 discriminators. These units (Vector Manufacturing Company, Model GD-10B) were of the phase-lock type with standard IRIG constant amplitude output filters. Pertinent specifications include an output voltage linearity with respect to frequency input to within ± 0.1 per cent of the ideal over the full bandwidth; a ± 0.5 per cent stability of full bandwidth in a four hour period after a thirty minute warm-up; an intelligence frequency response flat to within ± 0.5 db for an IRIG standard modulation frequency with a modulation index of 5; a 150,000 input impedance; and an output of ± 10 volts at ± 10 milliamps with full deviation.

The output of each discriminator was terminated at the Data Patch Panel where it was routed to the display and tape storage recorders. A meter indicator on the front panel of each discriminator allowed visual monitoring of the input and output signal levels. Controls on the same panel were available for adjustment of input signal level, center frequency, DC amplifier balance, and deviation sensitivity.

DATA RECORDERS

The main on-board recorder used for the real-time display of the flight data was a 24-channel light beam galvanometer type photographic recorder (Heiland Model 1104). The isolated input circuitry from 20 galvanometers installed in the recorder was routed to the Data Patch Panel where 20 independent resistive networks provided the damping required by each galvanometer and allowed for the independent adjustment of the deflection sensitivity of each display channel. The Data Patch Panel arrangement of this network in conjunction with the nominal 50 ohm coil resistance, 200 cps undamped natural frequency, and 25.5 microampere per inch deflection sensitivity characteristics of each galvanometer allowed the operator to select channel sensitivities of either, 1, 2, or 4 volts per inch deflection with a frequency response flat to within ± 5 per cent at 120 cps.

Operational features standard to the recorder included adjustable chart speed and time lines, amplitude grid lines, and photographic superposition of numerical digits on the chart paper to identify each test. A latensification lamp assembly located at the top of the recorder permitted the flight data to be viewed in real time with minimal development time. The unit was also equipped with a removable amber light shield which could be placed over the exposed portions of the chart paper. Thus the flight data were made visible in increased black and white contrasts offered by laboratory type chemical development procedures.

Pushbuttons at the top of the console synchronized the actuations of the chart motor drive of this recorder with the record operations of the recorder used for storage of the data. The latter unit was a portable 7-channel magnetic tape recorder/reproducer (Ampex Corp. Model CP-107) equipped with one direct AM channel and six FM channels. The direct channel was used to record the composite output signal of the telemetry

receiver which contained all of the telemetry information. By directing the playback signal of this channel through the discriminators, the telemetry data could be reproduced in the laboratory in case of malfunction of the on-board display recorder. Because of the signal-to-noise ratio limitations of wide-band direct-recording systems, this channel served only as a backup in case of loss of the display recorder data.

The other six channels of the recorder were used to store the analog output signals of the discriminators associated with the BCG-$\ddot{X}$, BCG-$\ddot{Y}$, BCG-$\ddot{Z}$, ECG-X, ECG-Y, and ECG-Z measurements. With the flexibility of the Data Patch Panel, data from other measurement channels could be stored by simple interchange of patchcord assignments. With the 30 ips tape speed used for the airborne data collection operations, the frequency response of the direct channel extended from 100 to 50,000 cps at the 3 db points while the response of the FM channels extended from DC through 10,000 cps at the 3 db point.

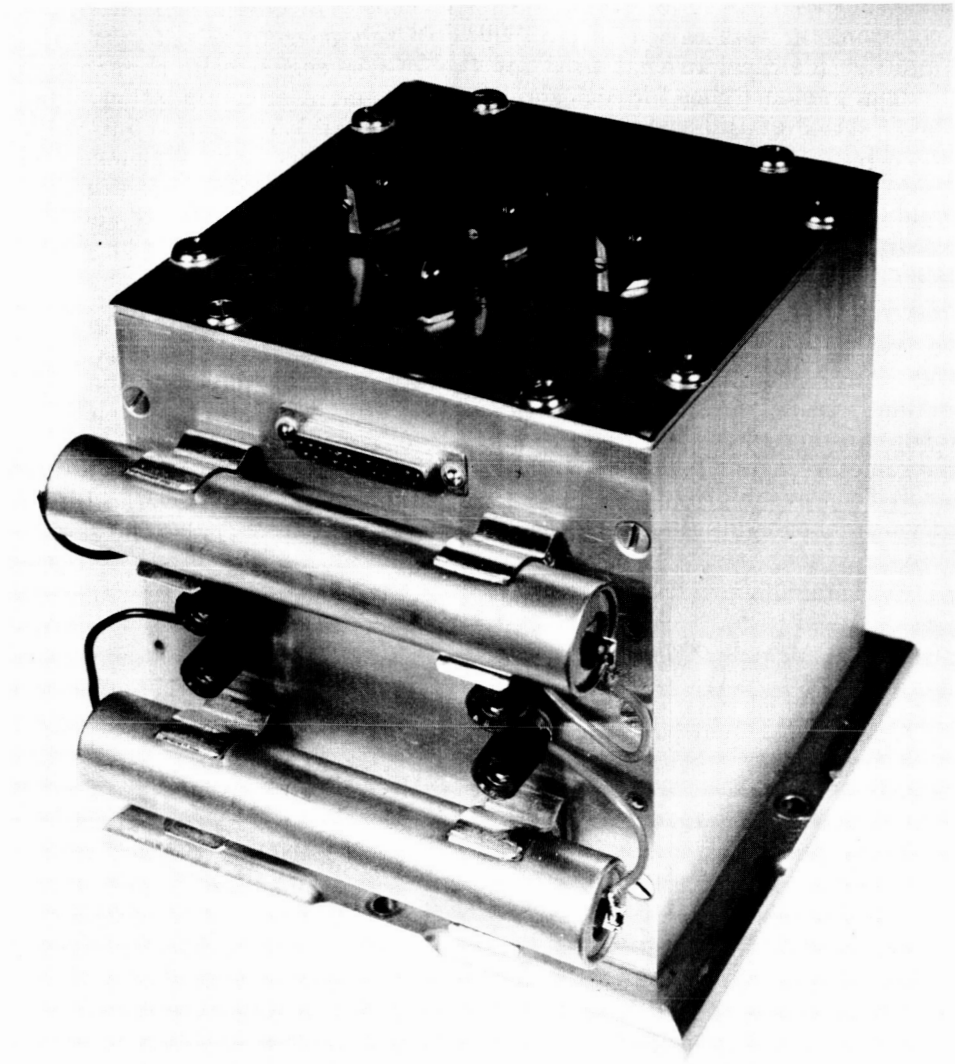

Figure 6.7 Triaxial Aircraft Accelerometer used to measure the linear accelerations of the KC-135 aircraft along its roll, pitch, and yaw axes.

As noted previously, the third on-board recorder was a single channel heat stylus galvanometer unit which was used for setup of the system. A multiposition selector switch mounted on the Telemetry Console and terminated at the Data Patch Panel allowed the individual monitoring of the output signals derived from the 10 discriminators as well as the output from the Triaxial Aircraft Accelerometer.

TRIAXIAL AIRCRAFT ACCELEROMETER

A photograph of the instrument constructed to quantify the acceleration profile of the KC-135 during its zero g maneuvers is shown in Figure 6.7. This unit, identified as the Triaxial Aircraft Accelerometer, measured simultaneously the linear accelerations of the aircraft along its roll, pitch, and yaw axes with the resultant output signals designated as $\ddot{x}$, $\ddot{y}$, and $\ddot{z}$, respectively. The transducers used to collect these data were three orthogonally mounted force-balance type linear accelerometers with a full-scale sensitivity of ± 15 g to produce ± 15 volts. The current output of each accelerometer was raised in level by a DC chopper-stabilized operational amplifier identical to that used for the BCG measurement channels. Individual gain switches for each accelerometer-amplifier combination allowed the selection of full-scale acceleration ranges of ± 1.5, ± 2.5, ± 5.0, ± 10.0, or ± 15.0 g with a choice of either a 25 cps or 2.5 cps upper frequency roll-off at a 6 db/octave rate based upon a filter network with a constant gain bandwidth product. The higher g sensitivities were included to facilitate application to acceleration environments produced by vehicles or devices other than the KC-135 aircraft.

The unit was installed inside the aircraft at the Telemetry Receiving Station location and its output routed to the L1 through L6 cells of the Data Patch Panel. The $\ddot{x}$, $\ddot{y}$, and $\ddot{z}$ signals were then displayed on the multichannel optical recorder. When the data were to be stored in electrical form, the signal was routed through a voltage divider to make the accelerometer output level compatible with the 1.5 volt tape recorder input level. To prevent ground loop problems, the unit was self-powered by two 24 volt nickel-cadmium cells identical to those used to energize the Biotelemetry Module.

7. DATA COLLECTION PROCEDURES AND NOMENCLATURE

PREFLIGHT PREPARATIONS

Laboratory Phase

Upon completion of the Constraint Platform and its associated instrumentation, the entire system was passed through a series of composite tests to evaluate its over-all performance. During these laboratory tests, the subject was placed in the Constraint Platform which was supported directly on the upper bearing of the commercial air-bearing BCG bed previously mentioned. The entire system was activated and the measurement data telemetered to the Telemetry Receiving Station where they were displayed on the photographic recorder and stored on the magnetic tape recorder. The signals present at the output of the BCG and ECG signal-conditioning amplifiers were also recorded simultaneously with their telemetered counterparts to ensure that the telemetry link did not introduce significant phase or amplitude distortion of the data.

The function of these tests was to determine the gain and drift stability characteristics of the signal-conditioning amplifiers as well as the linearity and deviation stability of the telemetry oscillators and discriminators. The tests also served as training sessions for the subject and experimenters who would be aboard the KC-135 aircraft during its flight maneuvers. Emphasis was given here to coordinating the efforts of the experimenter responsible for setup of the Constraint Platform equipment with the duties of the experimenter responsible for display and storage of the data at the Telemetry Receiving Station. By placing the subject in the Constraint Platform for several hours at a time, it was possible to detect and eliminate pressure spots within the contoured couch which could lead to discomfort during the flights.

To familarize the subject with the weightless environment, arrangements were made for him to serve as an observer on several zero g flights of a C-131 aircraft. During the zero g maneuvers of the aircraft, he was allowed to free-float to obtain a feel for the environment. These flights, as well as vestibular tests performed in the laboratory, established that the subject was not susceptible to air or motion sickness.

Field Phase

For implementation of the actual airborne operations, a field laboratory was set up in a building on the flight line adjacent to the KC-135 aircraft hangar. The laboratory housed equipment for ground checkout of the system, an automatic chemical developer for the airborne data collected with the on-board photographic recorder, and personnel support supplies. At the same time as the equipment was installed in the aircraft, the flight personnel went through a program of indoctrination to the KC-135 aircraft relative to their operational responsibilities, survival lectures, parachute and bail-out training, water ingress practice, and a flight physical examination.

A photograph of the actual installation of the Telemetry Receiving Station in the KC-135 aircraft is shown in Figure 7.1. The aluminum angle frame on the left supported the Telemetry Console by means of shock absorbers located at each side and the bottom of the unit. The multichannel light-beam galvanometer recorder, the single channel direct-writing recorder, and the Triaxial Aircraft Accelerometer are shown at the top of

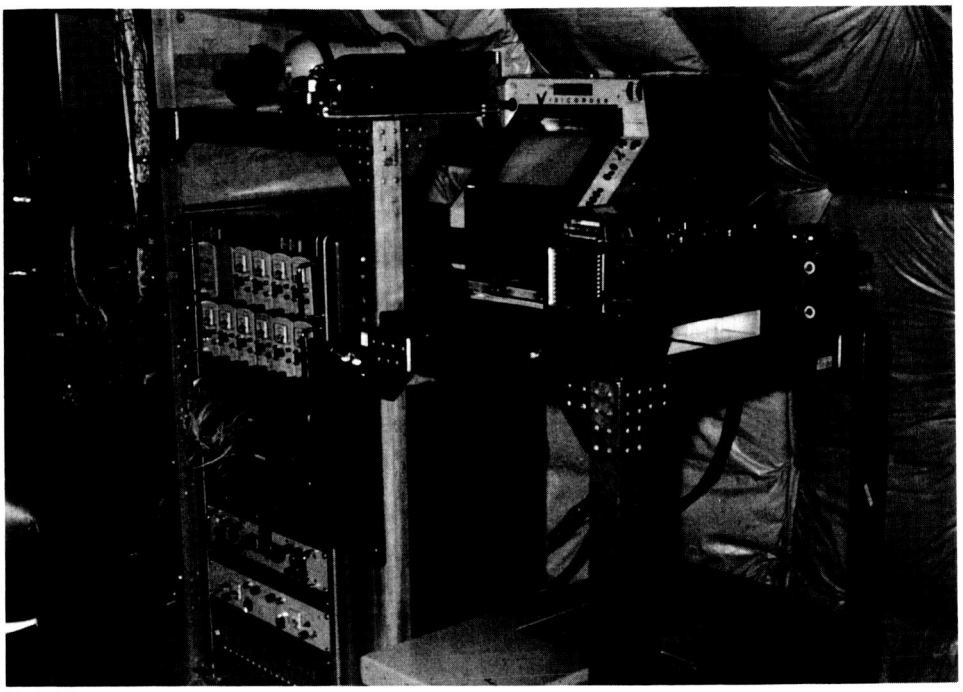

Figure 7.1 Telemetry Receiving Station as installed in the KC-135 aircraft.

the aluminum frame on the right. Part of the magnetic tape recorder is seen at the bottom of the same frame. All of this equipment was powered from a 115 VAC, 60 cps, single phase inverter installed aboard the aircraft specifically for instrumentation applications.

Upon completion of the installation of the Telemetry Receiving Station and associated transmitting and receiving antennas, the system was passed through a series of composite tests with the subject placed in the Constraint Platform and all AC powered equipment energized from the aircraft inverter source to determine if ground loop or telemetry transmission problems existed. These tests were also performed with all aircraft radio-frequency equipment used during normal flight operations in the on position to ensure that operation of the aircraft instruments did not introduce artifacts to the BCG data collection system, and more importantly, that the BCG telemetry system did not interfere with aircraft operations.

FREE-FLOTATION PROCEDURES

The photographs shown in Figures 7.2 through 7.8 were taken during actual flight operations of the KC-135 aircraft and are presented to illustrate the various phases of typical zero g maneuver. Figure 7.2 is an over-all view of the free-flotation area with the subject-Constraint Platform combination being readied for a zero g maneuver. Two different launch procedures were used for the actual release of the subject into the free-flotation state. In the first procedure, the two launch personnel lifted the subject several feet from the deck after the zero g state was reached and then released him taking great care not to impart any significant linear or angular velocity components to the platform. This procedure is illustrated in Figure 7.3. In the second procedure, shown in Figure 7.4, the subject was held to the deck by the launch personnel until the zero g state was

Figure 7.2
In-flight KC-135 photograph: Interior view of the aircraft free-flotation area showing the subject positioned in the Constraint Platform and being readied for a series of zero g maneuvers.

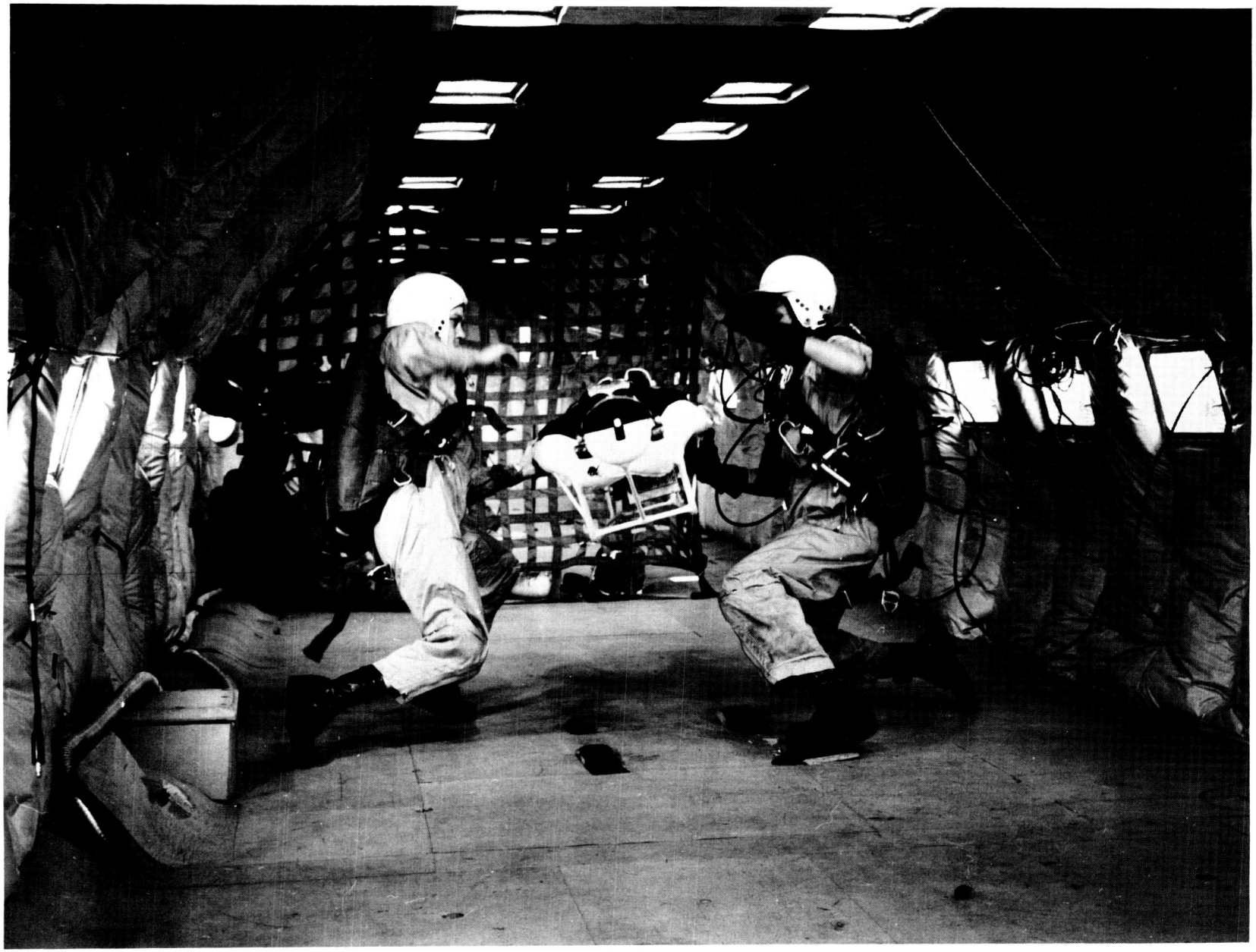

Figure 7.3
In-flight KC-135 photograph: View of the subject being manually released into the free-flotation state by the two launch personnel.

Figure 7.4
In-flight KC-135 photograph: View of the subject being released into the free-flotation state by pilot controlled application of negative acceleration to the flight profile of the aircraft.

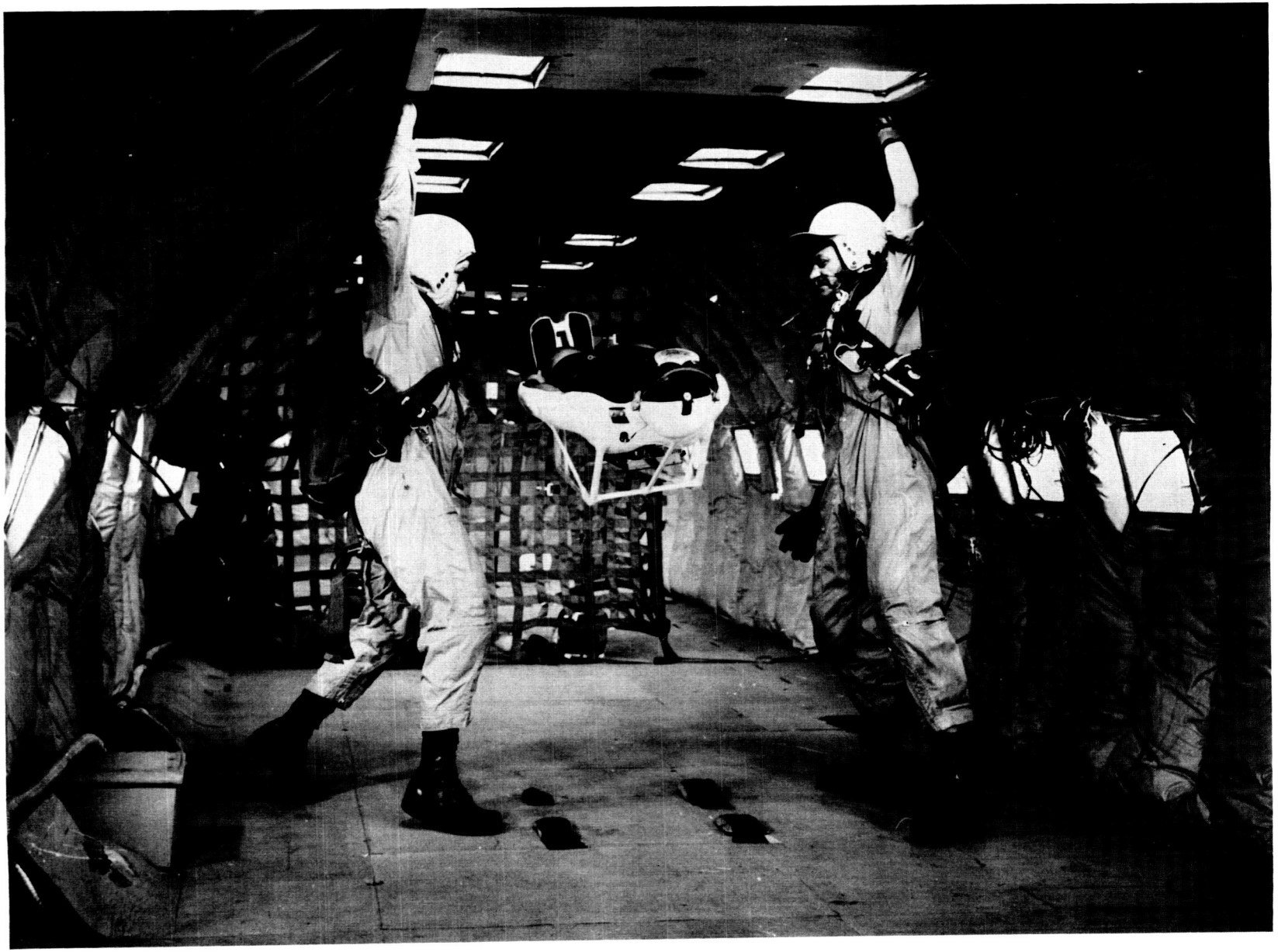

Figure 7.5
In-flight KC-135 photograph: View of an actual free-flotation of the subject during which his triaxial ECG and BCG signals were telemetered to the on-board Telemetry Receiving Station.

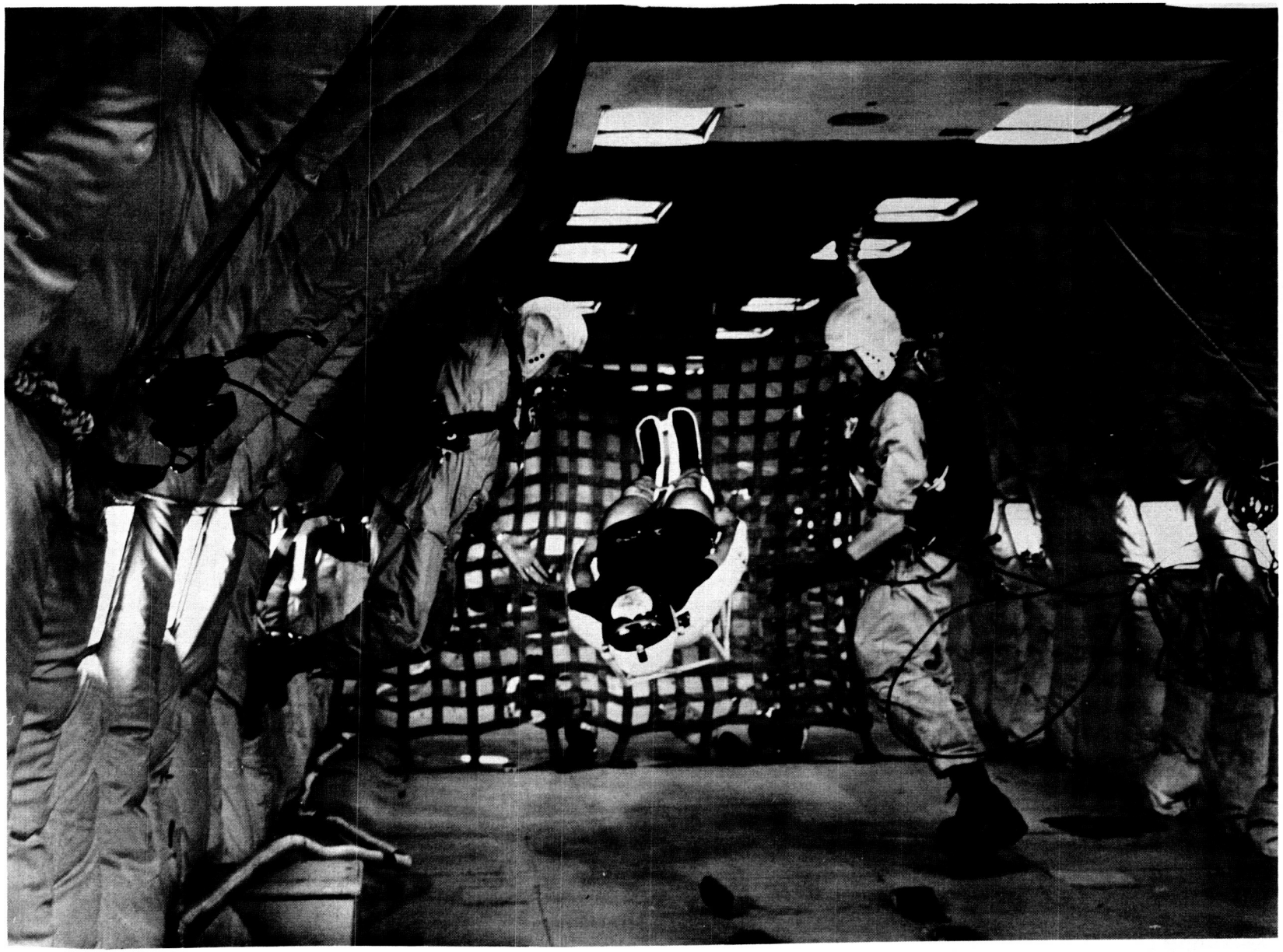

Figure 7.6
In-flight KC-135 photograph: View of an actual free-flotation of the subject showing the two launch personnel ready to assist if impact with the aircraft should become imminent.

Figure 7.7
In-flight KC-135 photograph: View of the launch personnel retrieving the Constraint Platform on signal of the pilot that the zero g maneuver is nearly completed.

Figure 7.8
In-flight KC-135 photograph: View of the launch personnel returning the Constraint Platform to the deck of the aircraft immediately before the free-flotation state was terminated by the pull-up phase of the zero g maneuver.

reached. The pilot then applied a slight negative acceleration to the aircraft which lifted the subject from the deck and placed him in the desired free-flotation state.

Views of actual free-flotation of the subject are shown in Figures 7.5 and 7.6. Although the launch personnel did not touch the Constraint Platform at any time during the free-flotation period, they were always in position to grasp it in case air turbulence or aircraft velocity changes occurred. The recovery duties of these personnel included assistance to the subject before the aircraft began its recovery pull-up at the end of the maneuver and are illustrated in the Figures 7.7 and 7.8.

FLIGHT DATA NOMENCLATURE

Actual flight records with identifying nomenclature are shown in this portion of the report to facilitate the ready interpretation of the airborne data presented in the following section.

As noted earlier, the entire instrumentation system was calibrated during flight immediately before each set of profiles was initiated. A photograph of typical real-time telemetry calibration data as displayed on the multichannel light-beam galvanometer recorder is shown in Figure 7.9. Each of the 14 galvanometer traces is identified by circled numerals to indicate the related measurement channels. Measurements 1 through 10 were telemetered from the Constraint Platform to the Telemetry Receiving Station while hard wire connections were used to display measurements 11 through 14. The IRIG subcarrier oscillator channel assignment for each of the telemetered measurements is shown below the associated identifying nomenclature.

This nomenclature is as follows: Measurements 1, 2, and 3, identified as ECG-X, ECG-Y, and ECG-Z, respectively, represented the triaxial electrocardiogram of the subject; Measurements 4, 5, and 6, identified as BCG-$\ddot{X}$, BCG-$\ddot{Y}$, and BCG-$\ddot{Z}$, respectively, recorded the triaxial linear acceleration ballistocardiogram of the subject; Measurement 7, identified as BCG-$\ddot{\Theta}$, displayed the angular acceleration ballistocardiogram of the subject along a single preselected body axis; Measurement 8 recorded the respiration rate of the subject; Measurement 9 indicated the voltage level of the battery used to energize the telemetry element of the Biotelemetry Module; Measurement 10 served to indicate both the level of the positive polarity battery used to energize the signal-conditioning amplifier elements of the Biotelemetry Module and the operation of the Command Reset System which reduced the recovery time of the BCG channels when AC coupling was used; Measurement 11 displayed the signal responses of the on-board flight surgeon who visually monitored the free-flotation procedures; and Measurements 12, 13, and 14, identified as $\ddot{x}$, $\ddot{y}$, and $\ddot{z}$, respectively, recorded the linear acceleration of the aircraft along its roll, pitch, and yaw axes during the zero g maneuvers.

The calibration pulses shown in Figure 7.9 were produced by placing the TELEMETRY switch located on the Biotelemetry Module in its CAL position and alternately pressing the plus and minus calibration pushbuttons. Since the voltage levels of the calibration sources were accurately predetermined before each flight, this procedure quantified the modulation sensitivity of each telemetry channel and established the baseline whereby the position of the galvanometer trace was known for the zero signal level presented to the input of each telemetry oscillator.

When this calibration procedure was completed, the TELEMETRY switch was placed in the OPR position which then connected the input of each subcarrier oscillator to the output of its related signal-conditioning circuit. The AMPLIFIERS switch was then placed in its CAL position which connected the input circuitry of the three ECG amplifiers and the four BCG amplifiers to the calibration network. By alternately pressing the plus and minus calibration pushbuttons, the voltage gains of the cascaded signal-conditioning and telemetry equipment could be measured. Typical data obtained with this procedure are shown in Figure 7.10. The voltage gain of the electrocardiogram preamplifiers and the transducer sensitivity of the ballistocardiogram accelerometers are shown below the related channel nomenclature. With these data, the gain sensitivity of the entire system could be accurately established.

Other information presented in Figure 7.10 includes the zero g baseline and 1.0 g deflection sensitivity of the x, y, and z aircraft acceleration measurements and the trace interruption used to sequentially identify the 14 galvanometer assignments. By comparing the zero volt input baseline associated with the three electrocardiogram measurements as shown in Figure 7.9 with the baseline shown in Figure 7.10, it can be seen that the output levels of the ECG preamplifiers were not set to zero volts when the inputs to the preamplifiers were shorted. This offset adjustment is necessary when such data as ECG signals are to be transmitted over telemetry links which have limited signal-to-noise ratio capabilities. Since the peak-to-peak magnitude of an ECG signal is not symmetrical about its baseline, higher modulation sensitivities can be achieved if the input to the related subcarrier oscillator is offset so that the DC level represented by the center of the peak-to-peak ECG deflection corresponds to the center frequency of the telemetry channel.

The actual form used to present the majority of the flight data is shown in Figure 7.11. The nomenclature which identifies the pertinent measurements is at the left. Below each measurement is shown the peak-to-peak magnitude of the calibration marker entered on the actual record. For the ECG channels, 1.0 millivolt calibration markers are shown; for the three linear acceleration BCG measurements, 3.0 milli-g markers are indicated; while for the angular acceleration BCG data, 0.1 radian/sec^2 calibration marks are noted. These calibrations are used for all flight data presented in later sections. It should be noted that the subscript which follows the BCG-$\ddot{\theta}$ nomenclature indicates the body axis about which the angular acceleration measurement was recorded.

The operation of the Command Reset System is also demonstrated in Figure 7.11. When the Command Reset Transmitter is activated, the corresponding trace at the top of the record is deflected downward. This action momentarily returned the low end of the capacitor used to couple each BCG amplifier to its related telemetry oscillator to ground potential which removed any static offset accelerations from the dynamic BCG signals, thus allowing the telemetry oscillators to be deviated about their true center frequencies. Also shown is the upward deflection of the galvanometer controlled by one of the on-board experimenters when visual observation of the free-flotation state of the subject was first noted. This trace was included as a trouble-shooting measure should the flight operations prevent collection of the desired BCG data. The effect on the data of a normal impact of the Constraint Platform against the wall of the aircraft is also shown in Figure 7.11 (right).

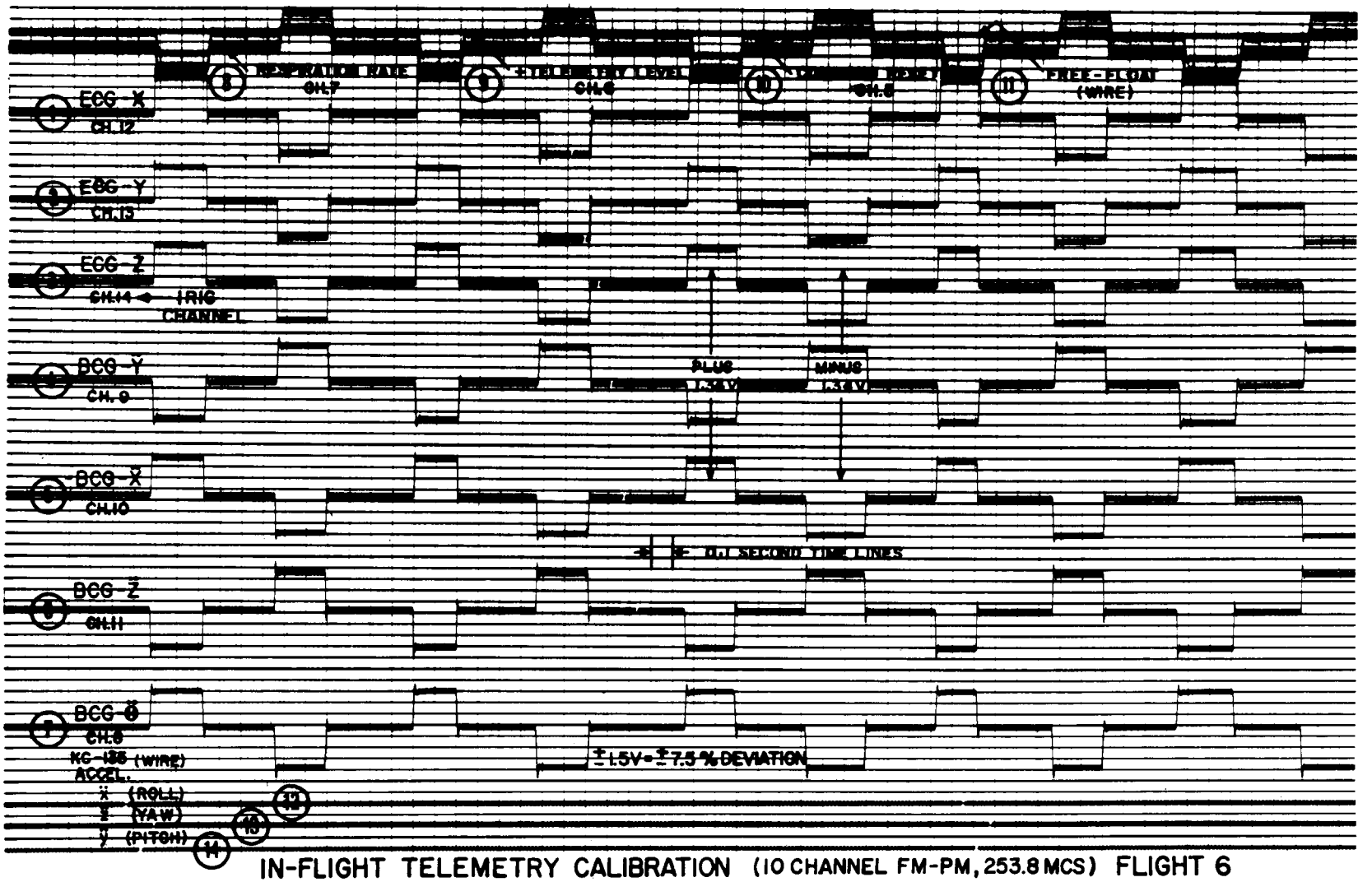

Figure 7.9

Photograph of airborne calibration data collected immediately before the initiation of Flight 6 zero g maneuvers demonstrating the quantification of the modulation sensitivity of the telemetry oscillators. Nomenclature has been added to the displayed data to identify each galvanometer trace and its measurement function. For these data, the input to each of the 10 telemetry oscillators was returned to a resistive network which allowed the manual application of sequential plus and minus 1.34 volt calibration signals to all oscillators simultaneously.

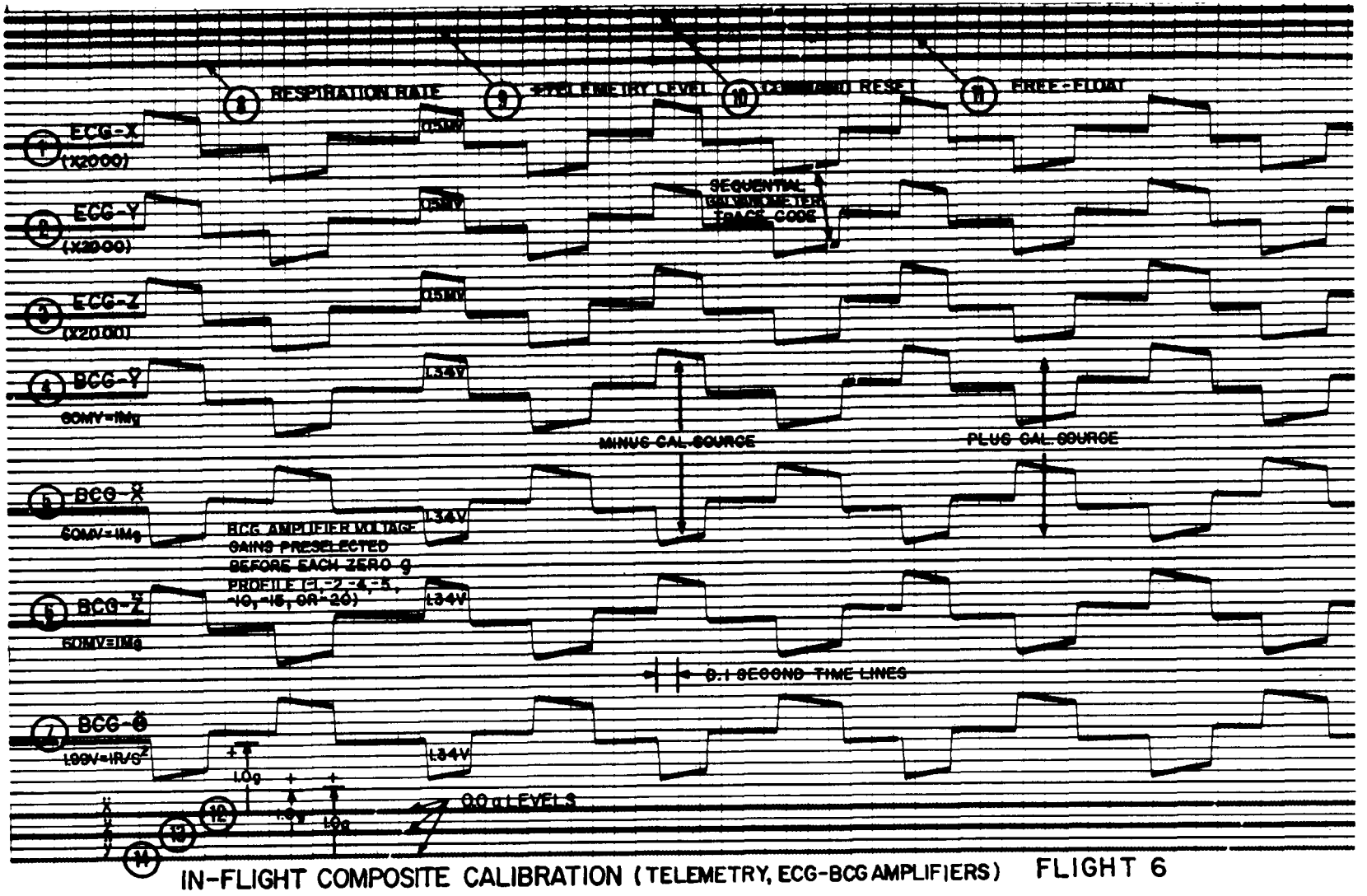

Figure 7.10

Photograph of airborne calibration data collected immediately before the initiation of the Flight 6 zero g maneuvers to facilitate the quantification of the display sensitivity of the composite signal-conditioning and telemetry circuitry. For these data, calibration pulses of known level were applied to the input of the ECG and BCG signal-conditioning amplifiers which in turn drove the telemetry oscillators. The sequentially applied calibration pulse permitted the voltage gain of these amplifiers to be measured and gave a galvanometer trace baseline for zero input signal voltage.

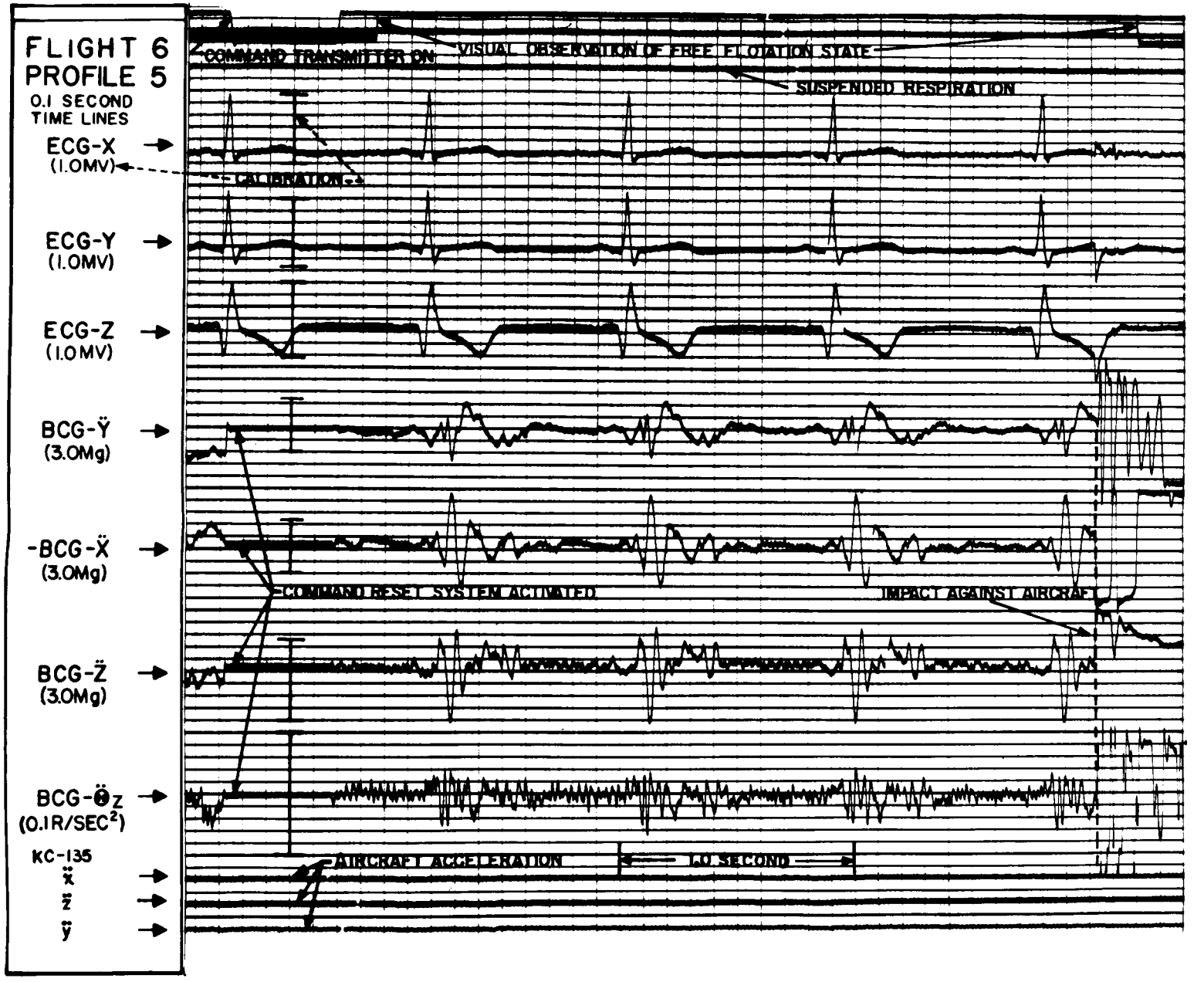

Figure 7.11
Photograph of the triaxial ECG and BCG data collected on Flight 6 during the free-flotation phase of Profile 5. Nomenclature has been added to identify the pertinent measurements, their calibration sensitivities, and over-all time profile.

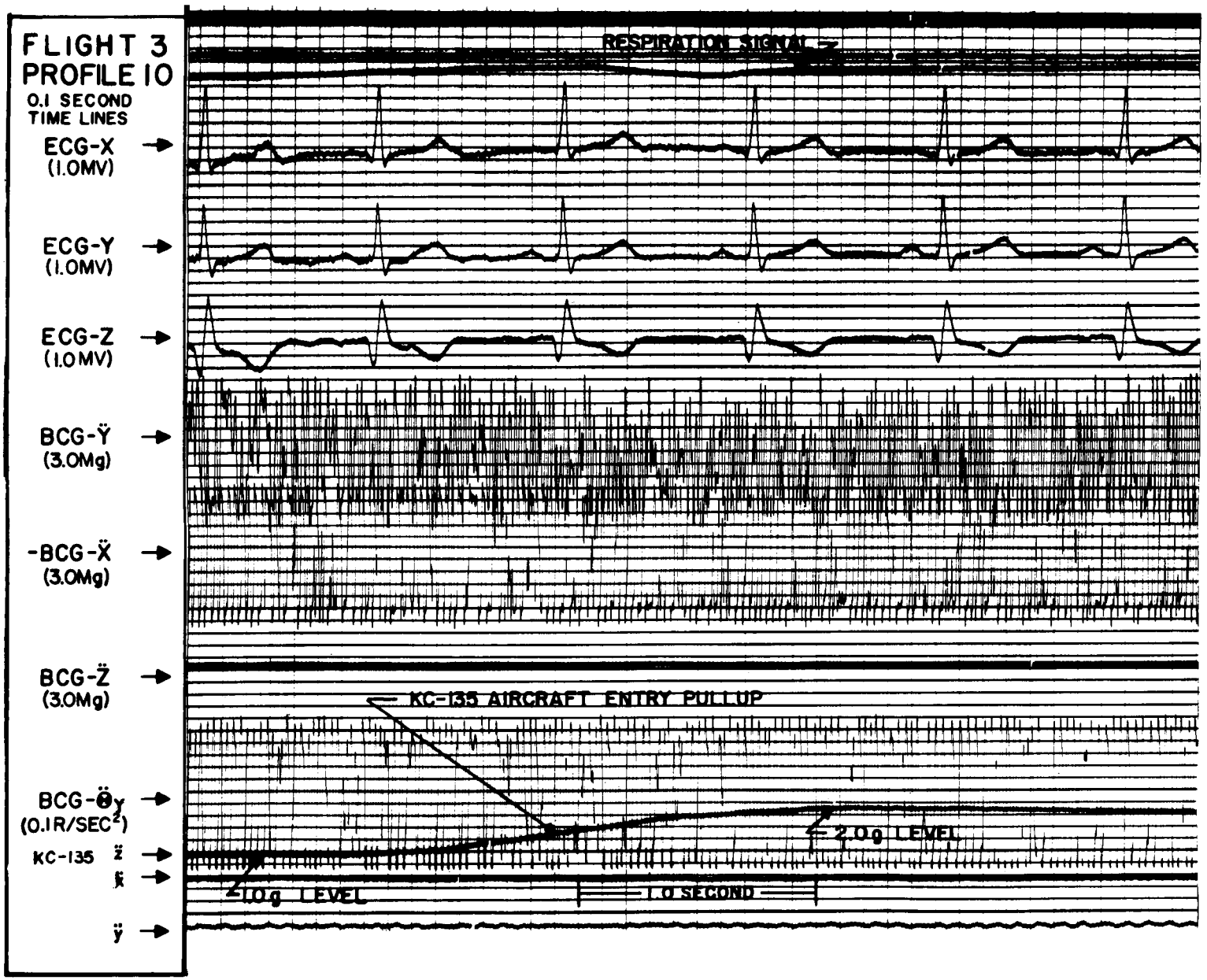

Figure 7.12

Photograph of the airborne data collected during the transition of the KC-135 aircraft from its initial 1.0 g level to its constant 2.0 g entry pull-up acceleration. These data are presented to illustrate the tremendous overloads to which the BCG channels were exposed.

A flight record is presented in Figure 7.12 to demonstrate the overloaded condition of the system before each zero g profile. This record was made at the time of the entry phase of the maneuver. The transition of the aircraft from its 1.0 g level before the maneuver to the 2.0 g pull-up acceleration is shown by the $\ddot{z}$ trace at the bottom of Figure 7.12. With the 250 milli-g full scale sensitivity of the linear BCG accelerometers, and the orientation of the subject relative to the aircraft, the BCG-$\ddot{Z}$ channel was always in the blocked state during this phase of the maneuver. The vibration of the aircraft and its coupling to the Constraint Platform resulted in the overloaded state of the remaining BCG channels. This figure also illustrates the functioning of the respiration rate circuitry. As stated before, the subject was instructed to maintain a suspended state of respiration only during the data collection phase of the free-flotation procedure.

8. TRIAXIAL BCG-ECG FLIGHT AND LABORATORY DATA

A total of six flights of the KC-135 aircraft was available for implementation of the data collection phase of the experiment (in September, 1962). A summary of these flight operations including related subject observations is given below, followed by the presentation of the resultant triaxial BCG-ECG flight data.

FLIGHT HISTORY

Flight 1 was scheduled to indoctrinate the on-board experimental personnel in their operational duties and responsibilities. Flight 2 on the afternoon of the same day served these same functions as well as providing time for in-flight testing of the BCG instrumentation system and practice of the launch operations associated with the placement of the subject in the free-flotation state. Five profiles were flown with the subject positioned in the Constraint Platform. On the fifth profile, a sudden change in aircraft speed resulted in a relatively high velocity impact of the Constraint Platform against the rear of the free-flotation area. No physical harm occurred to the subject or to the Constraint Platform except for a slight depression of the visor assembly. This event vividly demonstrated the correctness of the decision to place heavy design emphasis on protective constraint and proved the integrity of the system developed to provide this need.

Flight 3 represented the first attempt to collect preliminary quantified data. A total of 10 profiles were flown with the gain sensitivities of the BCG channels changed according to a schedule so that the nominal range of peak-to-peak accelerations produced by each measurement could be observed. After the eighth profile, the subject reported a slight stomach awareness and requested that the aircraft cabin temperature be raised slightly. The flight was terminated after the tenth maneuver at the subject's request.

During the following debriefing session, it was established that an operational procedure peculiar to this flight could have been the cause for the potential motion sickness problem. On the previous flight, the subject was instructed to close his eyes during the actual free-flotation period only. Following the Flight 2 impact of the subject against the aircraft, additional facial protection was afforded by attaching a 1 inch thick polyurethane foam liner to the interior surface of the clear polystyrene visor. On Flight 3, the then opaque visor inadvertently remained in place during all 10 maneuvers so that the subject was never visually cognizant of his environment during any portion of the flight, including the entry pull-in and recovery pull-out phases. It was concluded that this lack of a visual field in combination with a comparatively low (15°C) cabin temperature was the most probable source of the near motion sickness difficulties. For the following flights, the ambient temperature of the cabin was raised and the visor lifted after each profile, thus allowing the subject to orient himself between each maneuver. With these changes no indication of motion sickness was experienced by the subject during the remainder of the airborne program.

The peak-to-peak amplitudes of the BCG signals recorded in Flight 3

gave baseline reference data which allowed the gain settings of the measurement channels to be set closer to their optimal levels during Flight 4. A total of 10 profiles were flown during this flight with analysis of the resultant data determining the proper sensitivities of the linear acceleration channels, BCG-$\ddot{X}$, BCG-$\ddot{Y}$, and BCG-$\ddot{Z}$. During the 12 zero g profiles of Flight 5, optimal sensitivities for the angular acceleration channels, BCG-$\ddot{\Theta}_X$, BCG-$\ddot{\Theta}_Y$, and BCG-$\ddot{\Theta}_Z$ were determined.

Analysis of all these data established firm operating levels for each of the 10 telemetry channels so that all measurements could be transmitted simultaneously with minimal cross-channel interference effects and with optimal utilization of the signal-to-noise ratio capabilities of the entire system. This achievement of the basic operational criterion for the bioinstrumentation aspects of the project combined with the practice gained by the on-board experimental personnel in the performance of their tasks and the confidence gained by the subject in the safety of his environment allowed the final data collection phase of the project to be scheduled for the sixth flight.

On Flight 6, a total of 12 zero g profiles were flown. The first three were flown with the angular accelerometer oriented to collect BCG-$\ddot{\Theta}_Y$ data, the second three for BCG-$\ddot{\Theta}_Z$ data, and the last three for BCG$\ddot{\Theta}_X$ data. For the remaining three profiles, the subject was removed from the Constraint Platform and a putty-like glazing compound inserted into the couch to simulate the mass distribution of the subject. With free-flotation of this "dummy subject," data related to the over-all noise level of linear and angular acceleration measurement channels were collected.

FLIGHT DATA

Data collected on Flight 6 demonstrated the success of the program in meeting its basic objective, the quantitative recording of triaxial BCG-ECG information with a near perfect suspension system. The core of these data is presented in Figures 8.1 through 8.6 which are unretouched photographs of the telemetered triaxial BCG-ECG measurements as displayed in real time by the on-board optical galvanometer recorder for free-flotation of the subject on six different zero g profiles. Even a cursory examination of these data reveals the clarity of rendition of the BCG data, the presence of changes in cardiac activity which are marked by sharp and rapid transitions observable only with wide-band ballistocardiography techniques, the relatively low background noise present even though the measurements were made in an operational rather than laboratory type environment, and the excellent repeatability of the cardiac-originated acceleration data on successive zero g profiles.

The primary difference between each of these figures is the orientation of the angular accelerometer used for the BCG-$\ddot{\Theta}$ measurement. For Figure 8.1, the accelerometer was oriented to record BCG-$\ddot{\Theta}_Y$ data, i.e., the angular acceleration of the subject about his longitudinal body axis. Figure 8.2, with an identical accelerometer orientation, is presented to demonstrate the repeatability of the BCG-$\ddot{\Theta}_Y$ data. Figures 8.3 and 8.4 serve the same function for the BCG-$\ddot{\Theta}_Z$ measurement which represents the instantaneous angular acceleration of the subject about his dorsoventral axis. Similarly, BCG-$\ddot{\Theta}_X$ data describing the angular accelerations of the subject about his transverse (side-to-side) axis are shown in Figures 8.5 and 8.6. The capability to reproduce closely the three linear acceleration BCG meas-

urements can be seen by comparing the BCG-$\ddot{X}$, BCG-$\ddot{Y}$, and BCG-$\ddot{Z}$ data presented in all six figures.

The three components of the triaxial angular acceleration ballistocardiogram are shown in Figure 8.7 to facilitate comparison of magnitude and waveform. Each of the complexes was derived from different zero g profiles. Since the complexes did not occur simultaneously, and heart rate differed, Figure 8.7 does not allow the precise comparison of timing relationship between BCG-$\ddot{\Theta}_X$, BCG-$\ddot{\Theta}_Y$, and BCG-$\ddot{\Theta}_Z$. Instead, these relationships should be independently determined by reference to the related data of Figures 8.1 through 8.6.

For convenience to the reader the polarity conventions adopted for the display of the data are summarized below. The X, Y, and Z symbols define the transverse, longitudinal, and dorsoventral body axes, respectively, of the subject. For the three electrocardiogram measurements, an upward galvanometer deflection represents a positive signal referenced to the left of the body for ECG-X, to the foot for ECG-Y, and dorsal for ECG-Z. For the three linear acceleration ballistocardiogram measurements an upward galvanometer deflection represents rightward acceleration of the body for BCG-$\ddot{X}$, headward acceleration for BCG-$\ddot{Y}$, and dorsal acceleration for BCG-$\ddot{Z}$. For the three angular acceleration ballistocardiogram measurements, an upward galvanometer deflection represents clockwise angular acceleration as viewed from the subject's left for BCG-$\ddot{\Theta}_X$, from the feet for BCG-$\ddot{\Theta}_Y$. and from the front for BCG-$\ddot{\Theta}_Z$. When a minus sign prefix is assigned to a measurement in this report, particularly to the BCG-$\ddot{X}$ and BCG-$\ddot{\Theta}_X$ data, display polarities of opposite convention are implied.

Of the seven galvanometer traces of dynamic form shown in each figure, the top three traces depict the triaxial electrocardiogram, the next three traces describe the triaxial linear acceleration ballistocardiogram, while the seventh or bottom dynamic trace outlines one component of the triaxial angular acceleration ballistocardiogram; all of these data were collected and displayed simultaneously via the RF telemetry link to the subject. The time scale of each record is such that approximately 4.3 seconds of data are shown for each free-flotation phase of the related zero g profile. The display sensitivities of the three electrocardiogram measurements, defined by the 1.0 millivolt calibration markers, are nearly identical, thus allowing visual estimation of magnitude differences between the ECG-X, ECG-Y, and ECG-Z data.

Similarly, the BCG-$\ddot{X}$ and BCG-$\ddot{Y}$ data have near identical display sensitivities as shown by the length of the 3.0 milli-g calibration markers. However, because of the lower level accelerations occurring along the BCG-$\ddot{Z}$ axis, this channel has a display sensitivity approximately 1.5 times greater than that of the BCG-$\ddot{X}$ and BCG-$\ddot{Y}$ channels. Care also must be taken when comparing magnitude levels of the angular acceleration data as indicated by the length of the 0.1 rad/sec^2 calibration markers. All of the BCG data shown in these figures were collected using AC coupling which was controlled by the Command Reset System. The 0.25 cps low-frequency roll-off characteristics of this mode of transmission as well as the frequency response characteristics of the over-all system have been described in previous sections of the report.

At the end of Profile 9 of this flight, the subject was removed from the Constraint Platform and replaced by the glazing compound. The "dummy subject" was a commercial glazing compound (DAP Inc. Type 33)

Figure 8.1 Real-time flight data: Flight 6, Profile 2. Angular accelerometer oriented for collection of BCG-$\ddot{\Theta}_Y$ data.

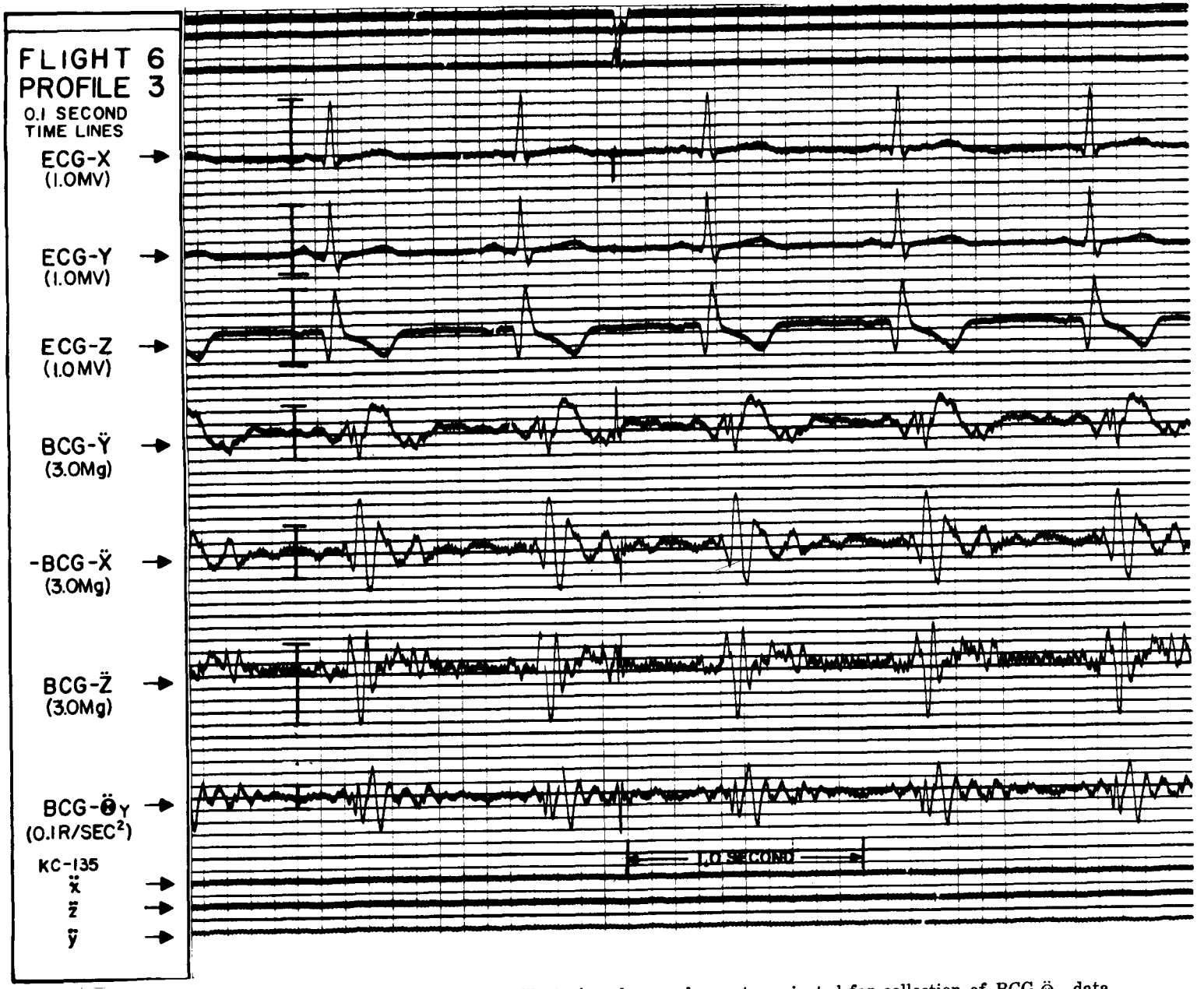

Figure 8.2 Real-time flight data: Flight 6, Profile 3. Angular accelerometer oriented for collection of BCG-$\ddot{\Theta}_Y$ data.

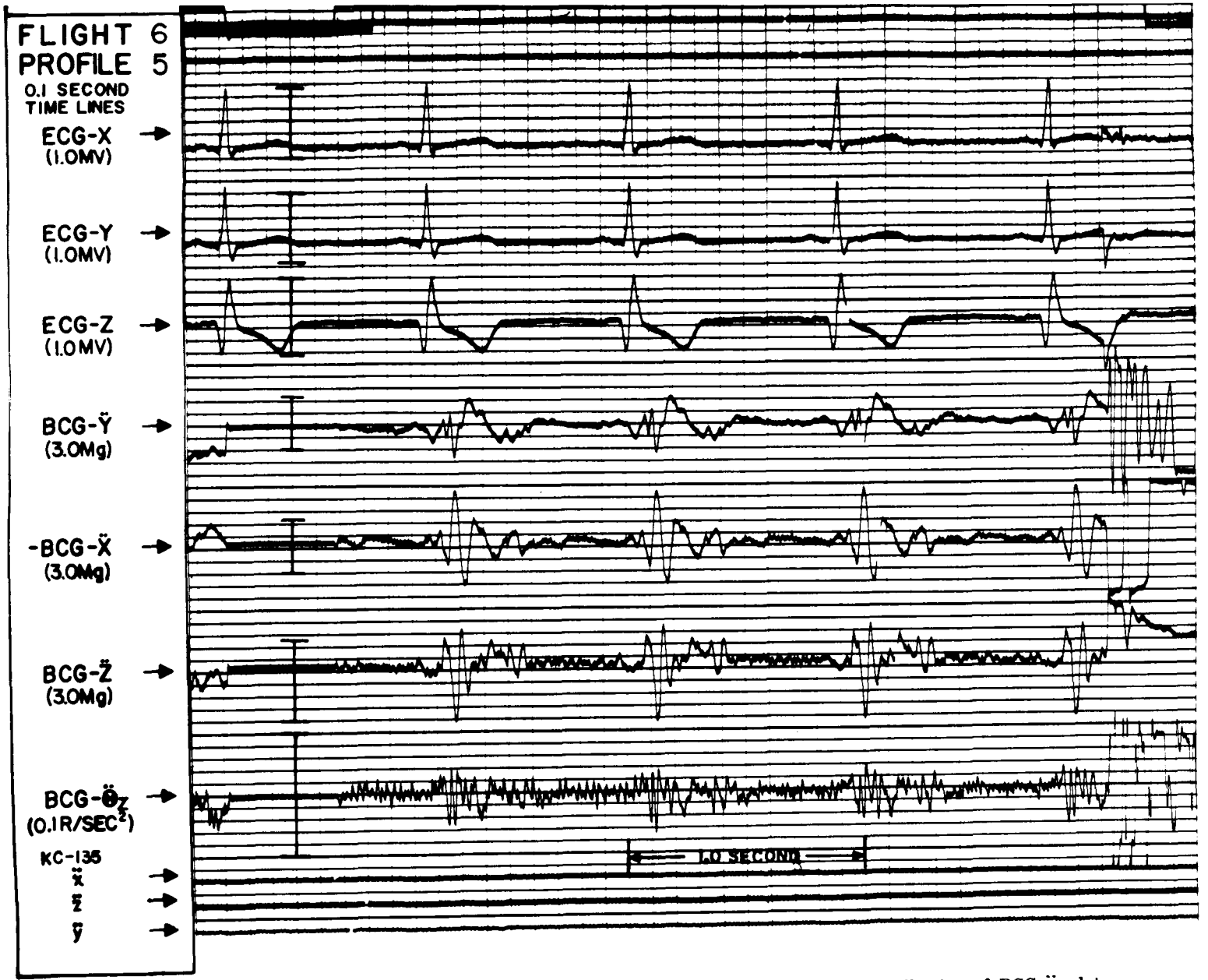

Figure 8.3 Real-time flight data: Flight 6, Profile 5. Angular accelerometer oriented for collection of BCG-$\ddot{\Theta}_Z$ data.

Figure 8.4 Real-time flight data: Flight 6, Profile 6. Angular accelerometer oriented for collection of BCG-$\ddot{\Theta}_Z$ data.

Figure 8.5 Real-time flight data: Flight 6, Profile 8. Angular accelerometer oriented for collection of BCG-$\ddot{\Theta}_X$ data.

Figure 8.6 Real-time flight data: Flight 6, Profile 9. Angular accelerometer oriented for collection of BCG-$\ddot{\Theta}_X$ data.

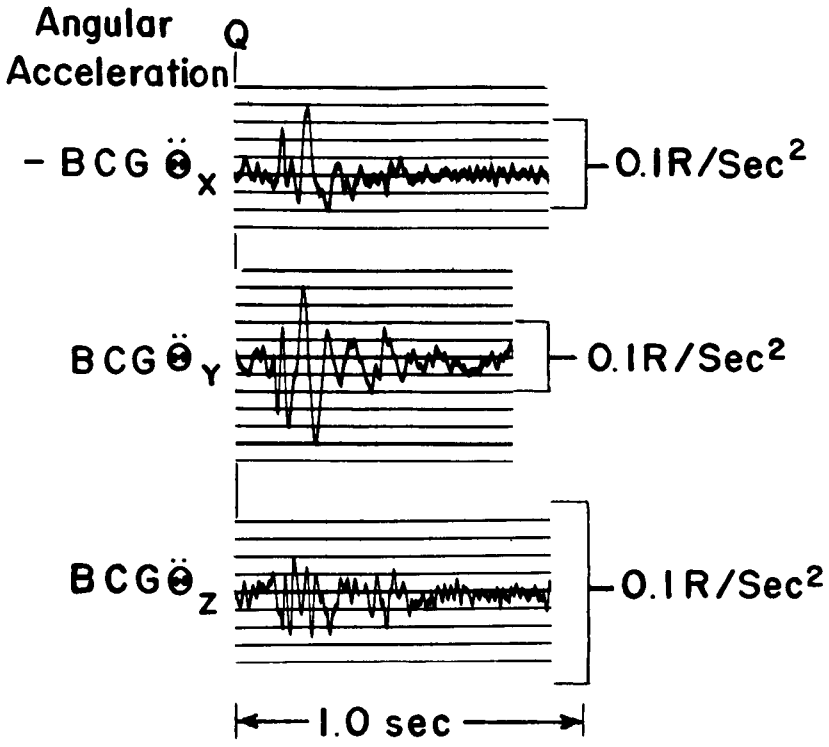

Figure 8.7 The triaxial angular acceleration ballistocardiogram.

of putty-like consistency, molded to approximate the mass and mass distribution of the human subject. On Profile 10, the Constraint Platform with dummy subject was placed into the free-flotation state using the launch procedures previously described. The BCG-$\ddot{X}$, BCG-$\ddot{Y}$, BCG-$\ddot{Z}$, and BCG-$\ddot{\Theta}_Y$ channels were in their normal operating modes and the resultant data displayed in real time on the optical galvanometer recorder. The same procedures were followed for Profiles 11 and 12 with the angular accelerometer orientation changed between maneuvers to collect BCG-$\ddot{\Theta}_X$ and BCG-$\ddot{\Theta}_Z$ data, respectively. The display sensitivities of each BCG channel presented in Figure 8.8 are set to their commonly used values. At the right of each channel's identifying nomenclature is shown the voltage gain of the Biotelemetry Module signal-conditioner amplifier associated with the measurement. Calibration markers quantifying the acceleration sensitivity of each channel are also shown.

LABORATORY DATA

Typical laboratory BCG data collected from the human flight subject are shown in Figures 8.9 and 8.10 under the same suspended respiration conditions used in the flight program. Figure 8.9 shows ECG-Z, BCG-$\ddot{Y}$, and BCG-$\ddot{X}$ data obtained with the subject positioned in the Constraint Platform and the resultant assembly placed on top of a support fixture mounted directly to the upper bearing of the commercial air-bearing BCG bed previously mentioned. The weight of this assembly was approximately 40 pounds as compared to 23.5 pounds for the Constraint Platform only. Laboratory data similar in waveform to the flight data always showed transitions that were neither so crisp nor so clearly defined as those pre-

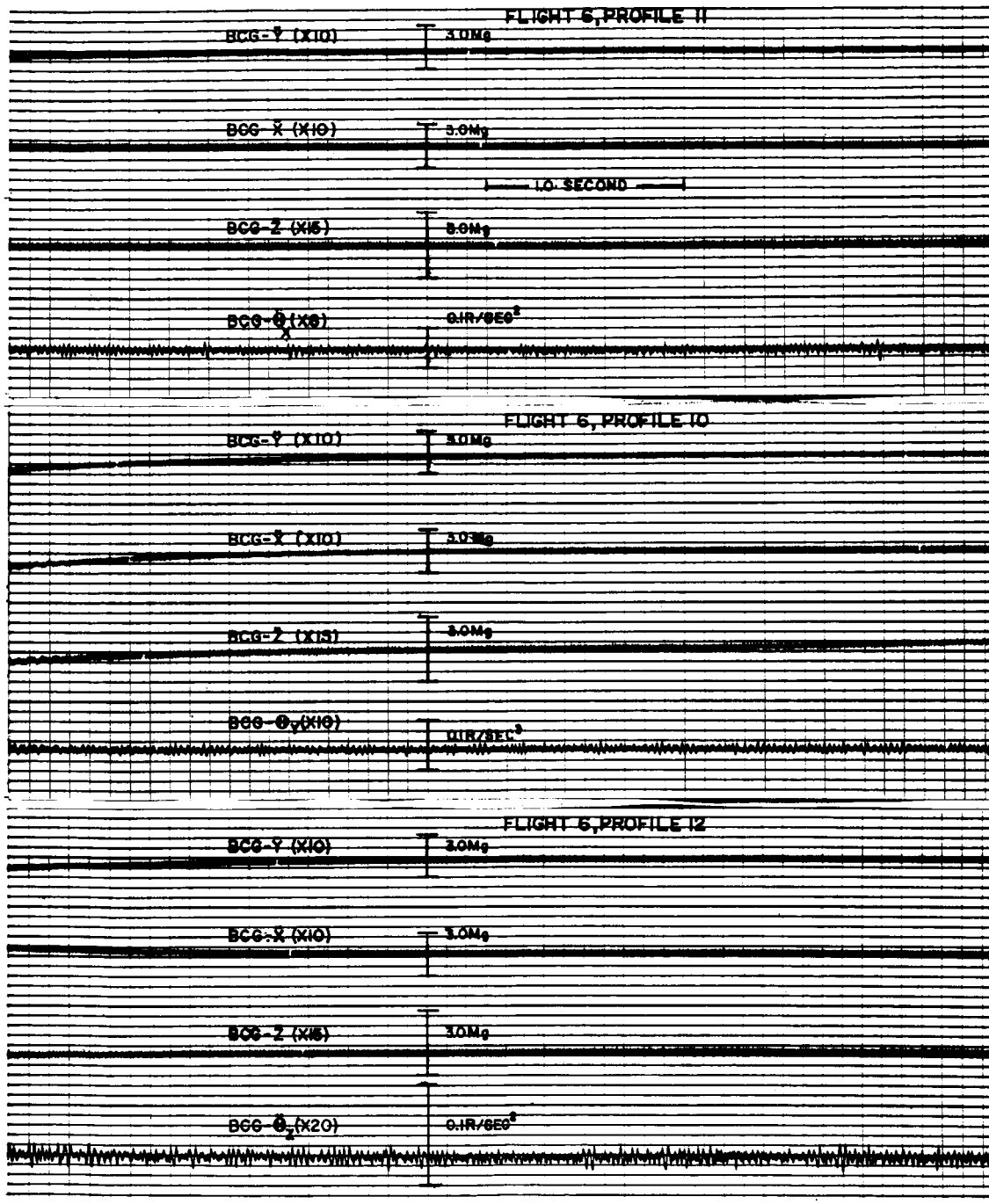

Figure 8.8 Real-time flight data: For these data, glazing compound of the same mass and general body configuration of the subject was inserted into the Constraint Platform to serve as a dummy subject for determination of the system noise characteristics. The voltage gains of the four BCG channels were set to their most commonly used values and the data collected while the Constraint Platform was in the free-flotation state. The orientation of the angular accelerometer was changed between profiles to obtain measures of the noise characteristics of the BCG-$\ddot{\Theta}_X$, BCG-$\ddot{\Theta}_Y$, and BCG-$\ddot{\Theta}_Z$ channels.

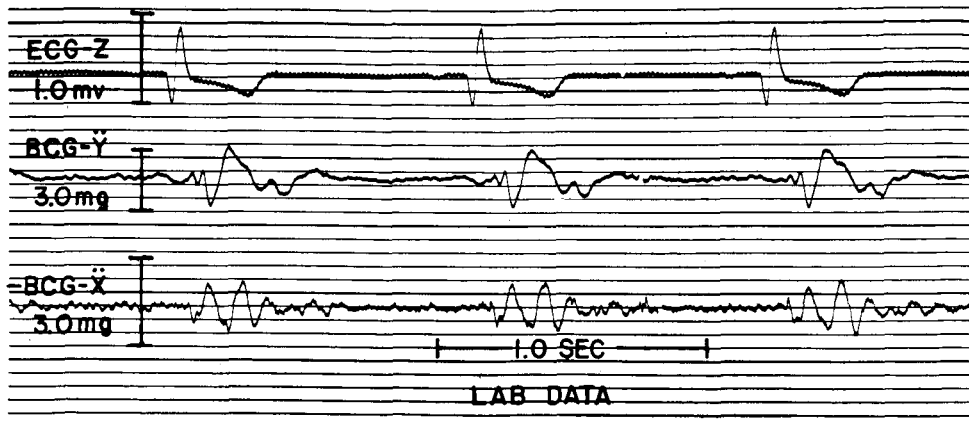

Figure 8.9 Laboratory data collected with the flight subject positioned in the Constraint Platform which was mounted on top of a support fixture affixed to the bearing of a two-dimensional air-bearing BCG bed.

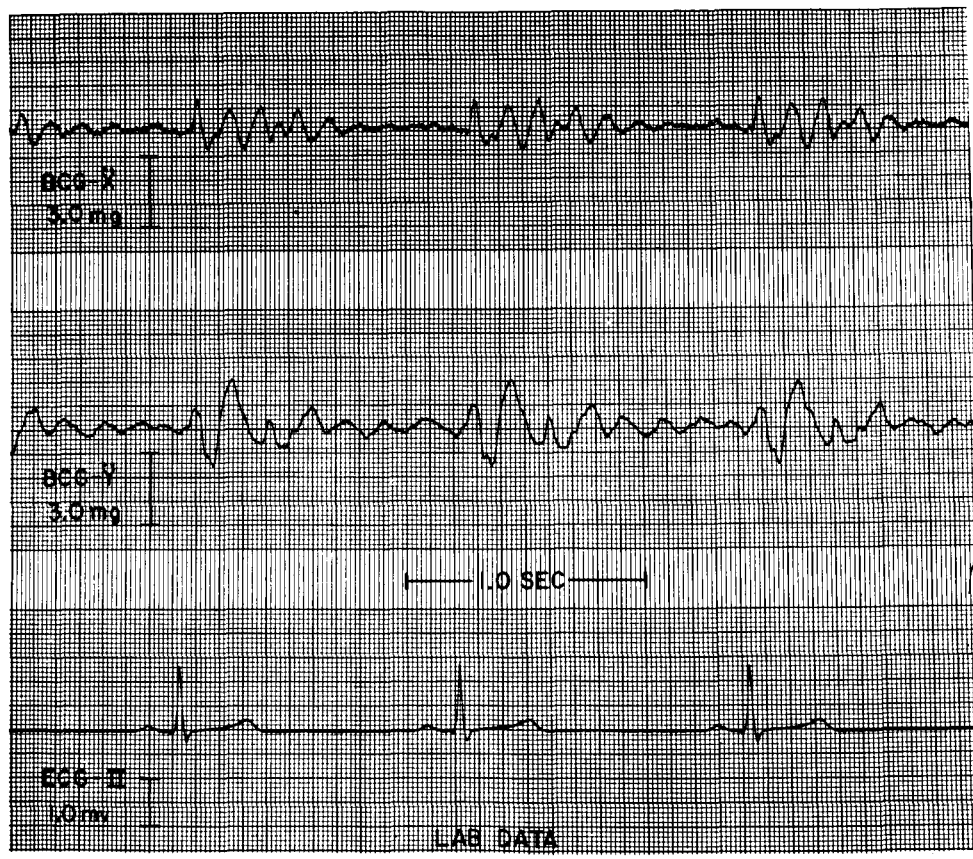

Figure 8.10 Laboratory data collected with the flight subject lying on the bed structure of a commercial two-dimensional air-bearing BCG bed with conventional foot-board and shoulder strap constraint.

sent in the flight recordings. For all laboratory measurements, the peak-to-peak value of BCG-Ÿ was greater than the corresponding value for BCG-Ẍ.

The typical laboratory data shown in Figure 8.10 were collected with the flight subject reclining on the 11.0 pound bed structure provided as part of the original equipment of the commercial air-bearing BCG bed. The lack of detail present in these recordings is due primarily to the less than optimal body-to-suspension coupling afforded by the foot-board and shoulder strap harness method of constraint. Comparison of this figure with either Figure 8.9 or the flight data reinforces the emphasis placed by ballistocardiographers on the importance of tight body-to-suspension coupling.

From all flight and laboratory data, it is readily apparent that the weightless environment can serve in both theory and practice as an idealized BCG suspension system allowing motion with a near perfect six degrees of freedom. Specifically, the data presented in Figures 8.1 through 8.6 define the first inertial triaxial ballistocardiogram data ever collected.

9. ANALYSIS OF DATA

To make laboratory and flight results more readily available for discussion the data were subjected to analytical procedures which ranged from simple averaging to computer treatment. This analytical treatment includes a certain amount of discussion which will be extended in Chapter 10.

AMPLITUDE OF SIGNAL

To facilitate a comparison of the relative peak magnitudes of the six BCG signals and to furnish data for calculation of the forces exerted by the cardiovascular system, amplitude measurements were performed on each complete cardiac complex shown in Figures 8.1 through 8.6. The measurements were based on determining the over-all amplitude of that portion of the complex which had the greatest peak-to-peak excursion during a single major directional transition. The means of the measurements for each profile are listed in Table 9.1 as well as the means, standard deviations, and ranges for the grouped profiles. Also shown is the average heart rate of the subject during each profile. The heart rate varied during a single profile with highest rates during time intervals of changes in acceleration of the subject.

The over-all mean data of Table 9.1 for the maximum peak-to-peak amplitudes of the three linear acceleration measurements give representative values of 5.0, 3.0, and 3.1 milli-g for BCG-$\ddot{X}$, BCG-$\ddot{Y}$, and BCG-$\ddot{Z}$, respectively. For all complexes of all profiles, the peak-to-peak transverse (side-to-side) accelerations of the body were always greater than those occurring along either the longitudinal or the dorsoventral axes. For the majority of the individual profiles, the dorsoventral accelerations were slightly greater than the longitudinal accelerations. As shown by the over-all means for BCG-$\ddot{Y}$ and BCG-$\ddot{Z}$, little difference exists with group treatment of the individual profile data.

Data of Table 9.1 show that the maximum peak-to-peak angular accelerations always occurred about the longitudinal axis of the body. The over-all means were 0.12, 0.24, and 0.047 rad/sec^2 for the BCG-$\ddot{\Theta}_X$, BCG-$\ddot{\Theta}_Y$, and BCG-$\ddot{\Theta}_Z$ measurements, respectively. These data indicate that the angular accelerations about the longitudinal axis of the body (yaw) were approximately two times as large as those about the transverse axis (pitch), and five times as large as those about the dorsoventral axis (roll).

It is interesting to speculate about the torque exerted by the cardiovascular system on the floating man-bed unit. Recently the moments of inertia of the living human body in a number of body positions have been determined experimentally (3). For the erect position with arms at the sides of the body the mean moments of inertia are 103.0, 11.3, and 115.0 lb. in. sec.^{2} about the transverse X, longitudinal Y, and dorsoventral Z axes. Although these values will probably not closely approximate the true body moments of platform and subject, their ratio may be applied to the present consideration. The values of torque, calculated by multiplying the angular acceleration with the moment of inertia for the different axes, rate in magnitude in the following sequence: the torque exerted by the

Table 9.1

Means of Peak-to-Peak Acceleration Magnitudes of Linear and Angular Triaxial Ballistocardiogram Data as Derived from the Flight Records Presented in Figures 8.1 through 8.6.

BCG Measurement		Maximum Peak-to-Peak Amplitude								
		Individual Flight Profiles						All Flight Profiles		
Channel	Units	2	3	5	6	8	9	Mean ±S. D.	Range	No. Obs.
BCG-$\ddot{X}$	milli-g	4.9	5.1	5.2	5.2	4.9	4.8	5.0 ±0.19	4.7 -5.3	23
BCG-$\ddot{Y}$	milli-g	2.4	3.0	3.1	3.4	2.9	3.1	3.0 ±0.30	2.4 -3.5	23
BCG-$\ddot{Z}$	milli-g	3.0	3.4	3.4	3.4	2.9	2.8	3.1 ±0.28	2.7 3.5	23
BCG-$\ddot{\Theta}_X$	rad/sec²	—	—	—	—	0.12	0.12	0.12 ±0.004	0.11 -0.13	8
BCG-$\ddot{\Theta}_Y$	rad/sec²	0.22	0.26	—	—	—	—	0.24 ±0.023	0.22 -0.27	8
BCG-$\ddot{\Theta}_Z$	rad/sec²	—	—	0.046	0.049	—	—	0.047±0.005	0.044-0.056	7
Heart Rate	cpm	71	75	69	72	66	65	69.7		

cardiovascular system to move the bed and subject about the Y axis is the smallest, the torque about the Z axis is larger, and the torque in relation to the X axis is largest, being about double the Z and five times the Y value.

LOOP DISPLAY

The scalar form of the three orthogonal linear acceleration BCG measurements shown in Figures 8.1 through 8.6 allows ballistocardiographers to obtain the basic magnitude and direction relationships of the spatial ballistocardiogram. To facilitate such an analysis, these data, as well as related ECG data, are displayed in Figure 9.1 in spatial loop form as photographed from the oscilloscope screen. In the top row is shown the vector-ballistocardiogram as observed in the frontal, horizontal, and right sagittal planes of the subject. In the second row is shown the triaxial vector electrocardiogram which was recorded simultaneously with the BCG data as the subject was free-floating in the weightless environment. The BCG and ECG loop data were derived from the identical cardiac complex. In the third row are shown ECG loop data recorded immediately before the zero g maneuver was initiated when the subject was still in a 1g environment. In the fourth row is shown the same display recorded in the middle of the 2g entry pull-up phase of the zero g maneuver. All of these data were collected during the same zero g profile of the aircraft.

For the BCG loops (Figure 9.1), the body axis reference directions are shown on each side of the individual loop displays. The reference directions for the ECG loops are similarly presented. The calibration sensitivity for the 1.0 centimeter display grid of the oscilloscope is shown below the loop identification nomenclature at the left of the figure. The 2.0 millisecond intensity modulation markers are in the form of arrows, and decreasing brilliance indicates the direction of motion. The data source for these displays was the magnetic tape instrumentation recorder which stored the DC analog BCG and ECG output signals of the telemetry discriminators on six individual FM record channels.

THREE-DIMENSIONAL DISPLAY

Figure 9.2 shows a mode of display in which the vectors in their true spatial orientation are attached to a vertical supporting rod which serves as time axis. These vectors have been derived from simultaneous measurements of BCG-$\ddot{X}$, BCG-$\ddot{Y}$, and BCG-$\ddot{Z}$ amplitudes for a single cardiac complex of the flight data. The display starts at the lower part of the rod, and the vectors with scalar markers in 1 milli-g distance are attached to the time axis in intervals corresponding to 10 milliseconds. Vectors which represent H, I, and J in BCG-$\ddot{Y}$ are marked with tags. Such a display demonstrates convincingly that the singular points of the acceleration pattern in the head-foot direction are not necessarily distinguished in an arrangement of spatial vectors.

VECTOR CALCULATION BY ANALOG COMPUTER

To provide further clarification of the relationships of the individual scalar components of the flight data, analog computer type instrumentation was used to present a display of the absolute value of the instantaneous magnitude of both the BCG and ECG vectors. A block diagram and a

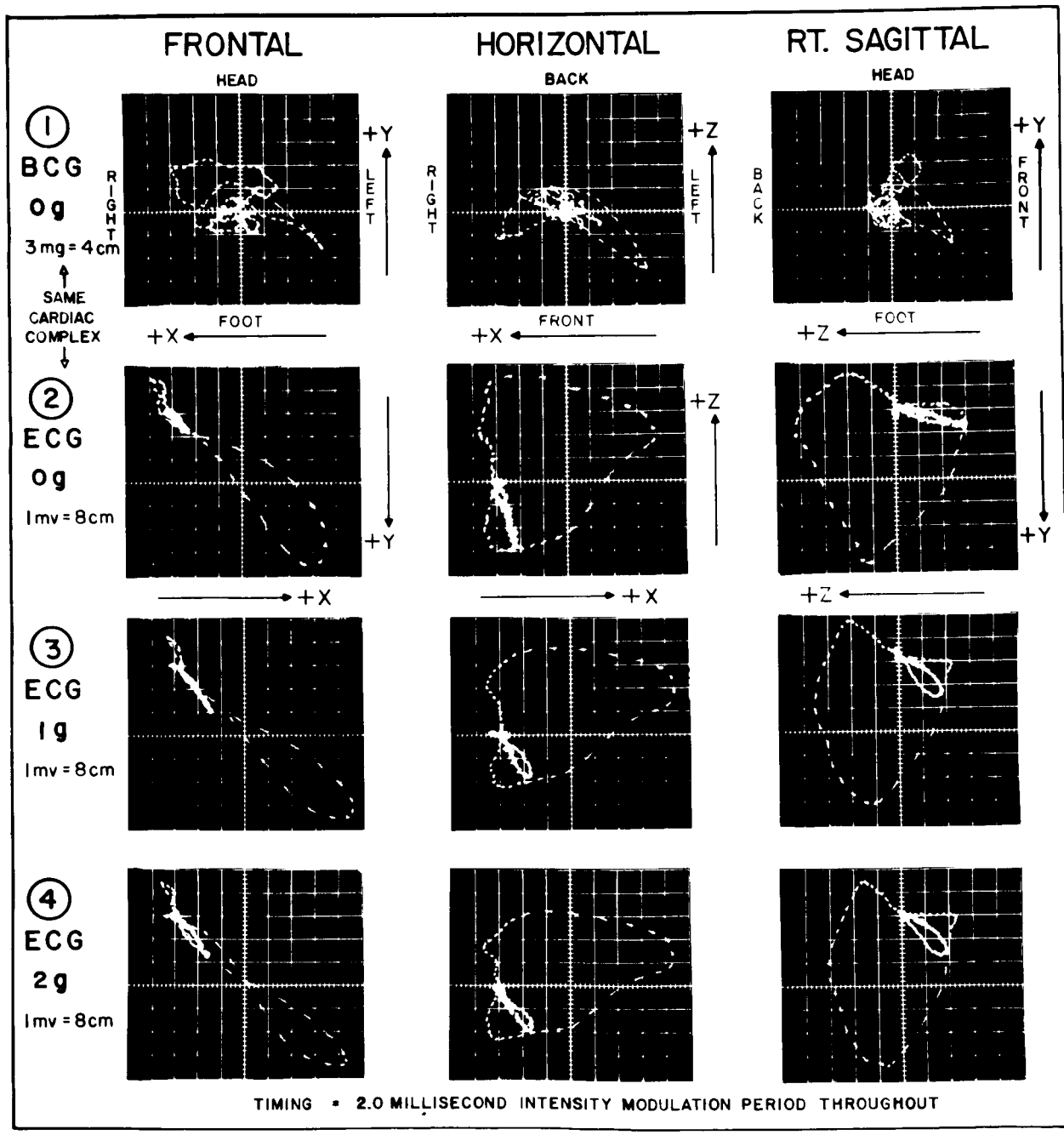

Figure 9.1 Display of vectorballistocardiogram and vectorelectrocardiogram data as projected in the frontal, horizontal, and sagittal planes (1 cm grid lines).

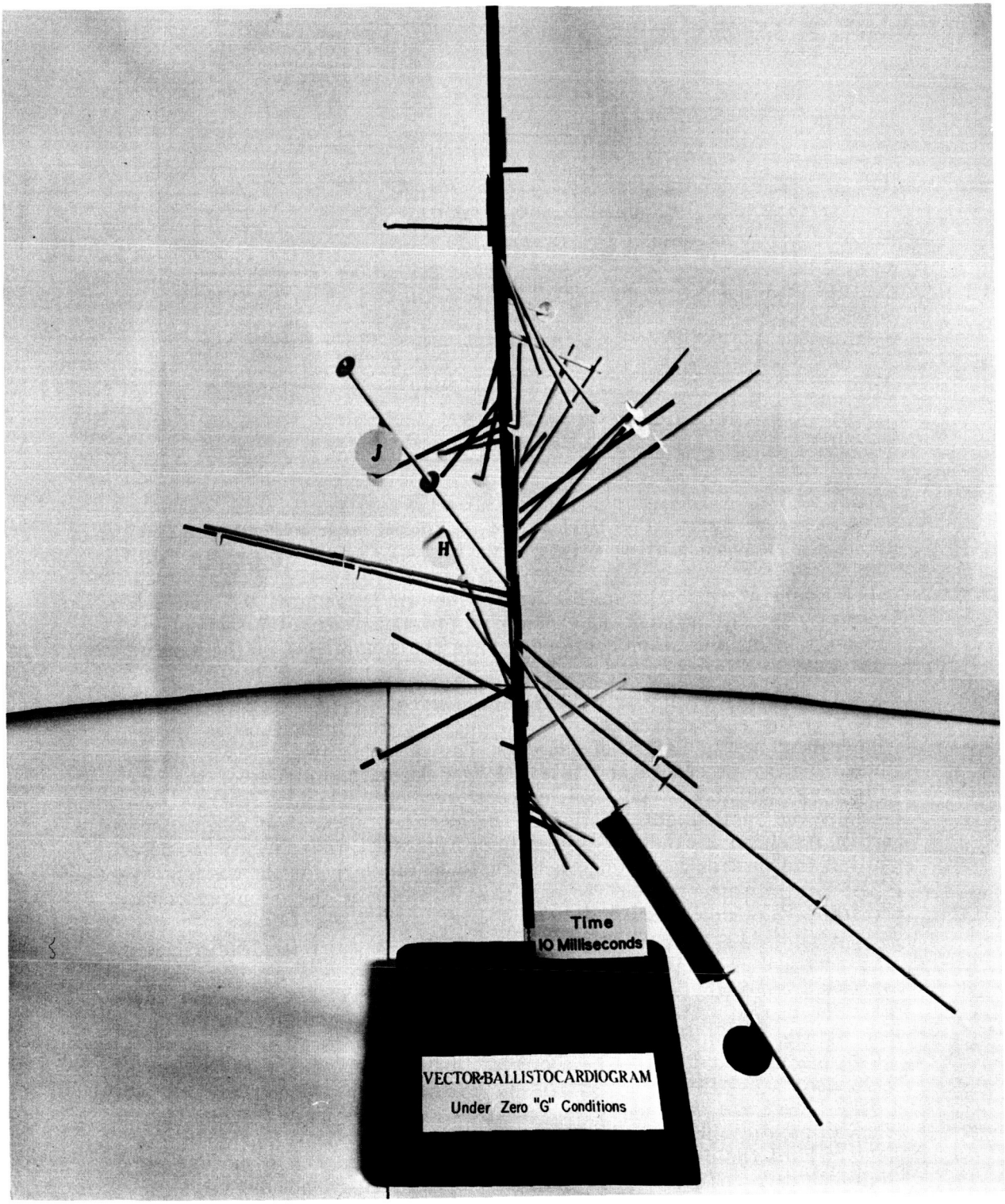

Figure 9.2 Three-dimensional display of vectorballistocardiogram. Vectors are attached to a vertical time axis in 10 millisecond intervals, starting at the lower part of the time axis. Extreme values of the BCG-Ÿ trace (H, I, and J) are marked.

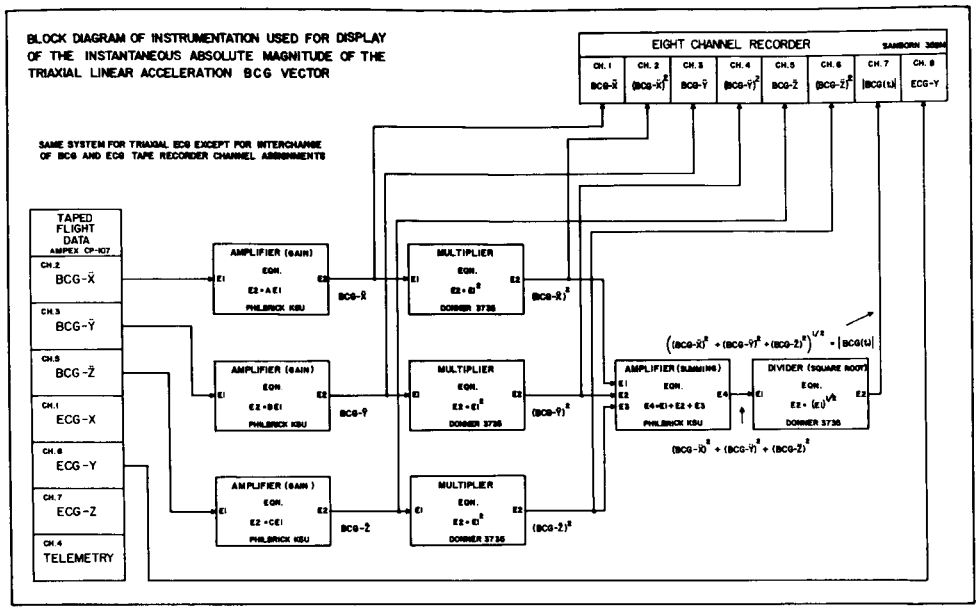

Figure 9.3 Block diagram of instrumentation used to determine the absolute value of the instantaneous magnitude of the triaxial linear acceleration ballistocardiogram vector and the triaxial electrocardiogram vector.

photograph of this instrumentation are shown in Figures 9.3 and 9.4, respectively. This system, long standard to analog computer technology, presents in instantaneous continuous form the square root of the sum of the squares of three input functions.

The essence of any triaxial measurement of time-varying spatial activity is the ability to recognize and quantify the instantaneous three-dimensional vector nature of the data. The cathode ray tube two-dimensional display procedure and intensity modulation techniques of the engineering field have been used by electrocardiographers to describe pictorially the spatial configuration of the electrical element of cardiac activity. As shown by the BCG loop data of Figure 9.1, this method has permitted the mechanical cardiac activity to be similarly displayed and, in fact, for the same cardiac complex used to describe the simultaneously recorded VCG loop.

It is obvious that such data cannot be said to describe ideally either the electrical or mechanical element of cardiac activity. The triaxial ECG suffers from such factors as the nonorthogonality of the measurement axes for a given vector lead system and the many assumptions involved in the nature, orientation, and movement of the theoretical dipole or sets of dipoles used to describe the source of the activity. Though the triaxial BCG does not suffer in the orthogonality of its measurement axes, it is obvious that the compliance and elasticity characteristics of the body elements and coupling media will also result in distortions. Though these factors limit the degree of precision attainable in analysis of cardiac activity, they do not seriously restrict the practical benefits arising from the research and clinical application of the data, as may be witnessed in the rapid progress of the VCG field.

For the BCG solution, the input functions were the BCG-$\ddot{X}$, BCG-$\ddot{Y}$, and BCG-$\ddot{Z}$ flight data signals stored on three FM channels of the on-

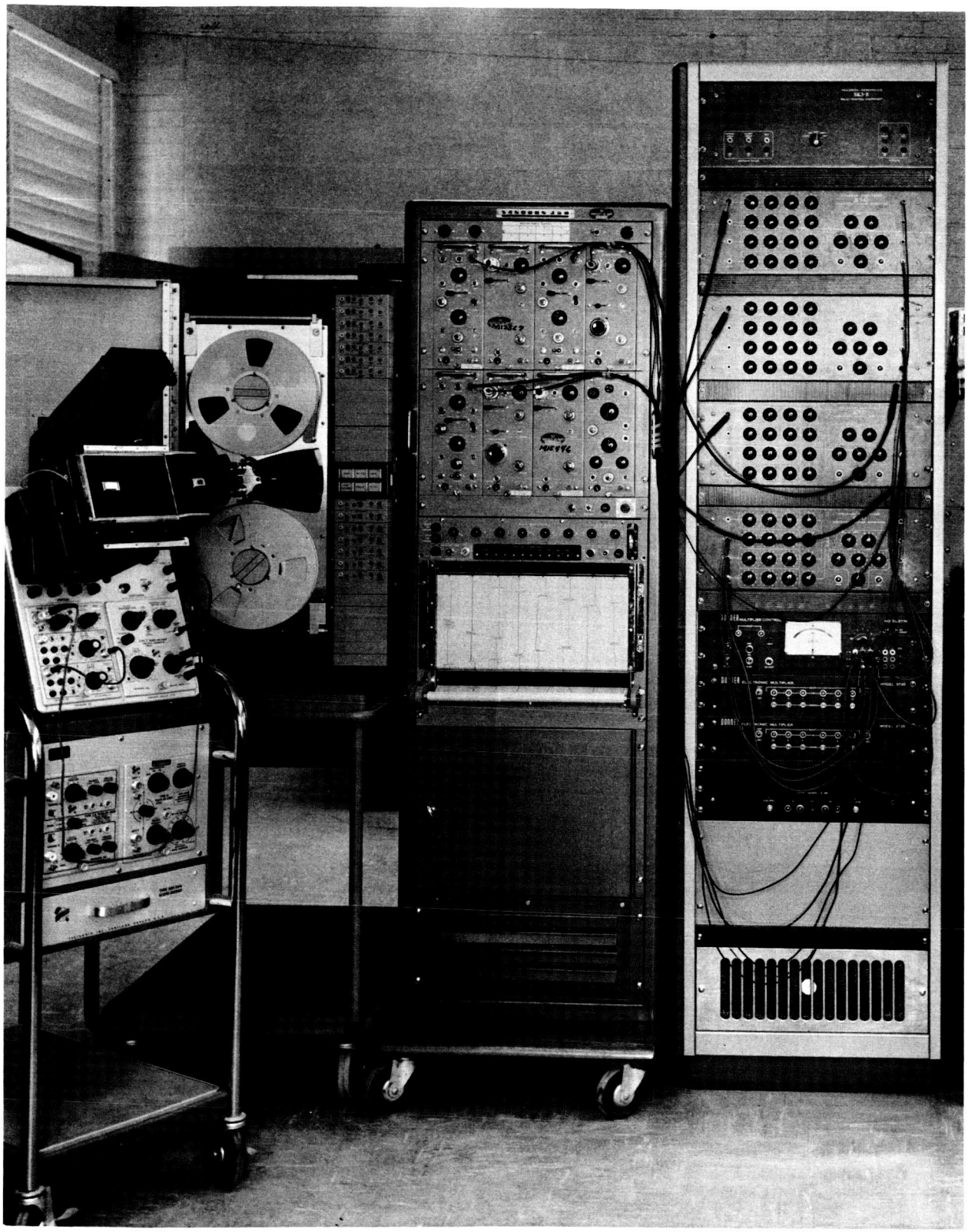

Figure 9.4 Photograph of equipment used for BCG and ECG vector analysis.

board magnetic tape instrumentation recorder. These signals, recorded at 30 ips and played back at 1-7/8 ips, were separately routed to three amplifiers which were independently adjusted to provide equal acceleration sensitivities at their outputs at a relatively high voltage level. Each BCG signal was then passed through an electronic multiplier whose output was proportional to the square of its input. The resultant $(BCG\text{-}\ddot{X})^2$, $(BCG\text{-}\ddot{Y})^2$, and $(BCG\text{-}\ddot{Z})^2$ functions were then added by means of a summing amplifier and routed to an electronic divider which performed a square-root operation on the sum.

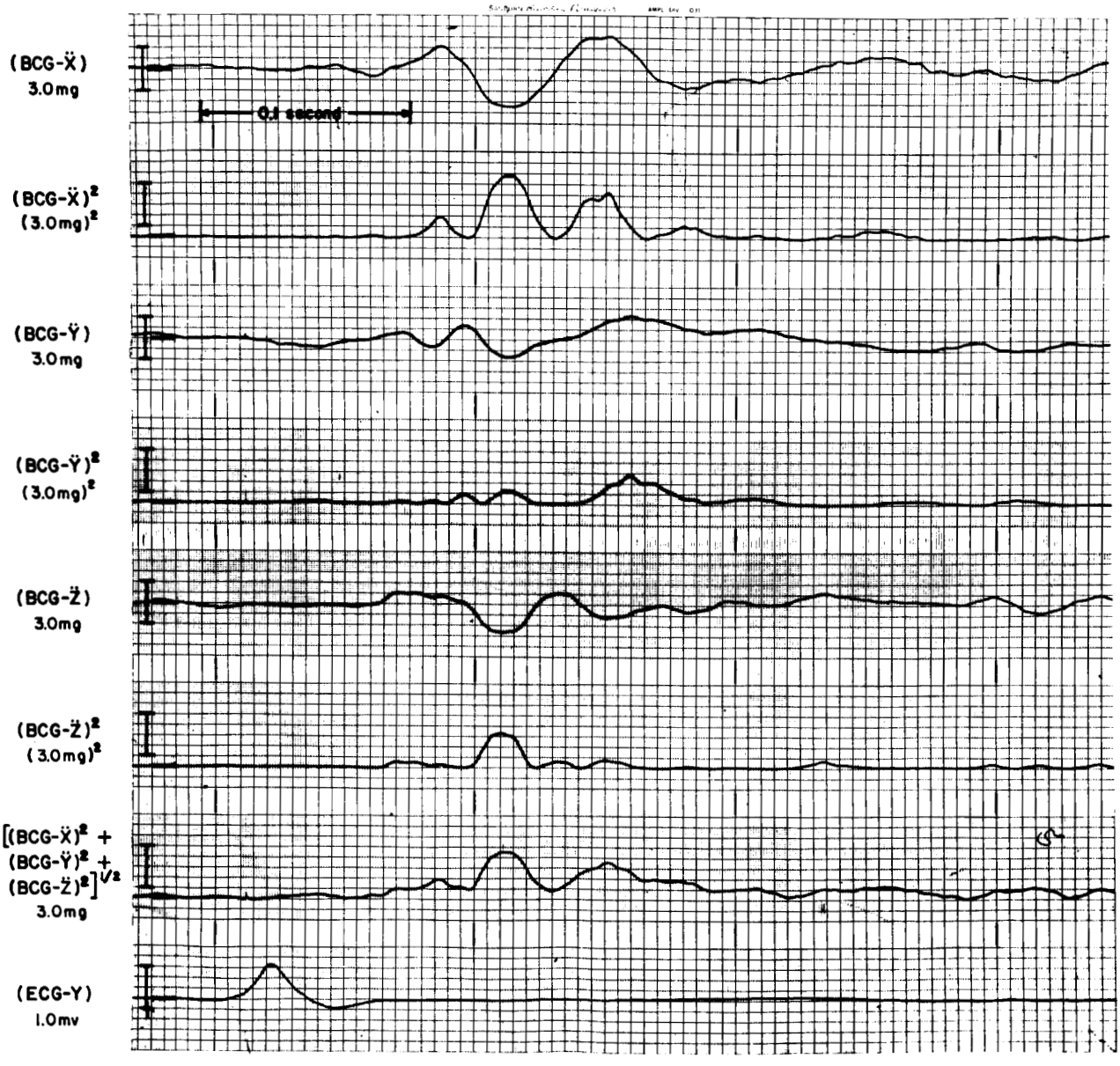

Figure 9.5 Analog computer solution of the absolute value of the instantaneous magnitude of the BCG vector for a Flight 6, Profile 8 cardiac complex. The ECG-Y data shown in the bottom channel serve as a time reference for the ECG vector solution shown in Figure 9.6 which was derived from the identical cardiac complex.

The output of this latter unit, $[\text{BCG-}\ddot{X})^2 + (\text{BCG-}\ddot{Y})^2 + \text{BCG-}\ddot{Z})^2]^{1/2}$, represented the desired solution for the absolute magnitude of the instantaneous BCG vector. This solution is identified as $|BCG(t)|$ to expedite later discussion. By removing the BCG signals from the input of the system and connecting each amplifier to the simultaneously recorded ECG-X, ECG-Y, and ECG-Z data channels, an identical solution, identified as $|ECG(t)|$, could be produced for the triaxial electrocardigram data.

The solutions for $|BCG(t)|$ and $|ECG(t)|$ for a single Flight 6 cardiac complex are shown in Figures 9.5 and 9.6, respectively. The top six channel

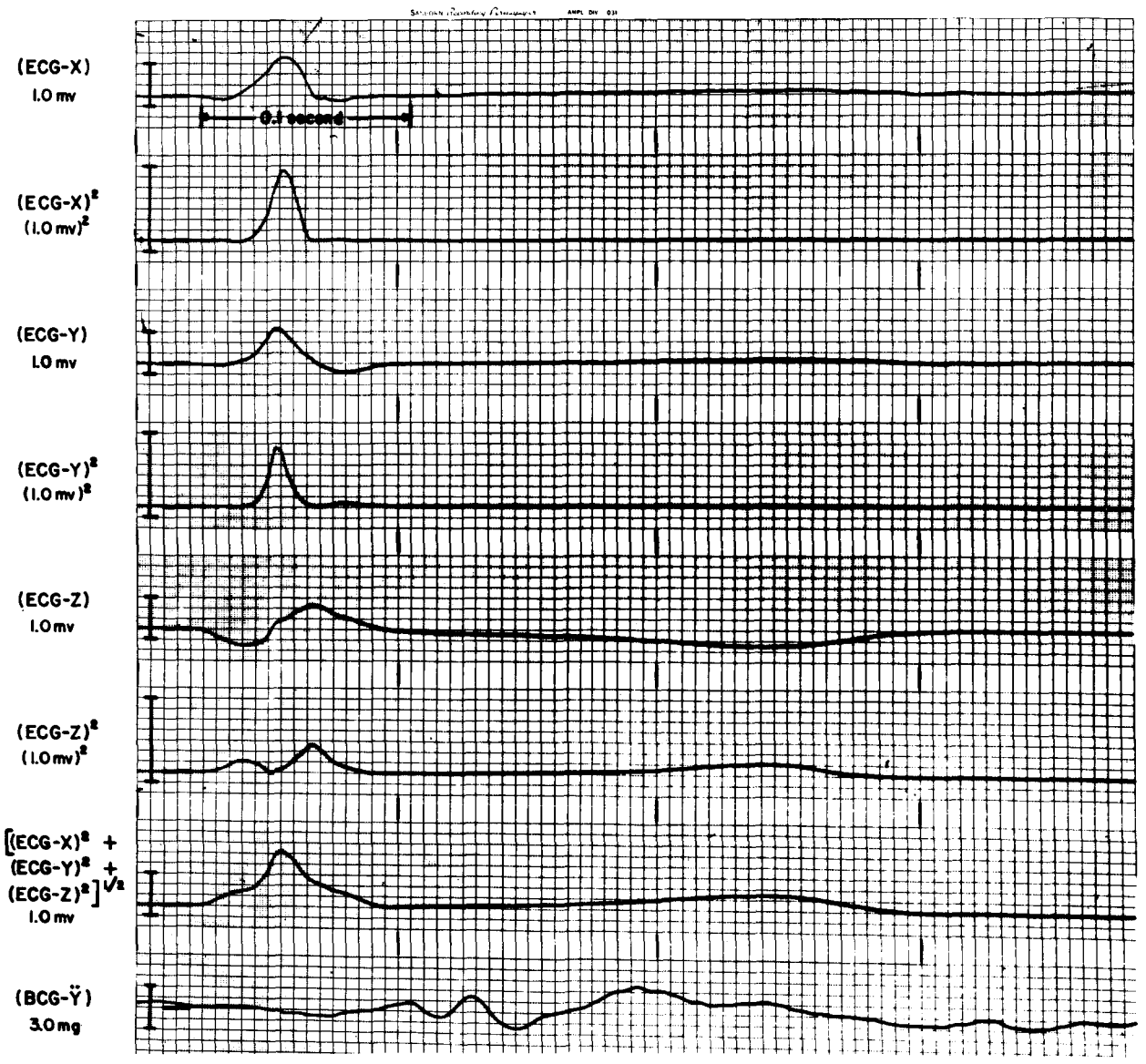

Figure 9.6 Analog computer solution of the absolute magnitude of the instantaneous ECG vector for a Flight 6, Profile 8 cardiac complex. The BCG-$\ddot{Y}$ data shown in the bottom channel serve as a time reference for the BCG vector solution shown in Figure 9.5 which was derived from the identical cardiac complex.

assignments of Figure 9.5 sequentially describe the instantaneous linear BCG accelerations occurring along the three reference axes and their instantaneous squares. In the seventh channel is shown the square root of the sum of these squares which has been identified as $|BCG(t)|$. The bottom channel shows the ECG-Y data which serve as a time correlate for the $|ECG(t)|$ data presented in Figure 9.6. The channel assignments of this latter figure follow a pattern identical to those of Figure 9.5 with time correlation provided by the BCG-$\ddot{Y}$ data shown at the bottom. The magnitude of each calibration marker is at the left immediately below the channel identification nomenclature.

Also shown in these figures at the left of each channel is a short line which denotes the zero reference signal level selected for the computer operations. For the BCG data, the relatively quiescent period immediately preceding the major complexes served as the zero reference. For the ECG data, the baseline occuring during the T-P interval served as zero reference. It should be carefully noted that, when squaring and square root computer operations are undertaken, small changes in these reference baselines can produce rather large changes in the absolute magnitude of the solution. In fact, a zero signal baseline reference is a difficult problem in biomedical computer applications requiring the precise quantification of the absolute magnitude of a time-varying physiological function. For this reason, analysis of the data of Figures 9.5 and 9.6 should give emphasis to the waveform of the $|BCG(t)|$ and $|ECG(t)|$ displays and the time correlations of the three originating scalar input functions.

To further emphasize these relationships, the scalar and vector data of Figures 9.5 and 9.6 have been consolidated into a single plot of simultaneously occurring BCG accelerations and ECG potentials (Figure 9.7). At the top are shown the three scalar ECG potentials, at the bottom the three scalar BCG accelerations, and at the center the related $|ECG(t)|$ and $|BCG(t)|$ quantities. The time base for these data, referenced to the onset of the Q wave of the electrocardiogram, is shown at the top and bottom of the figure. The polarity convention and zero baseline for each channel are shown at the left. The vertical dashed lines, identified as T1 and T2, signify the time of peak ECG activity and peak BCG activity, respectively.

The longitudinal BCG-$\ddot{Y}$ component of the flight data closely resembles data collected by an ultra low frequency suspension system with firm body-to-suspension coupling features; e.g., the BCG bed developed by Reeves, Jones, and Hefner (4). For comparative purposes, the nomenclature used by Reeves, Hefner, Jones, and Sparks (5) is applied to the data of this study. Their symbols are placed adjacent to the major events of the BCG-$\ddot{Y}$ complex shown in Figure 9.7. It is intended that this nomenclature serve only as a reference aid to facilitate the immediate identification of the cardiac events occurring in each of the six BCG measurements, not as a final definitive identification. It is obvious that the data of this study as well as those which will be collected in future explorations of triaxial BCG events will establish the need for new identification standards. It is felt that the key to these new standards will be the spatial BCG vectors to which events occurring in the three orthogonal scalar components can be time referenced and symbolically identified.

Figure 9.7 shows that the peak magnitudes of the ECG and BCG vectors occur approximately 47 and 153 milliseconds, respectively, after the onset of Q, which represents a 106 millisecond lag of the peak mechanical

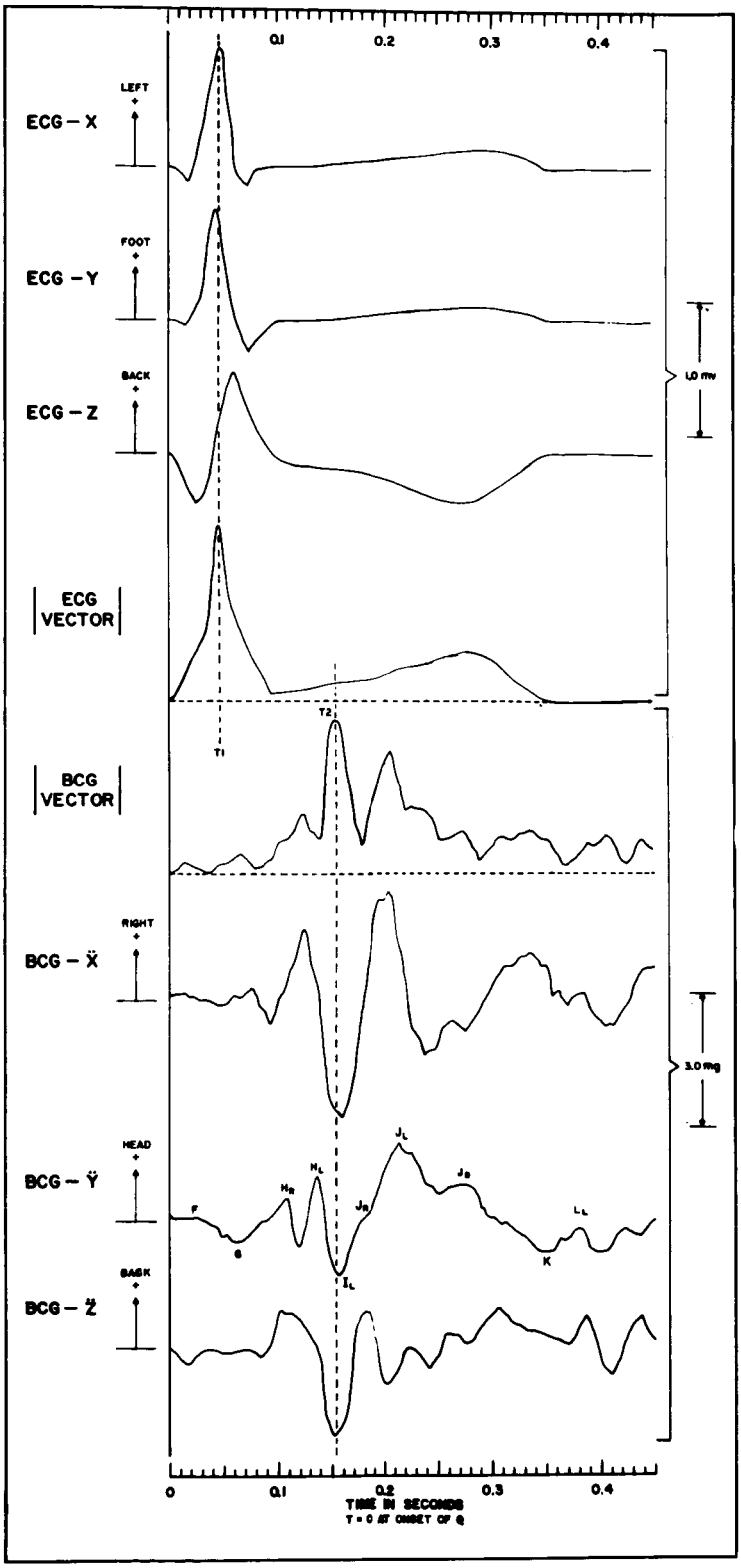

Figure 9.7 Plot of the scalar BCG and ECG data and their associated vector magnitudes as derived from the data of Figures 9.5 and 9.6.

activity behind the peak electrical activity. The R waves of ECG-X and ECG-Y are the principal components describing the peak magnitude of the ECG vector. Peak BCG activity occurs in the immediate vicinity of I_L in the BCG-$\ddot{Y}$ complex and is described by a simultaneous leftward, forward, and footward acceleration of the body. The events occurring at H_L contribute more to the BCG vector than those occurring at H_R. The valley between H_R and H_L on BCG-$\ddot{Y}$ is closely time related to a peak rightward acceleration event present in BCG-$\ddot{X}$. As expected, the waveform of the absolute magnitude of the BCG spatial vector clearly displays events which are not fully defined, or possibly even present, in any given single axis scalar measurement.

Information on the BCG vector in Figure 9.5 or 9.7 allows one to make a good estimate of the forces effective in the cardiovascular process at any time during a single cardiac complex. With a peak magnitude of the BCG vector of 3.5 milli-g and a total mass of the Constraint Platform including the subject of 206.5 pounds the maximal force exerted during the cardiovascular movement is 3.2 newton or 0.72 pound. The thrust of 0.72 pound represents the maximal force of ventricular ejection and is probably a valuable measure of cardiac efficiency.

TIME INTERVALS OF BCG-$\ddot{Y}$

From measurements performed on the original flight records shown in Figures 8.1 through 8.6 and using the nomenclature of Figure 9.7, means, standard deviations, and ranges of the time intervals between the onset of Q in the ECG and the major events of BCG-$\ddot{Y}$ were calculated. The resultant data for the individual and grouped profiles are shown in Table 9.2. Similar calculations were made for measurements obtained from BCG-$\ddot{Y}$ data collected from the flight subject in a laboratory environment. The results for six different laboratory runs, treated individually and as a group, are listed in Table 9.3. The raw data for these laboratory measurements were collected with the subject-Constraint Platform assembly resting on a two-dimensional air-bearing BCG bed as described in the previous section of the report (Figure 8.9). Comparison of the standard deviation and range of data of Tables 9.2 and 9.3 indicates that the flight measurements of the BCG-$\ddot{Y}$ time intervals showed less variation than those measured in the laboratory. This would be expected since the Figure 8.1 through 8.6 flight data were collected within a single ninety minute period while the laboratory data were recorded sequentially over a one week period. Comparison of the over-all mean data of Tables 9.2 and 9.3 indicates that, except for H_R, the major events of the BCG-$\ddot{Y}$ complex as measured in the zero g environment always preceded those recorded in the laboratory. For the two initial events, H_R and H_L, the standard deviation and range data showed little difference between the two environments. However, for all following intervals except Q-J_D, the over-all flight means never fell within the range of the data recorded in the laboratory. Similarly, the means of the laboratory measured Q-I through Q-L_L intervals did not fall into the range of the flight measurements except for Q-J_D. To summarize, little difference existed between the flight and laboratory data for the Q-H_R, Q-H_L, and Q-J_D intervals. The Q-I_L, Q-J_R, Q-J_L, Q-K, and Q-L_L flight data intervals preceded the corresponding laboratory measurements by approximately 19, 34, 24, 32, and 48 milliseconds, respectively.

Before considering the significance of this time delay, the mean, standard deviation, and range portions of Tables 9.2 and 9.3 are grouped

Table 9.2

Means, Standard Deviations, and Ranges of BCG-Ÿ Time Interval
Measurements Derived from the Flight Data Presented in Figures 8.1 through 8.6

BCG-Ÿ Interval	Mean Intervals in Milliseconds								
	Individual Flight Profiles						All Flight Profiles		
	2	3	5	6	8	9	Mean ±S.D.	Range	No. Obs.
Q-H_R	100	96	98	99	101	99	99±2.6	90-104	22
Q-H_L	130	126	126	128	130	129	128±1.3	124-132	22
Q-I_L	150	144	148	148	150	148	148±3.3	142-154	22
Q-J_R	170	165	168	167	—	171	168±3.2	161-173	18
Q-J_L	214	209	204	203	213	206	209±5.5	201-220	22
Q-J_D	265	248	253	253	265	264	258±7.9	246-268	22
Q-K	341	333	339	334	345	342	339±5.5	331-346	22
Q-L_L	370	357	365	365	374	371	368±6.2	354-378	22
Heart Rate	71	75	69	72	66	65	69.7		

Table 9.3

Means, Standard Deviations, and Ranges of BCG-$\ddot{Y}$ Time Interval Measurements Derived from Laboratory Data Collected with the Subject-Constraint Platform Assembly Supported on a Commercial Air-Bearing BCG Bed

Mean Intervals in Milliseconds

BCG-$\ddot{Y}$ Intervals	Individual Profiles						All Profiles		
	A	B	C	D	E	F	Mean ± S.D.	Range	No. Obs.
Q-H_R	96	95	99	98	93	95	96±3.9	87-103	30
Q-H_L	129	129	138	140	132	138	134±5.2	124-143	30
Q-I_L	163	161	172	171	162	173	167±5.8	156-174	30
Q-J_R	—	—	—	198	—	205	202±4.3	193-209	10
Q-J_L	227	226	240	237	222	244	233±9.5	217-252	30
Q-J_D	267	264	269	260	255	—	263±7.4	242-273	22
Q-K	375	369	357	377	368	383	371±9.8	352-397	30
Q-L_L	419	424	412	406	412	424	416±9.3	401-436	30
Heart Rate	55	54	58	57	55	51	55.0		

Table 9.4

Comparison of Means, Standard Deviations, and Ranges of Flight and Laboratory Based Constraint Platfrom BCG-$\ddot{Y}$ Time Interval Data with Similar Data Collected on 20 Normal Subjects with an Ultra Low Frequency Force BCG Bed.

Interval	Flight Data—1 Subj.		Lab. Data—1 Subj.		ULF BCG Bed—20 Subj.*		No. Obs.
	Mean ± S. D.	Range	Mean ± S. D.	Range	Mean ± S. D.	Range	
Q-H_R	99±2.6	90-104	96±3.9	87-103	85±10	60-100	100
Q-H_L	128±1.3	124-132	134±5.2	124-143	116±13	80-140	99
Q-I_L	148±3.3	142-154	167±5.8	156-174	142±13	120-170	100
Q-J_R	168±3.2	161-173	202±4.3	193-209	177±19	140-220	95
Q-J_L	209±5.5	201-220	233±9.5	217-252	217±19	180-260	100
Q-J_D	258±7.9	246-268	263±7.4	242-273	250±27	210-320	58
Q-K	339±5.5	331-346	371±9.8	352-397	305±24	260-370	86
Q-L_L	368±6.2	352-378	416±9.3	401-436	390±30	330-460	100

*These data were derived from Table 1 of Reeves,et al (5).

in Table 9.4 with similar data recorded by Reeves, Hefner, Jones, and Sparks (5) from 20 normal subjects on an ultra low frequency (ULF) BCG bed. Remembering that the flight and laboratory data represent repeated measurements on a single subject while the ULF data were collected on 20 subjects, a comparison of the Table 9.4 data can be made. Comparing first the flight and ULF data, most of the flight means fell on the high side of the ULF data. However, all flight means fell within the range of the ULF data, and the greatest differences occurred in the Q-H_R and Q-K intervals.

A similar comparison of the laboratory and ULF data indicates that all of the laboratory means fell on the high side of the ULF data, and, except for Q-K, all of the laboratory means fell within the range of the ULF data. The most prominent difference, as defined by the individual combination of the mean and standard deviation data, was the Q-K interval.

In general, the data of Tables of 9.2, 9.3, and 9.4 indicate that the BCG-$\ddot{Y}$ time interval data collected with the Constraint Platform in the flight and laboratory environment are reasonably similar to those which would be measured with a wide-band ULF suspension system. These data also indicate that the I_L, J_R, J_L, K, and L_L events recorded with the flight suspension did significantly precede the corresponding events as recorded by the air-bearing suspension of the Constraint Platfrom in the laboratory.

Though it might be tempting to attribute these changes primarily to the physiological effects of the weightless environment, one would be limited in this extrapolation by such potential cardiovascular controlling factors as the effect of the 2 g entry pull-up acceleration, the effect of heart rate on the interval data (Tables 9.2 and 9.3), or the effect of the higher mass loading placed on the subject in the laboratory. Because of these factors, it would seem necessary to restrict such an extrapolation and to place equal emphasis on the fact that the physical characteristics of the zero g and terrestrial suspension systems differed significantly.

ELECTROCARDIOGRAPHIC DATA

In Figure 9.1, electrocardiogram data were presented in vector loop form for three different intervals within the same zero g profile. Loop sets were presented for the 1 g environment occurring immediately before the entry pull-up phase began, the 2 g environment present in the middle of the pull-up maneuvers, and the zero g environment during free-flotation of the subject. These data indicate that, besides a general widening of the R loop, the most prominent changes occurring in the ECG loops recorded in the zero g environment were the compression of the T loop in the frontal plane, an increase of amplitude, and a forward-headward swing of the T loop noticed in the horizontal and sagittal planes.

Similar data, but of triaxial scalar form, are presented in Figure 9.8 on three different profiles of Flight 6. In all zero g recordings, the amplitude of T decreased in ECG-X and ECG-Y and increased in ECG-Z. An increase in the amplitude of the R wave in ECG-Z is also observed in this figure.

To gain further insight into the nature of these changes, the Flight 6 triaxial ECG data were investigated by using the computer instrumentation described by Figure 9.3, and the instantaneous absolute magnitude of the ECG spatial vector identified as $|ECG(t)|$ was obtained. Typical data

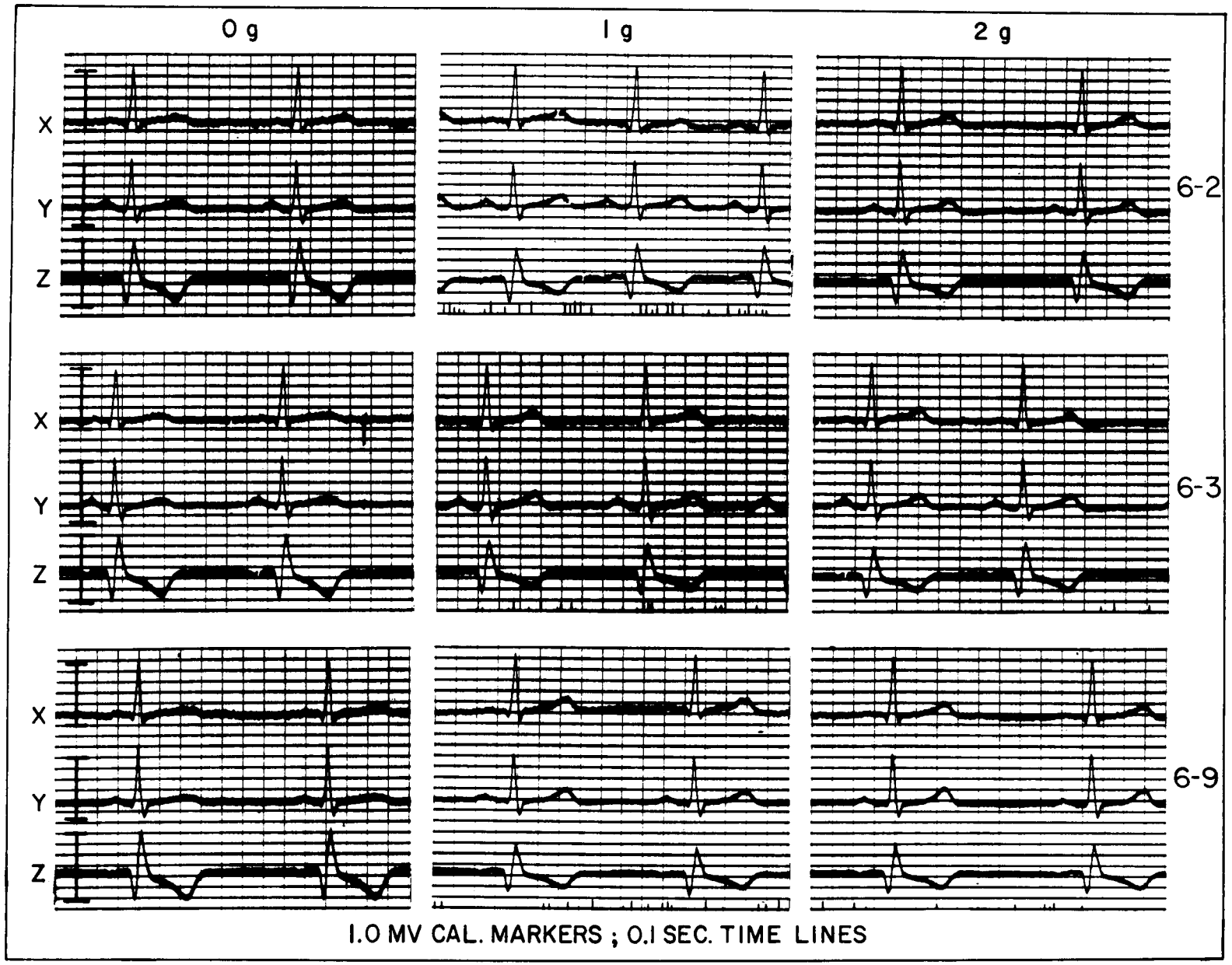

Figure 9.8

Comparison of triaxial electrocardiogram data collected during the free-flotation state (0 g) immediately before the beginning of a zero g maneuver (1 g) and during the entry pull-up phase of a maneuver (2 g) for three different Flight 6 profiles.

for the 2 g, 1 g, and zero g phases of the same maneuver are shown in Figures 9.9 through 9.11, respectively. The nomenclature for these figures is self-explanatory.

As typified by these data, little consistent over-all difference existed between the 1 g and 2 g environments in either the waveform or the magnitude of $|(ECG(t)|$. For the zero g data, a general rise in the amplitude of the T wave portion of $|ECG(t)|$ was observed, indicating that the directional changes of the T vector were accompanied by a small increase in magnitude. Also noted occasionally in the zero g case was the absence of the flat spot in the S portion of the $|ECG(t)|$ waveform usually observed in the 1 g and 2 g measurements. This difference came about as a result of the instantaneous magnitude relationship between the S wave of ECG-Y and the descending portion of R in ECG-Z.

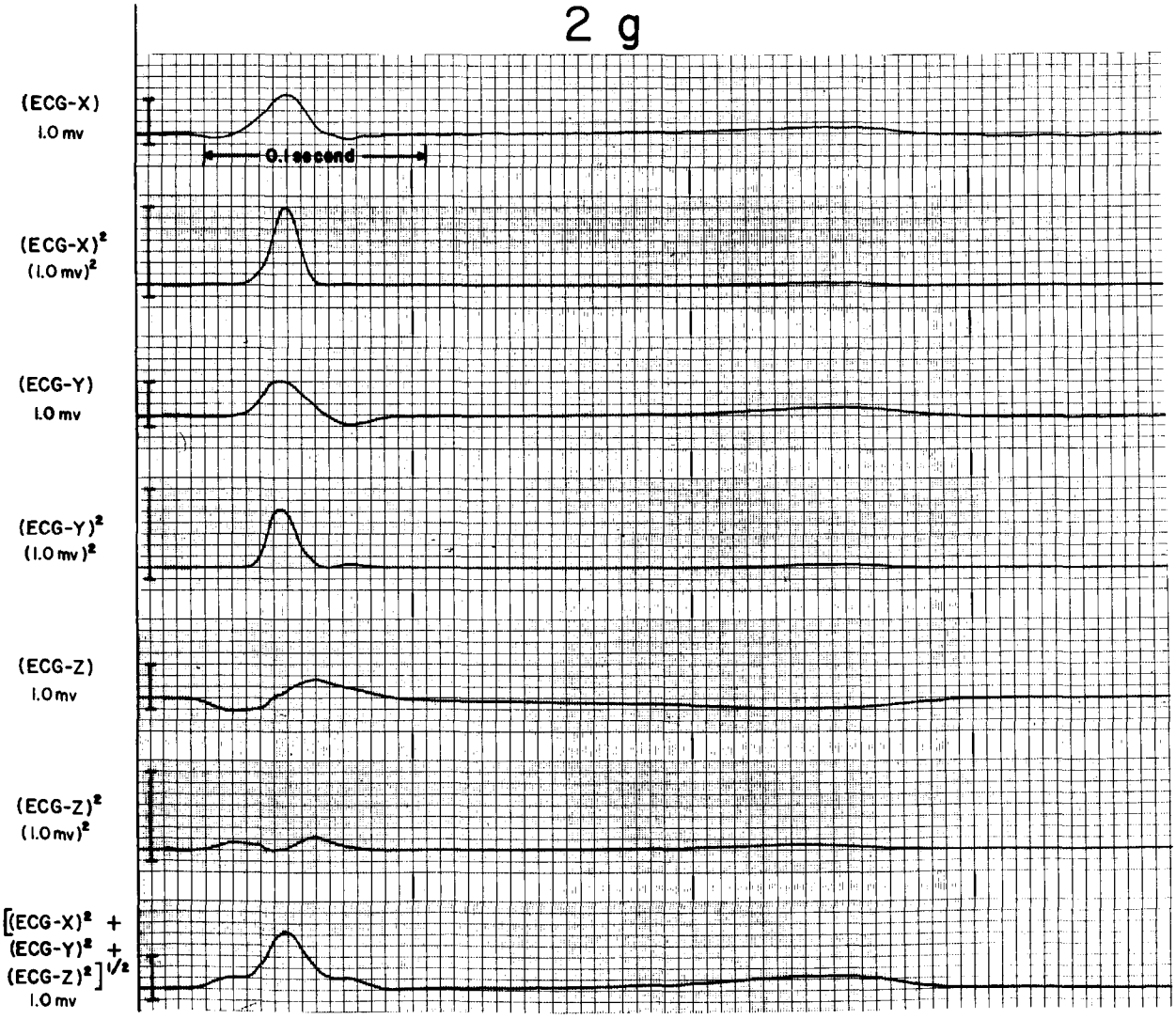

Figure 9.9 Typical analog computer solution of the absolute magnitude of the spatial ECG vector as recorded in the 2 g environment occurring in the middle of the entry pull-up phase of the zero g maneuver.

Again, as with the BCG data, it would be natural to attribute these changes to the physiological effects of weightlessness. Although the method of constraint is not so significant as in the BCG data, the effect of heart rate would have to be considered. However, a much simpler explanation is offered to account for the major portion of the differences in T wave amplitude. In the zero g environment, the subject maintained self-controlled suspension of his respiratory processes, while he exerted no such control in the other phases of the maneuver. Repeated laboratory observations of ECG-X, ECG-Y, and ECG-Z showed that the suspension of respiration produced comparable ECG changes, particularly the increase of the R and T wave portions of ECG-Z. It could possibly be said that the laboratory changes in ECG-Z were not quite so large as those noted during the

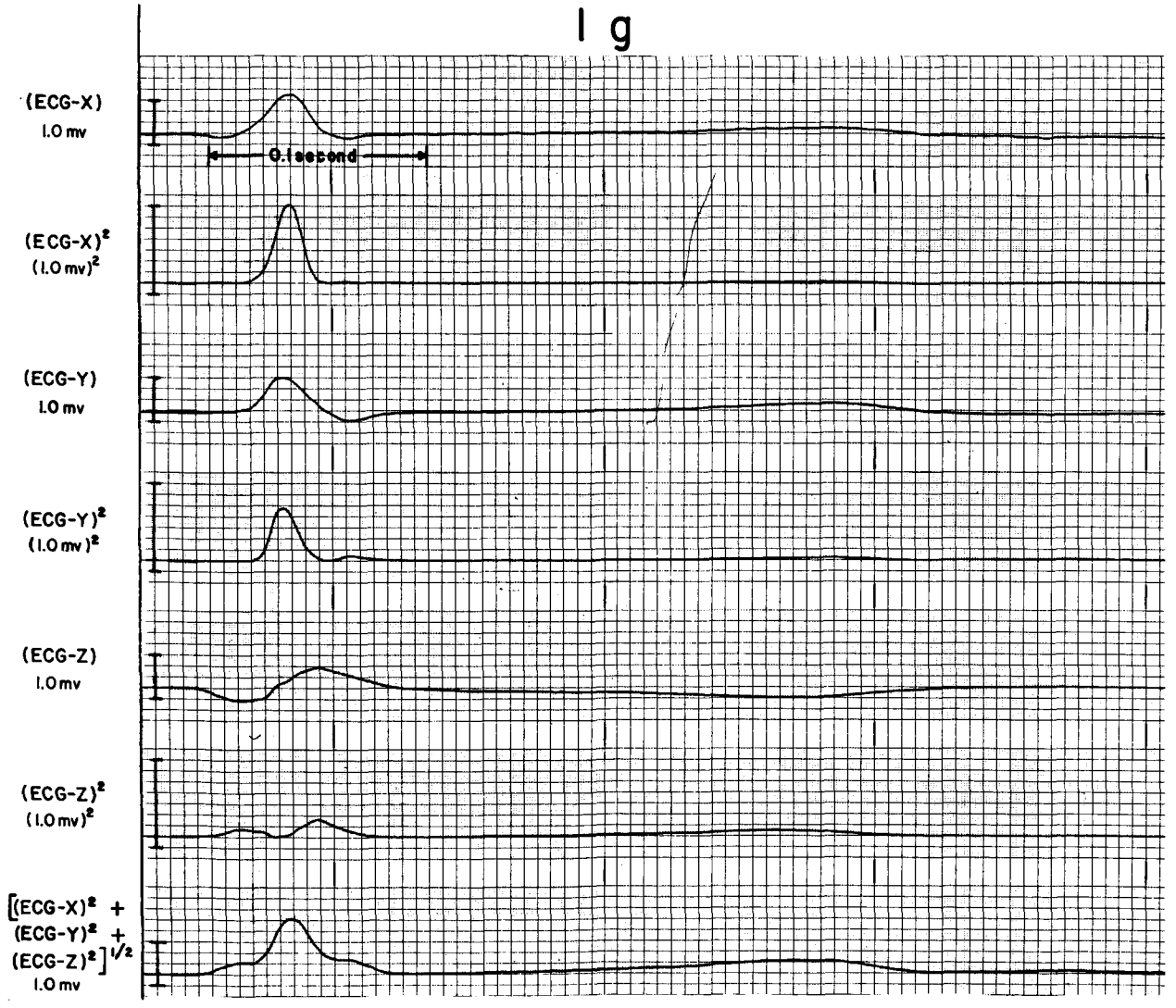

Figure 9.10 Typical analog computer solution of the absolute magnitude of the spatial ECG vector as recorded in the 1 g environment occurring immediately before initiation of the entry pull-up phase of the zero g maneuver.

free-flotation phase of a zero g maneuver so that the differences could have been caused partly by the zero g environment.

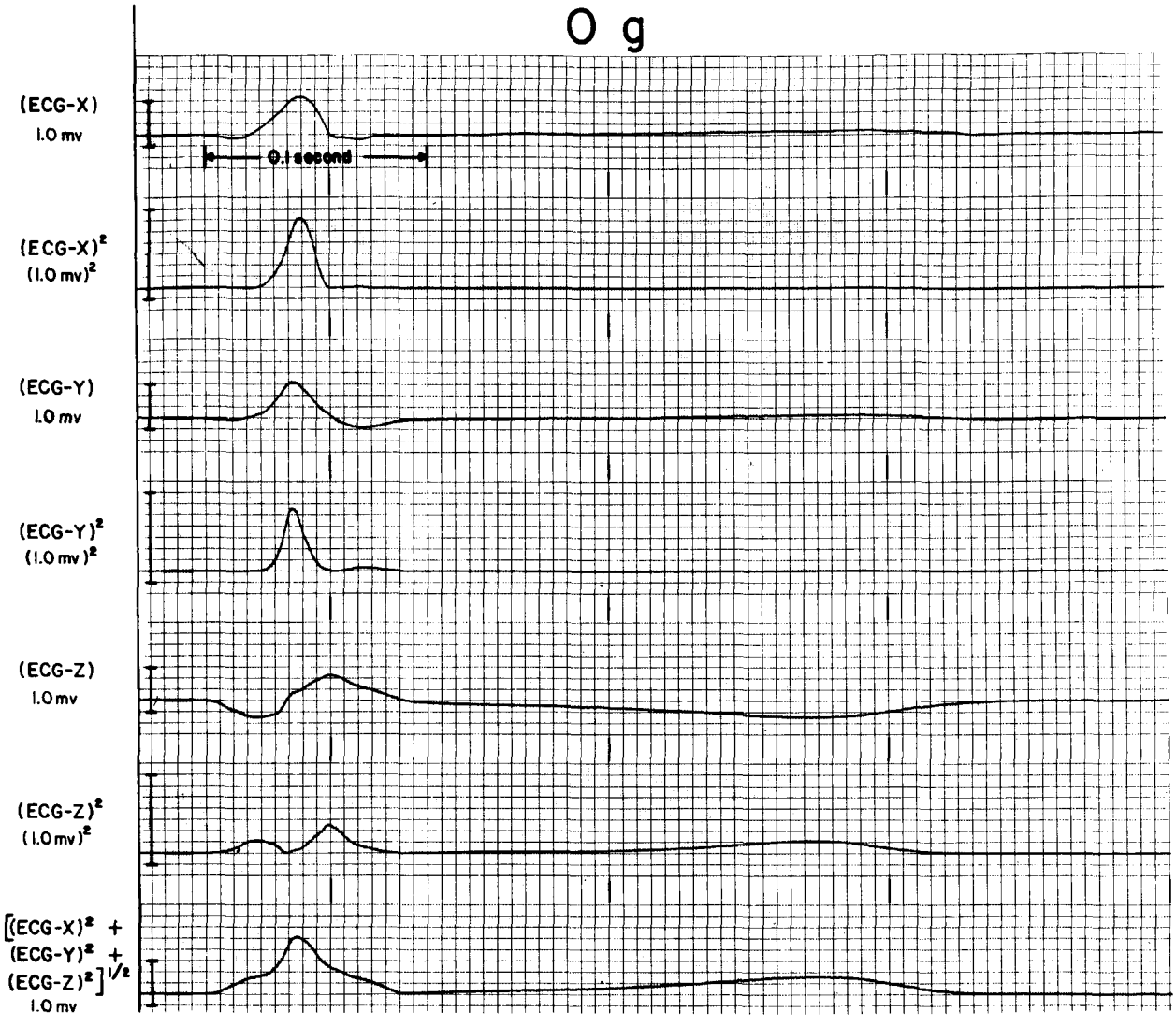

Figure 9.11 Typical analog computer solution of the absolute magnitude of the spatial ECG vector as recorded during the zero g free-flotation period.

10. DISCUSSION AND FUTURE APPLICATIONS

The experimental approach of this study was based on measuring the cardiac-originated, whole-body, inertial accelerations of a human placed in a suspension system allowing motion with a near perfect six degrees of freedom. The state of weightlessness generated by free-flotation during the zero g maneuvers of the aircraft served primarily as a suspension system and not as a stimulus variable whose effect on cardiovascular dynamics was under study. Only when space technology advances to a point where time is available for the subject to adapt to his environment and weightlessness can be considered as one of the primary stimuli can such a study be undertaken. The entry acceleration, the short period of weightlessness, and the recovery acceleration of each zero g maneuver defined a relatively short acceleration-time profile. Since little is known about the characteristics of the time response of the cardiovascular system to sudden transitions in acceleration, extrapolation of data collected in this environment is not sufficient to define the effects of weightlessness on the performance of the cardiovascular system. Therefore, the present discussion concentrates mainly on instrumentation aspects and their possible improvement in future airplane and satellite flights.

When the project was initiated, little *a priori* information was available on the physical characteristics of the environment produced by free-flotation of a subject within the KC-135 zero g aircraft. The background acceleration noise level which would be encountered during the collection of the BCG data due to the combined effects of the environment, the Constraint Platform, and the subject could not be predicted, nor could the level of offset accelerations that might be produced by the launch of the subject be estimated. Similarily, little *a priori* data were available on the magnitude and frequency characteristics to be expected of the BCG-$\ddot{Z}$, BCG-$\ddot{\Theta}_X$, BCG-$\ddot{\Theta}_Y$, and BCG-$\ddot{\Theta}_Z$ measurements since these data could not be readily collected in a terrestrial laboratory.

All of these factors necessitated special design features for the bioinstrumentation system which could be proven only in the operational environment. In the following sections, the information gathered from the flight program is used to discuss these factors and their relationship to the special design features of the system.

BCG BACKGROUND NOISE

The previously presented triaxial BCG data proved that such measurements could be made in an operational environment with a signal-to-noise ratio at least equal to that present in most terrestrial BCG laboratories. However, to establish a reference noise baseline for the data of Figures 8.1 through 8.6, three zero g profiles were flown at the end of Flight 6 with a "dummy subject" placed in the Constraint Platform.

The data of Figure 8.8 verify the low background noise observed in the three linear acceleration BCG measurements of Figures 8.1 through 8.6. These data also show the higher background noise of the angular acceleration BCG measurements which is to be expected for the extremely low-level signal. As may be seen, the system is free of low-frequency resonances, and the noise spectra are composed essentially of high-frequency components.

OFFSET ACCELERATION

As has been discussed, the potential impartation of angular velocity components to the free-flotation motion of the Constraint Platform by the launch personnel played an important role in the basic design of the instrumentation system. In fact, the lack of *a priori* data on the magnitude of these velocities and their resultant centripetal accelerations as measured by the BCG linear accelerometers required a) the design of a system with a dynamic range greater than that required to handle only the peak-to-peak levels of the BCG signals, b) the need for AC coupling of the BCG channels so that the full signal-to-noise ratio capabilities of the telemetry oscillators could be realized if these offset accelerations did exist, and c) Command Reset circuitry to minimize the loss of data due to the blocking effects usually encountered with the transmission of transient signals through capacitive coupling networks.

To determine if these offset accelerations did exist, zero g profiles were flown on Flight 3 with the three linear acceleration BCG channels direct coupled throughout the system. These data indicated that the dynamic zero baseline level, defined as the level where the time integral of the periodic signal above the baseline equals the time integral of the signal below the baseline, did not occur at the measured static zero acceleration. These offset differences between the dynamic and static baselines were approximately +0.4 milli-g, −0.2 milli-g, and +1.0 milli-g for BCG-$\ddot{X}$, BCG-$\ddot{Y}$, and BCG-$\ddot{Z}$, respectively.

If one were to assume that these offsets of the BCG baselines were due to centripetal accelerations produced by the angular velocity motions that might be imparted to the Constraint Platform by the release operations of the launch personnel, it would be fair to assume further that the magnitude of these accelerations would differ from profile to profile since the physical act of releasing the Constraint Platform could not be identically repeated on each profile. However, the Flight 3 data indicated that little change occurred in the exact magnitude of the offsets from one profile to another. It was concluded that the release operations did not produce measurable acceleration levels and that the offset was due to a small static bias always present in the output of each accelerometer.

Since the magnitude of the BCG-$\ddot{Z}$ offset level, acting in combination with its dynamic BCG signal, would result in modulation with pronounced nonsymmetry, it was necessary to capacitively couple the related signal-conditioning amplifier to its telemetry oscillator so as to optimize the signal-to-noise ratio of the channel. Although not technically necessary, the other BCG measurements were similarly coupled to permit all of the BCG signals to be displayed with identical low frequency response characteristics.

APPLICATIONS

From the knowledge gained during the implementation of this project, the following observations and recommendations are offered which are considered to be significant to the instrumentation aspects of future BCG explorations using a similar approach. Factors pertinent to the further study of the triaxial BCG in parabolic flight are presented first. Recommendations involving BCG considerations in actual space operations, specifically large scale manned space station laboratories, follow.

From the flight data phase of this program, it was shown that the instrumentation system could be greatly simplified for future studies. The greatest simplification would occur in the AC-DC coupling alternatives provided in the BCG channels of the system. Specifically, the flight data indicated that the manual launch operations which placed the subject into the free-flotation state did not produce measurable offset acceleration artifacts. Although offset signals were present in the linear acceleration BCG channels, they were attributed to small bias signals in the accelerometers. By specifying smaller zero signal tolerances to the transducer manufacturer, these bias signals could be made negligible. Thus, in future applications, the BCG signals could be direct coupled throughout the system without the need for the coupling capacitors or the Command Reset System included in the present Biotelemetry Module.

Simplification in future studies might also be achieved by eliminating the need for signal-conditioning amplifiers between the BCG transducers and their related telemetry channel. If FM-FM type telemetry is utilized, high sensitivity subcarrier oscillators have become available which would not require additional amplification of the transducer signals. However, attention must be given here to matching the impedance levels of the transducer output to the oscillator input. Equally important would be the need for some method of gain control not affecting the acceleration calibration of the system that would allow for the different levels of the BCG signals occurring along the various body axes. The operational amplifiers utilized in this project accurately provided this gain control feature as well as the impedance matching requirements.

For the selection of transducers, it is felt that transducers utilizing the force-balance principle offer the most advantages for both the linear and angular acceleration BCG measurements. Without imposing stringent demands on the gain characteristics of the chopper-stabilized amplifiers, linear accelerometers with a full-scale sensitivity of ± 0.25 g and angular accelerometers with a full-scale sensitivity of ± 5 rad/sec^2, all with natural frequencies of 100 cps or greater, would optimally serve for such applications. Such transducers are usually provided with damping ratios of 0.6 to 0.7 of critical to extend their amplitude response at the higher frequencies. However, a more idealized BCG transducer would result if a unit were designed with a higher natural frequency, and its damping set to equal or to exceed critical slightly. Such a transducer would offer the same flat frequency response over the BCG spectrum but eliminate the pre-emphasis of noise frequencies near its natural frequency as well as overshoot for fast rising waveforms.

One further consideration would be to minimize the ratio of the mass of the Constraint Platform and instrumentation to the mass of the subject. Emphasis on packaging techniques would reduce the mass of the instrumentation system. The three linear accelerometers and three angular accelerometers could be mounted in a single case. The ECG and BCG signal-conditioning amplifiers could be similarly packaged as well as the telemetry components. The weight of the battery sources could be decreased by reducing the operating time demanded for the system. These reductions are considered as immediately achievable and do not depend on the initiation of feasibility studies or the development of new concepts, devices, or components.

With this approach, the 11.0 pound weight of the existing instrumentation package could be reduced using commercial equipment that is available

and operationally proven. The limiting factor would be the weight of the angular accelerometers currently available. However, in the case of the Constraint Platform, it is felt that little weight reduction can be accomplished without materially sacrificing its safety functions in the operational environment. In effect, the efforts to reduce the over-all weight would be restricted to the mass of the instrumentation.

For manned space applications, specifically for large scale orbiting laboratories providing freedom of motion to on-board personnel, the BCG instrumentation problem becomes greatly simplified. Constraint of the subject need be provided only to maintain a fixed body posture of the subject. The removal of the safety functions of the system would result in a most significant reduction of its weight. A second simplification would be the elimination of the need for telemetry of the BCG signals to the on-board data collection station. Since the relative motion between the free-floating subject and the vehicle will be stabilized for this environment, hard-line interconnections would be feasible. In fact, with a central data collection station, which will surely be provided regardless of what specific in-space physiological measurements will be recorded, there will be no need for signal-conditioning circuitry at the subject. Only a lightweight constraint platform, three linear accelerometers, three angular accelerometers, and ECG electrodes will be required to collect the triaxial BCG-ECG data.

Justification for the utilization of BCG measurement techniques in such space ventures is easily established. First, the instrumentation techniques are simple and do not require significant additions to the payload or power demands. These external whole-body measurements do not place any physical demands on the subject or introduce disturbances to physiological functions. With the empirical background data currently available in the ballistocardiography field, a valid measure of cardiovascular performance directly related to the originating cardiac forces will result, its greatest contribution being detection of changes in the mechanical cardiac activity after prolonged exposure to the space environment.

However, terrestrial ballistocardiography will also profit from the results of the flotation method. For the first time, estimates of the nature and degree of impairment by spring connection to the ground can be verified by comparison of the earthbound with the gravity free method. It will also be possible to derive undistorted quantitative data on the intensity of the driving force of the cardiovascular system and the pattern in which it reaches the surface of the human body. Distortions of the BCG introduced by the nonrigid coupling of the heart with the surface of the human body are not eliminated by the new method, but the estimation of their influence on the BCG will be simplified. The suspension in a weightless environment presents ideal conditions for evaluation of the effectiveness and limitations of terrestrial suspension systems.

REFERENCES

1. Frank, E., An accurate, clinically practical system for spatial vectorcardiography. **Circulation, 13**:737-749, 1956.

2. Scarborough, W. R., and Talbot, S. A., Proposals for ballistocardiographic nomenclature and conventions: Revised and extended report of Committee on ballistocardiographic terminology, with technical appendix. **Circulation, 14**:435-450, 1956.

3. Aerospace Medical Division, 6570th Aerospace Medical Research Laboratories, Wright-Patterson AFB, Ohio, Rpt. No. AMRL-TDR-63-36. Moments of inertia and centers of gravity of the living human body. May, 1963.

4. Reeves, T. J., Jones, W. B., and Hefner, L. L., Design of an ultra low frequency force ballistocardiograph on the principle of the horizontal pendulum. **Circulation, 16**:36-42, 1957.

5. Reeves, T. J., Hefner, L. L., Jones, W. B., and Sparks, J. E., Wide frequency range force ballistocardiogram: Its correlation with cardiovascular dynamics. **Circulation, 16**:43-53, 1957.